TERRESTRIAL PHOTOGRAMMETRY FOR VELOCITY MEASUREMENT OF KRONEBREEN CALVING FRONT

Mari Svanem

Norwegian University of Life Sciences
Department of mathematical science and technology
Master Thesis 30 credits 2010

Preface

As a Geomatics student at The Norwegian University of Life science (UMB) one can choose from a variety of interesting subjects for a master thesis. The choice of this master thesis became a reality because I wanted to use my knowledge from study in a realistic, unknown and development case of work. Landscape, glaciers and climate are fascinating and exciting parts of the environmental changes. I was curious about practical science work in this field, and wanted to be a part of it.

This thesis uses terrestrial photogrammetry as equipment for measuring velocity. This application has indicated which challenges can appear when using the method on an area of continuous change. The experience from this work makes me more prepared for the same challenges in new and similar cases. It has been interesting to learn about glacier motion and calving, that was a new knowledge for me. I have also become dependent of MATLAB and learned to use new and different kinds of computer programs.

The decision and agreement of this master thesis was taken one year ago. A course at University in Oslo in January got me started on learning the computer programs I have been using through my work, and connected me to people working with glaciology science. The total ardency guided a way to a fantastic glacier course in July. The culmination was to be one of Anne Chapuis' field assistants in August. We were a team of four people who stayed at the beach of Kongsfjorden for 10 days to observe and capture data from the calving of icebergs from Kronebreen. The calving is a truly amazing event and I found it inspiring to be a part of a science project regarding these events in such a beautiful area.

The main work started when I arrived from Svalbard in August. I had more images than space on my computer, supervisors with a lot of ideas and engagement, some computer programs to learn and unread papers about glaciology. But instead of working with all my plans, much of the time was used trying to transform images into same reference frame, without success. I continue the work with a not satisfying solution of the problem, with a plan of deeper research later. The time always goes faster than wanted, but I am very happy for all the interesting kind of problems and unplanned work that showed up instead of just following all the plans. It lets me think in another way, ask people for good advises and ideas, and turn into surprises. By finishing the work, I see new and better ways of reaching representative results. However, the method works, I have tried to get good results, but it can always be done better.

Mari Svanem

Ås, 15th of December 2010

Acknowledgements

This work has leaded me to many helpful and clever people that give a lot of their interesting knowledge with their engagement and help.

First I will thank Anne Chapuis, one of my helpful supervisors. This master thesis would not have been created without her. Thanks for always taking time for my question, having a lot of good ideas, and generally being nice and very positive! The door is always open and the mail answered wherever she is in the world.

I send a lot of thanks to my supervisor Cecilie Rolstad Denby, who always tries to inspire me with her large engagement. Thanks for a nice and interesting trip to International Glaciological Society Nordic branch meeting in Copenhagen in October, and for suggesting me to go. My poster is found in appendix A.

Ivar Maalen-Johansen stepped in as a supervisor the last month. Thanks for helping me reaching the deadline, giving ideas and feedback! He has also been one of the trustful and helpful photogrammetry experts together with Øystein B. Dick early in the work.

The corridors at Department of Mathematical Sciences and Technology (at UMB) are generally filled with clever people answering questions as the largest matter of course. Four of them are already mentioned. Thanks to Jack Zeigler too, who has helped me with questions about MATLAB, and Håvard Tveite, who gave me the computer program ArcGIS. Thanks to Karin Smisetfoss for running around trying to find a cover to my poster.

Department of Geosciences at University of Oslo has many clever glaciological people. Here I will give a specially thank to Andreas Kääb, that have learn me, given me, and answered a lot of questions about his computer program, Cias. Ph.D. student Christopher Nuth has been available to answer questions, and has given me his GPS measurements to compare my results with. Thanks to Monica Sund who gave us some of her images. All the images taken in June, July and August 2007 are images from her camera.

Thanks to the committee of the legacy, “Kong Haakon den 7des utdannelsesfond for norsk ungdom”, by Viktorovna Svetlana Olsen at University of Tromsø, for giving us economic help to the field work excursion to Svalbard in August.

A special thanks to Anne Chapuis, Bas Altena, Damien Isambert and Imiaq, who were a great field company! Thanks for two fantastic weeks on Kongsfjorden beach. Thanks to Vojtech and the rest of the staff at The Norwegian Polar Research Institute in Ny-Ålesund for help and company.

Thanks to Martin Windju, Gunnhild Medhaug and Gjermund Kvernmo, for trying to rescue my English writing with emergency relief during the last weeks.

And final, but not less important, thanks to Astrid Hystad and all other incredible friends holding company with me during this last semester at Norwegian University of Life Sciences.

Abstract

Crevasse tracking in optical satellite images has successfully been used for mapping glacier velocities. Temporal resolution is restricted to the repeat orbit periods, and the spatial resolution according to recording geometry. Terrestrial photogrammetry offers an advantage in both temporal and spatial resolution, but introduces other challenges. We have applied terrestrial photogrammetry close to the calving front of Kronebreen, in order to map velocities close to the terminus.

Two cameras are placed near the front, one south and one north of the measured points on Kronebreen, recording photographs every hour and every sixth hour. This project aims to analyze images from June to August 2007, May to October 2009 and April to August 2010.

The velocity is found as displacement between matched image pairs. Displacement is then transformed into terrain coordinates by means of an elevation model and camera parameters. The preprocessing proved to be the main part of the work, as the images have different reference frame because of camera motion within the periods.

This transformation of images into the same reference frame includes the largest percentage of uncertainty of the results. Non satisfactory transformation, image quality, image matching and georeferencing process, elevation model and spatial resolution of the images make a total accuracy of 1.5 pixels in images taken from camera 1. The uncertainness is 0.84 m for a point 2500 m from the camera for every match. The absolute accuracy of the daily velocity belongs together with the numbers of days between the matched image pair, and will be 0.32 m with 4 days between the images.

By measuring velocity from images with 2, 4 and 8 days between, a temporal resolution of four days gives the best results. Choice of fewer days gives worse accuracy for daily velocity, but better temporal resolution.

The results are presented as velocity graphs showing temporal variations together with temperature and precipitation. Spatial variations are displayed in graphs as velocity across and along the glacier tongue.

Comparisons with earlier cross profiles from the same area, GPS measurement from the same time on the same glacier and velocity from satellite images with worse spatial and temporal resolution, support the results from terrestrial photogrammetry.

Samandrag

Satellittbilete har lenge vore bruka til å måle hastigheit på isbrear. Den tidsmessige nøyaktigheita for denne metoden er begrensa til banemønsteret, medan den romlege oppløysinga blir bestemt av opptaksgeometrien. Terrestrisk fotogrammetri gir meir detaljert informasjon både i tid og stad, men gir i staden andre utfordringar. Hastigheita er måla så nær kalvingsfronten på Kronebreen som praktisk mogleg. Det er satt ut to kamera for å fotografere brefronten: Eit står sør for Kronebreen og tek bilete kvar time, medan det andre fotograferer kvar sjette time frå nordsida av breen. Hastigheitsmålingane er utført i bilete frå juni til august 2007, mai til oktober 2009 og april til august 2010.

Posisjonsforskjellen mellom to matcha biletepar viser forflytning av breen i biletekoordinatar. Transformasjon til terrengkoordinatar blir gjort ved hjelp av ein høgdemodell og kjende kameraparametre. Hovudvekta av arbeidet viser seg å vere i forarbeidet, sidan bileta har ulik referanseramme på grunn av kamerabevegelse i løpet av opptaksperioden.

Den attverande forskjellen etter eventuell transformasjon til same referanseramme utgjer den største andelen av usikkerheit i resultata. Ingen kamarakalibrering, ikkje tilfredsstillande transformasjon, biletekvalitet, matching av bileta, georeferering, høgdemodell og bileteoppløysing gir ei total nøyaktigheit på 1,5 piksel i bilete teke frå kamera 1. På eit punkt 2500 m unna, utgjer dette 0,84 m feil i eit matcha biletepar. Dette gir ei nøyaktigheit på 0,32 m/dag dersom det er 4 dagar mellom bileta.

Ved å måle hastigheita frå bilete med 2, 4 og 8 dagar mellom, gir fire dagar det beste resultatet. Færre dagar mellom bileta gir dårlegare nøyaktigheit for dagleg hastigheit, men betre tidsmessig oppløysing.

Resultata er presentert som grafar med variasjon i hastigheit over tid. Desse er samanlikna med temperatur og nedbør i same tidsrom. Romleg variasjon er presentert som hastigheit på tvers og langs bevegelsesretninga på breen.

Samanlikning med tidlegare tverrprofilar i same område, GPS-målingar frå same tid, men lengre opp på breen, og hastigheit frå satellittbilete med dårlegare romleg oppløysing, viser samsvar med våre målingar frå terrestrisk fotogrammetri.

Contents

1 Introduction

1.1 Glacier dynamics and calving

Glaciers are made of fallen snow which have transformed into ice. That happens when snow lies long enough at the same place to be compressed. The weight of the additional snow, and the freezing of the melting water, let the density increase. When the density reaches 0.8 kg/l, the snow is air tight, and then called glacier ice.

Accumulation happens when it snows more on the top of the glacier than melts of, and is necessary for the existence of the glacier. The gravity helps the surplus of the mountain glacier down to the lower part of the glacier, the valley glacier, where ablation appears by melting. (Haslene, 2008) If the ablation zone of the glacier continues to the sea, is it a tidewater glacier, which also loose ice through calving. (Fig. 1-1)

Figure 1-1: Kronebreen calving front. Photo: Anne Chapuis

Glaciers stores and release large volumes of water which can cause motion, like a slowly moving river, by cooperation with gravity forces. The friction and cohesive forces in the ground retain the glacier from sliding. Velocity is a sum of these forces. The sliding velocity is very different between the glaciers, and depends for instance of climate, area and seasons. Because of the pressure in the lower layers, the glacier gets plastic attributes, and can be stretched in and out together with the changing landscape, which cause crevasses in the glacier. Because of friction, the upper layer moves faster than the lower.

Spatial variations are directly and indirectly decided by the landscape: More slope let the glacier move faster, and the margins decrease the velocity because of friction and ice thickness. Ticker ice increases the weight, and following gravity forces that makes the velocity. (Fountain & Walder, 1998; Haslene, 2008; Melvold, 1992)

Surface velocity of a glacier depends of seasonal and short-time variations. The distribution of surface water inputs to the sub glacier draining system and seasonal development of sub glacial channels influence the velocity of the glacier. Both the volume and the pressure of the water can decide the rate of glacier sliding. The seasonal variations are a result of penetration of surface water through the glacier ice. Typically time of melt season on Svalbard is between the beginning of June and August. The short-term high-velocity events arise from high and rapidly increase of water inputs, water pressure and water storage to the sub glacier drainage system.

Figure 1-2 displays the glacier dynamics. Melt water slides to the margins or makes ponds on the glacier surface. This surface water drains into moulins or flow into crevasses and englacial channels linked to the crevasses. The melt water continues using these moulins, channels and crevasses to reach the glacier bed during the melting period. The glacier slides on this slippery glacier bed towards the terminus, and out through drainage portals which earlier were frozen and trapped the melt water. A result of the first water release through the frozen terminus is increasing velocity, but later the water follows this new draining portals and makes a more rapidly transmission towards the glacier front. The Short time events arising early in the season, follow the established draining system from surface to glacier bed, and then to the outlet at the glacier front. The sub glacier water pressure and channels close by freezing ponds after cold periods. Resuming of surface melting after a cold period makes new events in the middle of the season. Large amount of precipitation on the surface is the predominant reason for rapidly rising water input to the draining system, but large increase of temperature can increase the effect, and even make the same result itself. (Copland et al., 2003; Fountain & Walder, 1998)

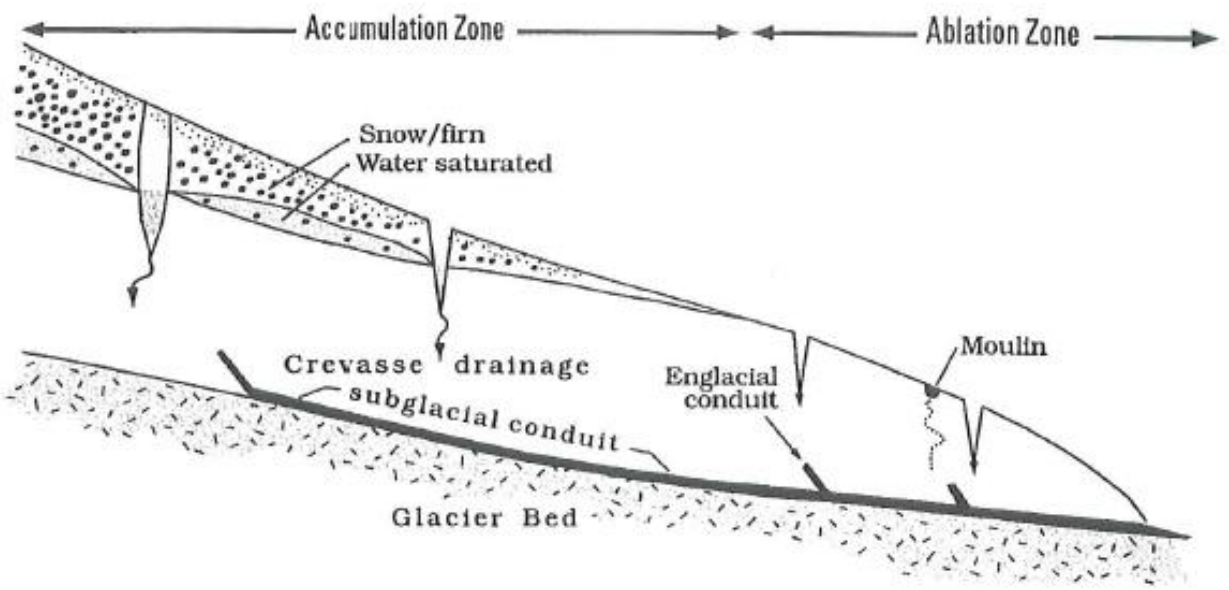

Figure 1-2: Hydrological components of the glacier dynamic. (Fountain & Walder, 1998)

Calving and melting are the two main reasons for ice loss from a tidewater glacier. A calving event appears when big pieces of ice, icebergs, break off the terminus of the glacier and fall into the sea. This happen because the crevasses behind the ice bergs, the motion of the glacier and the temperature of the water are too much to hold the glacier together. The whole sequences of calving consist of a lot of reasons with complex and partly unknown explanation.

Anne Chapuis is writing her doctoral dissertation about calving. She is studying calving with help of i.a. seismic and image observations. Her data is calibrated with observations in the field, and she also co-operate with measurement from ground-based radar. (Chapuis et al., 2010; Rolstad & Norland, 2009) A part of the calving study is to find the calving rate by equation (1-1).

$$U_C = U_{T-} \frac{dL}{dt} \tag{1-1}$$

U_C is the calving rate, U_T is the velocity and $\frac{dL}{dt}$ is the change in front position (Negative when retreat). – All in m/day. Calving rate is the speed of the calving, telling how much of the surface ice is lost by calving of ice bergs. (Benn et al., 2007; Ritchie et al., 2008)

According to equation (1-1), calving rate can be calculated if the velocity and the front position are known. The position of the calving front is modeled by stereo photogrammetry with terrestrial images from two different camera positions, and the velocity is found by this thesis.

The front position, calving rate and velocity are all time dependent. The calving events appear during the summer because of positive temperature, and make the front position retreat. The opposite happens within the winter, when negative temperature freezes the iceberg and the rest of the glacier together. The glacier retreats if the growing during the winter is less than the retreat during the summer. Kronebreen has retreated since 1948. (Melvold, 1992)

1.2 Problem description

The velocity close to the glacier front is interesting and necessary when finding the calving rate. Field work in this area will be very dangerous because of the vicinity to terminus and sea, fast unstable motion and big crevasses. A good and safe idea is to measure the velocity in images instead of physical measure the glacier itself. Traditionally, high resolution satellite images are used for this application. Satellite orbit decreases the possible terminal resolution, together with geometrical restriction on the spatial resolution.

Terrestrial photogrammetry will hopefully increase the spatial resolution compared to satellite images by coming closer to the object. The temporal resolution can increase by high frequency image recording from the same position.

- How good is the spatial resolution of the velocity measurements from our terrestrial images?
- Which temporal resolution can be used and contemporary give results with good accuracy?

Two different types of photogrammetric computer programs can be used together to obtain information (Velocity) out of the data (Images). They include matching of images and transformation to terrain coordinates. This is most likely the first time these two programs are used together for measuring velocity from terrestrial images.

- Can, and how can, these two photogrammetry computer programs be used to extract velocity from the terrestrial images?

There are a lot of steps in this method which can influence the accuracy of the results. An intention of this thesis is to find the different causes of uncertainness, and try to make as good accuracy as possible in all the steps.

- What cause the uncertainty of the results?
- How can the size of the uncertainty be calculated?
- What can be done to avoid the sources of uncertainty?
- How can already existing inaccurate results be better?

A sample of the results needs to be presented in a good way which makes them possible to be used as a measure of glacier velocity when calculating the calving rate in Anne Chapuis' doctoral dissertation.

- What information can be extracted from the velocity measurements?
- How can the information from the measurements be presented in an applicable way?

Hopefully this method will be a good improvement of measuring velocity from satellite images, both in temporal and spatial resolution, money and time. The aim of this thesis is to find out:

- Is terrestrial photogrammetry a good alternative to satellite images when measuring the velocity on the glacier front?
- What is the advantage of measuring velocity by terrestrial photogrammetry?

1.3 Work flow

There are many separate steps including in the method of getting the velocity from the images. Each of the steps is explained in the order they are used. The explanation includes the different techniques, the computer program, which requirement is necessary and the reason for doing the step. (Chapter 2) The steps give different challenges and cause different kinds of errors. The challenges are explained in the same chapters where they natural fell in. The source of errors are deeper explained together with the accuracy of the results. (Chapter 4)

The velocity of the glacier front is the result of the measurements, and the reason of finding a good method for extracting velocity from terrestrial images. Chapter 3 includes the graphs showing temporal and spatial variations of the velocity.

The method, source of errors and uncertainty are the main work of this thesis. An additional to the results will therefore include the accuracy of the results. (Chapter 4) This chapter is extended with test work, comparison and explanation about the sources of uncertainty.

The accuracy of the measurements is the most interesting part of the method and is already discussed in chapter 4 about accuracy of the results. The discussion in chapter 5 makes comments to the result of the velocity measurements, which are the graphs in chapter 3. A short look about glacier motion in chapter 1.1 makes it possible to compare the velocity with the climate data from the Norwegian Meteorological Institute. Earlier terrestrial photogrammetry measurement, GPS measurement on the same glacier and velocity from satellite images are also workable comparisons. A statement of the four days temporal resolution is also included in the discussion. Chapter 6 recommends some improvement which makes the results of the method better.

2 Methods

The different steps within the method of finding glacier velocity from terrestrial images are displayed in figure 2-1: Time-lapse cameras record images regularly during the whole summer. The difference between two images from the same camera position and at different moments shows the glacier displacement in the same time interval. The matching program, Cias (Kääb, 2008), finds the displacement in pixel coordinates. The computer program Geophotoref (Corripio, 2006) makes it possible to transform the displacement in the result file from Cias into terrain coordinates. Transformation of images into same reference frame before matching is the most time-consuming part of the work.

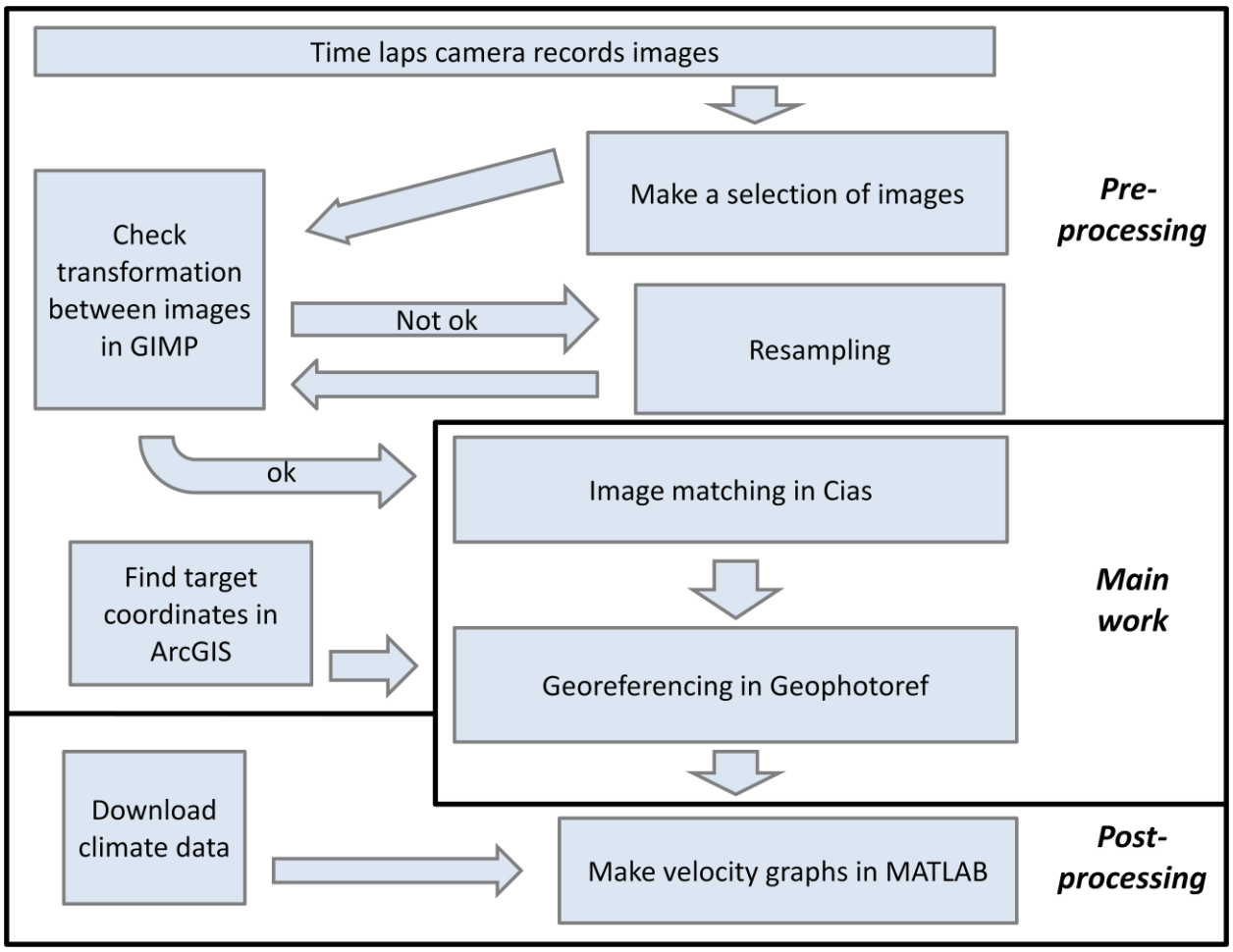

Figure 2-1: The steps included in the method of measuring velocity from terrestrial images.

2.1 Area

Kronebreen (Fig. 2-3) is the area of measureing. Kronebreen is a tidewater glacier calving into Kongsfjorden, 14 km southeast of Ny-Ålesund on Svalbard. (Fig. 2-2-b) The three mountain glaciers Isachsenfonna, Holtedahlfonna and Infantfonna are the accumulation area of the glacier tongue. Kronebreen lies south of Colletthøgda and Kongsbreen, and north of Kongsvegen and Grensefjellet. (Fig. 2-2a) (Chapuis et al., 2010; Lefauconnier et al., 1994)

Figure 2-2: a) Map of Kronebreen, Kongsfjorden and Ny-Ålesund. b) Map of Svalbard and Ny-Ålesund

Kronebreen is an active tidewater glacier. A draining area of 1375 km^2/year makes Kronebreen to the second largest on Svalbard. (Rolstad & Norland, 2009) The front of Kronebreen is 3.5 km long. The high of the front varies a lot during the year, and has been measured from 5 to 60 meters with stereo photogrammetry. (Chapuis et al., 2010)

Kronebreen is a very interesting study object because of the high activity. The proximity of Ny-Ålesund makes the glacier easy to reach for field work, together with similar climate data as the yearly continually Zeppelin research station. (Norwegian Meteorological Institute, 2010)

Figure 2-3: Kronebreen, 31st of August 2009 00:10 a.m.

2.2 Time-lapse cameras

Pictures are the main data in this project. Two time-lapse cameras are recording images of the glacier and glacier terminus during the summer session. The cameras are standing on each side of the glacier. Camera 1 is placed on Grensefjellet, south of Kronebreen, west of Grensebreen and east of Botnfjordbreen. Camera 2 stands on Colletthøgda, north of Kronebreen. (Fig. 2-4)

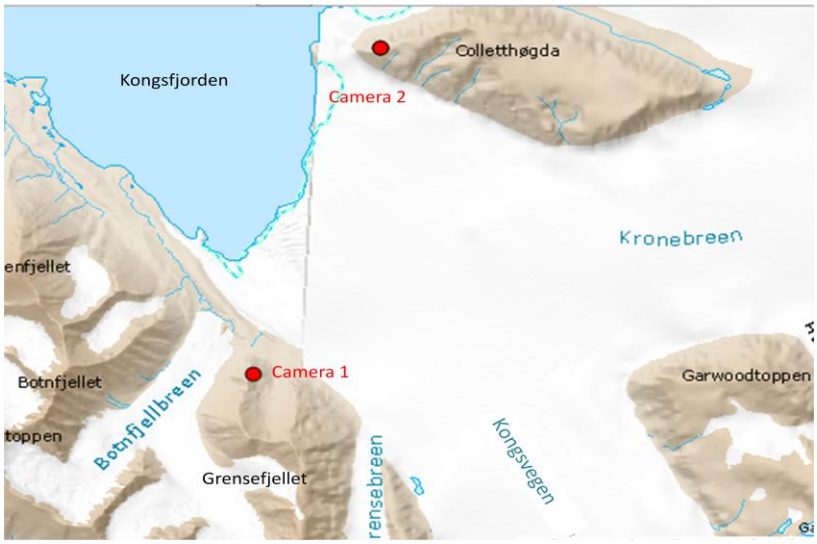

Figure 2-4: Position of the two cameras. (Norwegian Polar Institute, 2010)

The battery is charging with help of a solar panel. Because of the different light distribution on Svalbard during the year, the camera stops working in November and needs charged battery to start recording again in the spring. If the image shall be useful, it needs to be light enough for the glacier to be visible from the camera position. Time of measuring periods is displayed in table 2-1.

One of the cameras records images every hour, and the other one 4 times during the day. One image is chosen from each day, except from some days with too bad weather to make useful images for measuring. 2 p.m. is chosen as a good time regarding to light, shadow and percent of usable image. Images with different point in time are chosen some days, because of better weather conditions, mainly in proportion to fog and bad visibility. Basically is the time difference up to 3 hours (6 hours in 2007), but as showed in table 2-1, has it been necessary with some hours more in exception cases. Each period include one image more than number of days with velocity measurements. It is the image the day before first day of measurement. The velocity is measured as the displacement the 24 hours before the date itself.

Table 2-1: Dates of measuring velocity.

Period	Measuring period	Time	Days without images
2007	14th of June - 13th of August	2:00 p.m. ± 6 hours	2 of 61
Summer 2009	13th of May – 16th of August	2:02 p.m. ± 8 hours	12 of 97
Autumn 2009	17th of August – 29th of October	2:16 p.m. ± 7 hours	6 of 75
2010	17th of April – 10th of August	2:28 p.m. ± 5 hours	4 of 117

Camera 1 (Fig. 2-5) was brought to its position by Anne Chapuis in May 2009. We have access to all the images which is taken in 2009 and 2010, but the use is restricted to the working period of the solar panel. 24 images have been taken every day from the 11th of May to the 30st of November 2009. The pictures from 2009 are shared into two periods of measurement because of changing memory card at field work in August. The last month's images are not used because of less light for measuring. Camera 1 started working again 16th of April 2010. The memory card was changed on the field work, the 10th of August, and is the date of the last used images. All the newer images are still in the camera. (15th of December 2010)

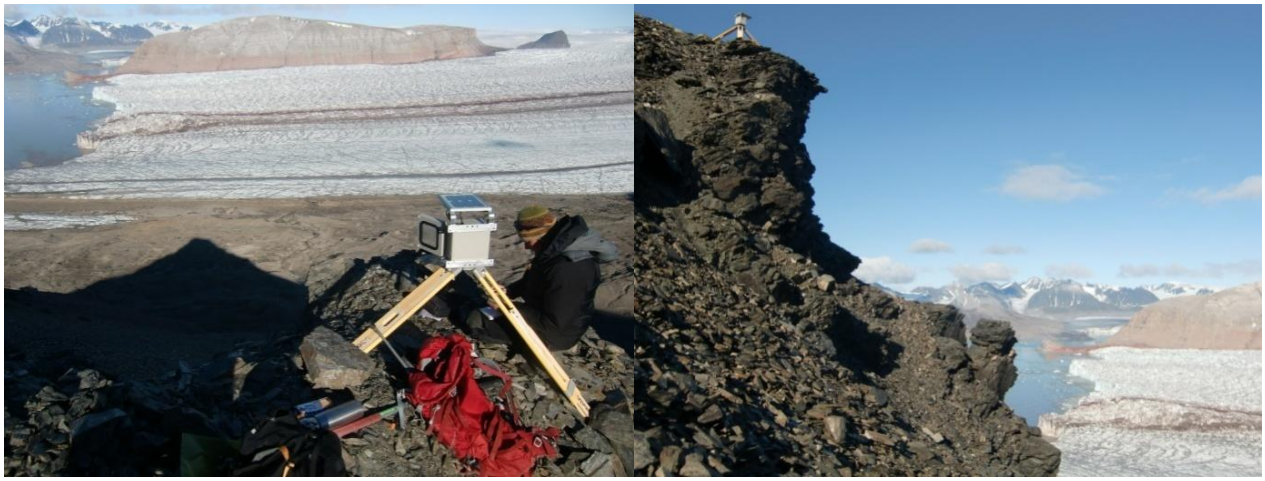

Figure 2-5: Camera 1. Photo: Mari Svanem

Images from 2 months in 2007 are received from Monica Sund in additional. Camera 2 (Fig. 2-6) is standing on the northwest side of the glacier. This camera gives better spatial resolution to the images because of longer focal length and shorter distance to the measured points on the glacier. The camera records images every sixth hour. Monica Sund is working with extracting velocity from these images. Supplementary information about the two cameras can be found in table 2-2.

Figure 2-6: Camera 2. Photo: Monica Sund

Table 2-2: Supplementary information about the two cameras used for measuring.

		Camera 1	Camera 2
Position		[445884, 8754603, 340]	[447609, 8759605, 375]
Owner		Anne Chapuis	Monica Sund
Camera type		Pentax K200D	Nikon D200
Sensor type		CCD	CCD
Image size, pixels	**Height**	2592	2592
	Width	3872	3872
	Size	$10.2 * 10^6$	$10.2 * 10^6$
Sensor format size, mm	**Height**	15.7000	16.1341 (Calibrated)
	Width	23.5000	24.0670 (Calibrated)
Resolution		6.07 µm (1648 dpcm)	6.07 µm (1648 dpcm)
Focal length, mm		18.0000	27.8928
Frequency		1 image/hour	1 image/6 hours
Viewshed		Fig. 2-7a	Fig. 2-7b

Figure 2-7: a) Image recorded by camera 1. b) Image recorded by camera 2.

The spatial resolution inside the same image varies, dependent of the position of the object in the image according to the terrain. Camera 1 (Fig. 2-7a) has the best resolution in the south, nearest Kongsvegen, and less close to Colletthøgda in north. Camera 2 (Fig. 2-7b) has best spatial resolution close to Colletthøgda and less in the south.

2.3 Photogrammetry

2.3.1 Basic theory

Photogrammetry is the science of using images for measurement. Instead of measuring size of an object, the photographed object is measured in the image. By knowing the scale of the image, easy formulas (Eq. 2-2) can transform the measurements from image scale to terrain scale. In this case displacement of a glacier is the measured object in the image. The real displacement in terrain coordinates is found with help of known camera parameters. A terrain model which covers the area of the image view is used to get the displacement of the terrain coordinates in all wanted points in just one operation.

Photogrammetry is a growing science. Except from land surveying, is it used in biotechnology, building and earth observing.

Digital images are the raw data of measuring. Each image is an array of many pixels. The sensor size of one pixel is calculated from image sensor size and numbers of pixels. (Eq. 2-1) The ground pixel size (spatial resolution) is computed from the distance. (Eq. 2-2)

$$\frac{Sensor\ size\ in\ m}{Image\ size\ in\ pixels} = size\ of\ 1\ pixel\ in\ m \quad \frac{0.0235\ m}{3872\ pixels} = 6\ \mu m/pixel \tag{2-1}$$

The accuracy of the pictured object depends of the spatial resolution. If the image consists of many small pixels instead of few large ones, more of the object details can be extracted from the image. That makes it possible to measure these details.

The spatial resolution varies in the image, dependent of the distance between camera and wanted area. (Fig. 2-8a)

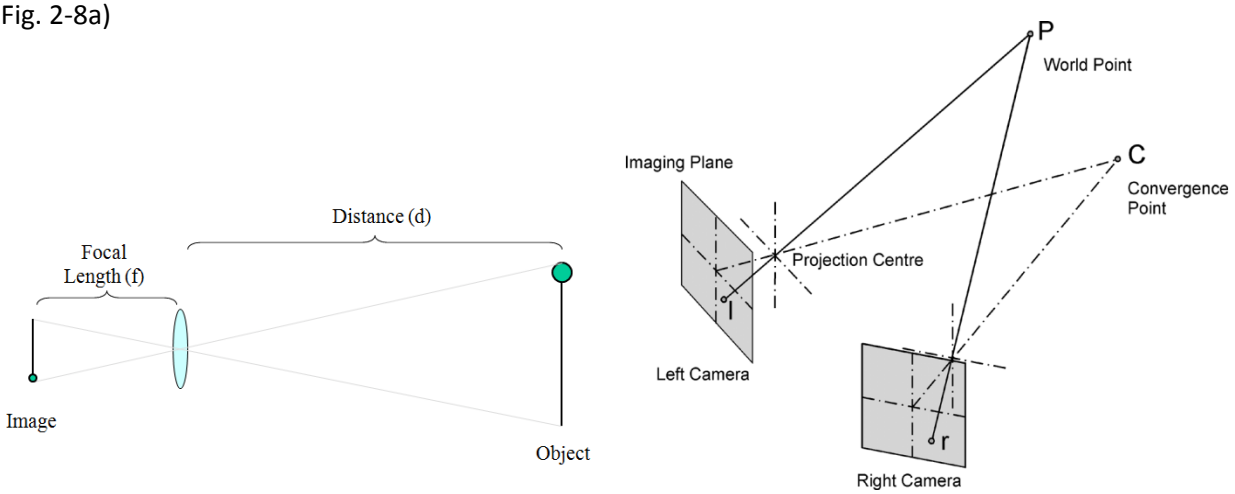

Figure 2-8: a) Object in scale of image sensor. b) Intersection of lines gives position by Stereo photogrammetry.

$$\frac{Size\ in\ image}{Focal\ length} = \frac{Size\ of object}{Distance} \tag{2-2}$$

The temporal resolution tells how detailed the measurements are in time. More measurements during a period give larger frequency and following better temporal resolution.

The position of an object can be decided by stereo photogrammetry: Measuring the image position of the same object in images recorded from two different positions with known coordinates at the same time. The intersection between the two photographed lines gives the position of the object. (Fig. 2-8b)

Stereo photogrammetry is also used to find the displacement of matched points. Then the object is moving according to a camera at same position. Still the intersection of the two lines between camera and point are used to find the displacement from the position.

An elevation model and mono photogrammetry can also be used together to find the position of the points. Ground control points and camera parameters connect the images to the terrain. (Andersen, 2003; Apogee Imaging Systems, 2010; Dick, 2003; Jacobsen & Mostafa, 2001)

2.3.2 Image matching

Image matching is to find the same object, point or pattern in different images. Manually matching is to find the image position of the same terrain points in two different images by looking in visually search in the images. In automatically matching, the program finds the different image positions of the points in the two different images that have the same terrain coordinates in real. The most possible position is selected as the correct match. In this thesis the computer program Cias (Kääb, 2008)is used to find correct match automatically.

Different matching methods are used to find the correct match. Object based/feature based matching extract an object, and try to find it in the other image. Useful objects can be found by edge detection or interest operator. Area based matching is usually used after object based matching. Cias jump over the object based matching and starts straight with the area based matching. The computer program uses the position of the point in one image as a basis for searching in the other one.

Area based matching use the gray levels to decide which area are the same in the two different images. The most common area is found by comparing the gray level distribution in a template of chosen size. (Fig. 2-9) This area can for example be decided as the area which gives highest correlation coefficient. A template is a small sub-image, usually fixed positioned in one of the images. The same area should then be found in the other image, inside a chosen search area. The search area is decided by fixed size around a position decided by one of the methods mentioned above. After trying all the different positions of the template inside the search area, the best position is chosen. It could be decided by least square matching or highest correlation coefficient. The size of the template decides how unique the match will be. The size of the search area decides the distance from the chosen start position. (Schenk, 1999)

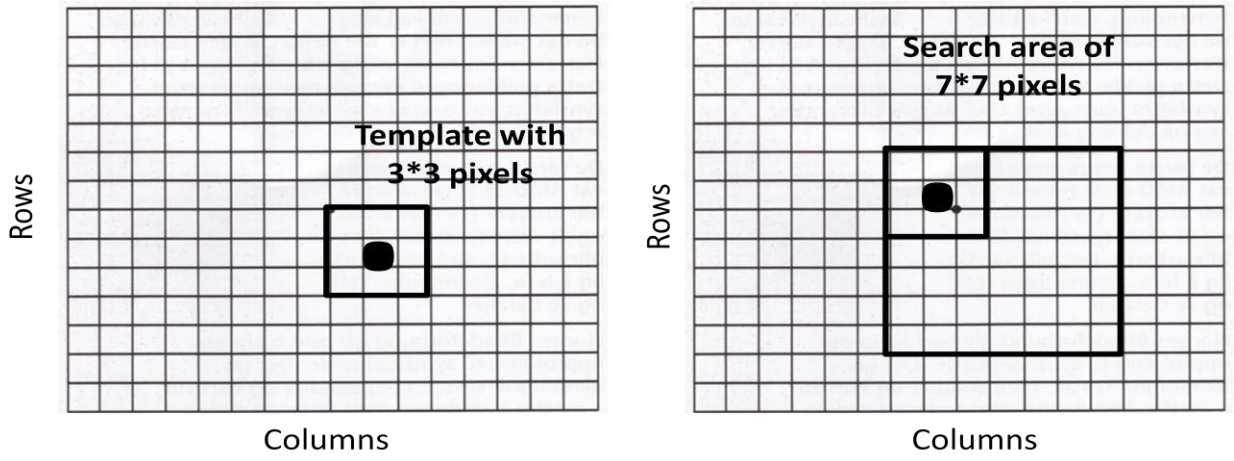

Figure 2-9: Template and search area.

2.4 Resampling

The wanted situation is to measure directly in the raw images. Since they are taken from the same position, the only difference between the images should be the position of the moving glacier. But all the images are not in the same reference frame. Other objects than the glacier show up to have different image position in the different images. Colletthøgda in the image background, for example, does not change terrain position according to the camera during the time of measuring. But this mountain get different image coordinates in some of the images taken in different time. Following, the photographed mountain is moving relative to the camera view. Since the mountain is not moving in real, the camera view is changing during time.

The largest difference in reference frame appears between the images from 2009, which was the first summer for camera 1. The camera moves mostly and continuous in May, and also a bit in September. Images from 2010 are almost in the same reference frame. Images from 2007 are recording with camera 2. These images looks to change a bit, but this is difficult to say, especially give a number of it, since we have no trustworthy and evident conjugate points to compare in the view of the images.

I visited the camera when we changed the memory card in August this year. It is a lot of wind where the camera is standing, but still it is standing very steady. To make motion of the tripod, big achievement is necessary. Grensefjellet, the mountain under the camera is just stone frozen together and the whole area is in conditionally motion because of the perm frost. That is why it probability could be the mountain under the camera that moves. This explanation fits with the dates of main motion, since this is in the periods with changing temperature, melting and freezing. But the difference between images from 2009 and 2010 shows that the tripod needed some time (a summer season) to be stable too.

The camera coverage (the camera view) changes remarkable every time the memory card is changed. The problem is solved by splitting the images from the different periods into several series of measurements. (Table 2-1) Different image positions are measured in the different reference frames. The points are given the same numbers, but the image coordinates are changed so it looks to be in the same terrain positions in all the images.

Figure 2-10: a) Rotation on image. b) Translation of image

An affine transformation rotates (Fig. 2-10a), translates (Fig. 2-10b) and scales the image. (Eq. 2-3 & 2-4) It is easier to find the different transformation parameters separately, and multiply the three different matrixes before they are used to transform the image.

$$\overrightarrow{X'} = \vec{R} * \vec{T} * \vec{S} * \vec{X} \tag{2-3}$$

$$\begin{bmatrix} x' \\ y' \\ 1 \end{bmatrix} = \begin{bmatrix} cos\theta & -sin\theta & 0 \\ sin\theta & cos\theta & 0 \\ 0 & 0 & 1 \end{bmatrix} * \begin{bmatrix} 1 & 0 & t_x \\ 0 & 1 & t_y \\ 0 & 0 & 1 \end{bmatrix} * \begin{bmatrix} s_x & 0 & 0 \\ 0 & s_y & 0 \\ 0 & 0 & 1 \end{bmatrix} * \begin{bmatrix} x \\ y \\ 1 \end{bmatrix} \tag{2-4}$$

The rotation angle needs to be found before the translation parameters if the different matrixes are found manually step by step. Rotated images will cause different offset between each other, but the relative angles (and therefore the rotation) will be the same between translated and not translated images.

The camera motion is too small compared to the distance between the measured points and camera to change the scale of the images. Therefore, no scale included in the transformation of the images.

2.4.1 Requirement for the reference image

One image is chosen to decide the reference system. All the images which are not already in the same reference system need to be transformed into it. Automatically matching in MATLAB (The MathWorks, 2005) is used to decide the transformation matrix. (Eq. 2-4)

A reference area is chosen to compare the two images, and decide the difference between them. The area needs to be quiet, not moving and homogenous. Colletthøgda is chosen since it is standing at the same terrain position relative to the camera all the time. (Change in the terrain coordinates of Colletthøgda will not be observed in the image view because of the small scale in this background position of the image.) The transformation is decided by giving the same points on Colletthøgda same image position in all the images.

The reference image ought to be clear and having sharp contrast. That makes it easier to pick out image coordinates for the same objects in the different images. That is important in both manually and automatically matches for deciding transformation matrix.

The image clearness itself is not enough. The different amount of snow during the recorded period together with changing in light, shadow and weather, makes the image different and following different gray scale distribution in the images. This is one of the main problems in automatically matching to decide the transformation matrix. One solution is to use an already transformed image as a reference image for the rest of the images.

2.4.2 Rotation

As mentioned (Ch. 2.4) the camera has been moving during the period the images were taken. Basically the camera is moving downwards, but not necessarily coincides at the whole level. The camera makes a sharper pitch, which results in lower image y coordinate, if the whole camera front is moving down at

the same time. In opposite, a rotation in image level appears if one side sinks more than the other side of the camera. (Known as roll in air photos) Rotation appears in our images, and makes a change from the first to the last image in one period, but is not a large problem between consecutive images. The placing of the tripod makes the rotation small because one foot is standing in the front, and two feet behind the view direction. Because the mountain and camera mainly sink in the front, only one foot is retreated, and following both sides sink in same amount, which cause no rotation.

The unknown rotation is found by comparing the consecutive images and find the position relation in degrees between chosen points in the image. The free computer program, GIMP (Kimball & Mattis, 2010) is a good remedy to find the possible rotation. The image coordinates of wanted object is found by zooming 800%, which is as much as possible in the program. It is very important to choose an object which is clear and easy to see in the plurality of the images. The points ought to be visually unchanged during the season, which makes points beside snow and water unsuited. Obvious it cannot be a point in motion, like the glacier. It is more openly to see if there is a rotation or not if the chosen points are in total different part/side of the image. The rotation angle according to the reference image will be the same anyway.

The images are singly opened in GIMP, where the image coordinates of at least two chosen evident points are written down. The rotation angle is the difference between α (Eq. 2-5) in the reference image and the other images. $\frac{dy}{dx}$ is the difference in image coordinates between the two chosen points. The images are rotated in for example GIMP or MATLAB according to the rotation angle, α.

$$\alpha = atan\left(\frac{dy}{dx}\right) \tag{2-5}$$

The method above is a totally manually way to find the rotation angle and rotate the image. The rotation need to be found automatically to be useful in the following method I will present. Implementing of deciding the rotation angle in a total transformation in MATLAB will be most overall.

The rotation angle can be found by matching the images in the frequency domain reached by fast Fourier transformation (FFT). MATLAB has a lot of implemented formulas to follow the suggestions from MATLAB's own web sides and papers. This method was tried with both the originally colored images and gray scaled images, but it did not come out with the wanted results. (Tested with manually deciding in GIMP and false rotated images, degrees and radians, large and small angles) The rotation angle came out like integers, but the largest rotation angle is 0.23 degrees. (Between the first image in May and the last one in August) After working too long with programming to find rotation angle, the manually method described above seemed to be the only and better way.

The results from this method do not give satisfactory results in accuracy. It is too easy to choose the pixel beside the correct one because of unclearness in the images. The standard derivation is then two pixels, which cause uncertainty in same order as the rotation will rectify. (More in ch. 4)

The rotation angle according to the reference image is found manually in GIMP (Appendix B), but not used for rotating the images. It only includes rotation of the images from summer 2009, since they were

the test of the manually method which did not work out to decide the rotation. A sample of the images from 2010 was checked in GIMP, with the following conclusion: Neglecting rotation. The images from 2007 have no points which are evident enough to be trustful when comparing the images. None of the images are rotated to each other. The rotation step is skipped by jumping directly to translation.

2.4.3 Translation

With translation the images are moved in x and y direction, to be placed in the same reference frame. As described earlier (Ch. 2.4.2), the main motion results in a shift in y direction, as a result of the down moving camera. Images recorded after the reference image will have a positive shift in y. The translation will then give the image a smaller y value to lift the image, since the image coordinate is (1, 1) in upper left corner. The opposite will happen with the images taken before the reference image.

A shift in x direction can appear by motion caused by wind, which is rotation through the zenith angle of the camera (A difference in the heading direction of the view) in reality. A shift in x value is the easiest way to treat the eventually rotation around the zenith axis. Down going motion of the mountain in one direction (left or right) will also cause shift in x because no rotation included in the transformation. The images from summer 2009 show a small difference in x direction. (Appendix B) It seems to be motion against the left (North west). Probably it could be caused by wind always coming from east (right) this part of the year. Another reason could be counter clock rotation caused by ground motion.

The offset (Shift in both directions) can also be found or checked in GIMP. The easy equation (2-6) gives the offset with help of just one point in each image. Because of quality assurance is four points used to decide the offset, but some of them are more trusted than other. The method is mainly used for checking the automatically method. Because of trouble with automatically matching, the equation decides the offsets between the autumn images from 2009.

$$Offset, in\ direction\ 1 = \ Difference\ in\ image\ position\ 1\ of\ same\ point \qquad (2\text{-}6)$$

Deciding of offset by matching in MATLAB is a more effective and accurate way. A predefined area with same properties as conjugate points (Ch. 2.4.1) is chosen as search area in the reference image. The template is chosen as a smaller area inside the trimmed print. Resultantly the square around Colletthøgda becomes the search area in the clear and contrasted reference image. The image coordinates of the square are found in GIMP. The chosen area is matched with the reference image according to the explanation in chapter 2.3.2.

A MATLAB script decides the offset in x and y direction between the two images with matching. The offset is used to transform the image into the reference image by equation (2-7). The main script does this operation as a loop with all the jpg files in the selected folder (Appendix C)

$$\begin{bmatrix} x' \\ y' \end{bmatrix} = \begin{bmatrix} 1 & 0 & t_x \\ 0 & 1 & t_y \end{bmatrix} * \begin{bmatrix} x \\ y \\ 1 \end{bmatrix} \qquad (2\text{-}7)$$

It is easy to see if the decided offset is totally incorrect compared to small mistakes. The offset shall fit in the series of offsets in continually order. The offset usually works in the same direction. Trouble with matching is usually caused by different light, snow conditions, weather, shadow and sun.

The mountain Colletthøgda is the best reference area found in images recorded with camera 1. Automatically deciding of offset works quite well with the images from summer 2009.The process is done around seven times (with change of reference image to an already transformed image) before all the images pass with translation based on the correct match. Some of them are transformed even more than twice because of incorrect decided offset. An already transformed image with more similar weather and snow amount is chosen as a new reference image in the new lap of processing for the rest. The transformed images are checked in GIMP to be sure the offset is correct.

The automatic method has more problems finding correct offset for the autumn images from 2009. Testing with match in all the different layers, colored and gray scale does not make the result better. Different area and size of the search area does not help either. Checking in GIMP shows remarkable motion just twice during the period. Based on this research, the offset in images recorded summer 2009 is decided by equation (2-6), by using 4 points for comparison. The offset of the foggy images is decided by tightening the gap to let it fit in the series. Following MATLAB is used to translate them with the decided matrix (Eq. 2-7) from GIMP observations.

The images from 2010 are already in the same reference frame according to checking in GIMP. The motion between the images is not remarkable. (Appendix B)

The camera view changes the image position of visual points in the images recorded with camera 2 in 2007. The camera coverage does not include any clear area without snow, which makes it difficult to choose a reference area for comparison. The translation of these images is leaved out too, on the background of better spatial resolution and proportionally small motion.

2.4.5 File format

The matching program, Cias (Kääb, 2008), assumes the image file to be saved as a Geo TIFF (Tagged Image File Format) in gray scale. Geophotoref (Corripio, 2006) also needs the image as TIFF, but colored. The images from camera 1 are saved as jpg (Joint Photographic Experts Group) files. The 2007 images from camera 2 are received as raw files, in NEF (Nikon Electronic format). Both the raw and jpg files need to be transformed into TIFF.

The transformation from jpg to both the different types of TIFF is done in MATLAB, together with the translation. (Appendix B)The same is done also if translation is not necessary. The script read jpg files, and save them in wanted file formats. Changing of file format included in the MATLAB script makes a big advantage by creating fewer steps.

MATLAB are not able to read the file format NEF. A computer program of converting images (ReaSoft, 2010) change the file format NEF to jpg. Continuation with transformation in MATLAB is already described above.

2.5 Image matching gives displacement in pixel coordinates

A terrain point has the same image position in all images within same reference frame. Displacement in the terrain exists if the terrain point gets different image position in different images in same reference frame. The displacement can be shared into 2 dimensions in an image, change in x (column) and y (row) direction between the two images. The change in image position of glacier points show displacement of the glacier in image coordinates.

The image position of photographed objects can be decided visually/manually. Cias (Kääb, 2008) is a program which automatically match chosen image points. The program is made with IDL codes by Andreas Kääb at University of Oslo. It is therefore necessary to have the free software IDL (Stern, 2010) when using Cias.

Cias match chosen image points in two images from different times, and find the displacement of them in image coordinates. The operator decides images, points, size of template and search area, save the result file and wanted images, and does this for all consecutive image pairs.

The combination of image pair for matching needs to be decided before using the computer program. A good system with image name, date and matching number of the series in a notebook beside the computer, is necessary for keeping track of file names and belonging results. The chosen images are a result of wanted intervals, which is 2, 4 and 8 days in this thesis.

The images need to be in gray scale. A TFW file which explains the size and scale of the image are loaded together with the two TIFF world files at different time.

Measuring is done without using the implemented Helmert transformation (Conform transformation), since the images are in same reference frame after eventually transformation. It makes it unnecessary to choose conjugate points for deciding transformation, which also makes the process less time-consuming. In additional it keeps the same image position of the physical objects. An opposite choice, by deciding the transformation in Cias, would not give images in same reference frame during the whole period. (Image in time 1 is transformed into nr. 2, and nr. 3 into untransformed nr. 3, etc.) It will results in velocity measured in different terrain coordinates of the same image coordinates. (Ch. 2.6). We want to measure velocity in the same terrain points during the whole period, and therefore need to transform into same reference frame in advance.

Image coordinates for velocity measurement is imported as predefined points in a txt file. It is the fastest way of matching several points and gives same image position in all the different matches, and is therefore a good alternative to choose polygon or single points, which probably would results in different points from time to time. (It also avoids the program weakness of impossible to choose a point with x coordinate less than 1000) This method gives images and velocity measurement in same reference frame during the whole measuring period. A point with same image position will not be the same physical points, but velocity measurement in the same terrain point.

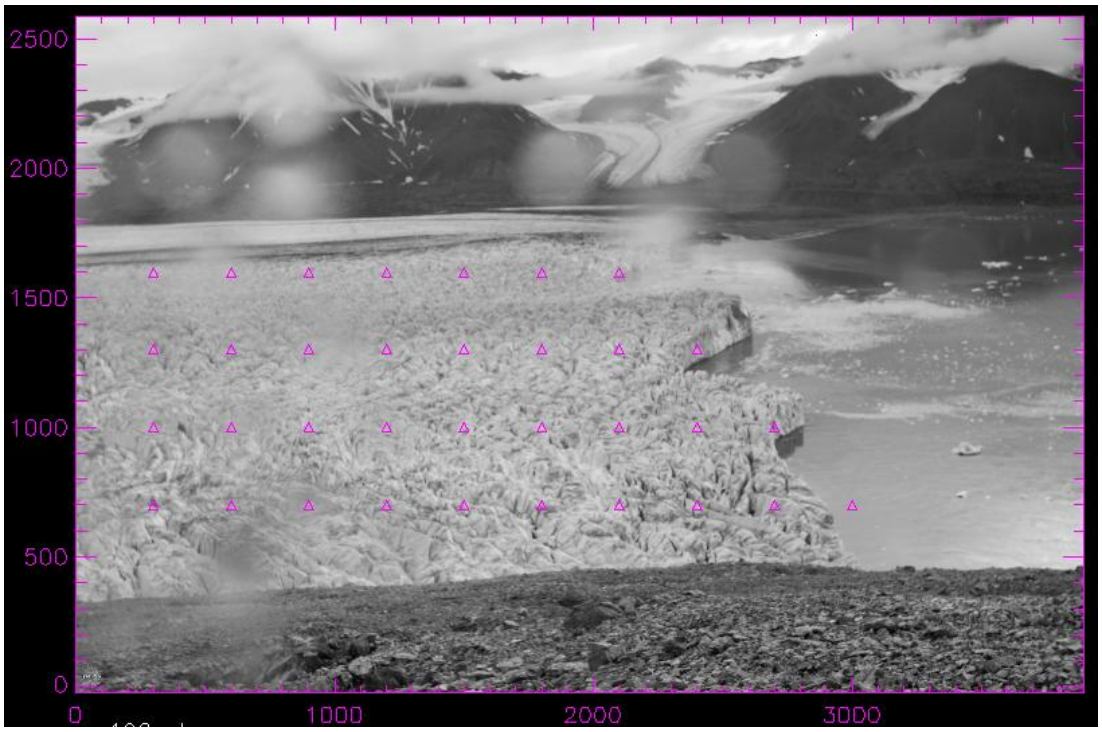

Figure 2-11: Point distribution in images from 2007.

Figure 2-12: Point distribution in images from 2009 and 2010.

The measured points are chosen as four lines along the motion direction of the glacier, from the glacier front to the end of interest area. (Fig. 2-11 & 2-12) The distance between each point and the front of the

glacier changes during the time, since the front position changes through the seasons. The image positions of the points are decided by iteration between txt file and use in Cias. Four different txt files are used together with the four different measuring periods (Table 2-1) because of their different reference frames. Then almost the same terrain points are obtained in measurements during the whole time of image recording. The axis in figure 2-11 and 2-12 (And all following images from Cias) are divided into pixel as in the original terrestrial images.

Area based matching (Ch. 2.3.2) is used to find the chosen points in the image at time 2.The user decides the block size of the template and the size of the search area in pixels. The size is vital for the results because the correlation coefficient and following the correct match depend of this choice. In principle gives a small sized template larger correlation coefficient because of increasing chance of finding similar areas. Larger template increases the chance of correct match because of more unique solution, but the time and data amount grows exponentially. Large pattern change between the images, which could happen if the glacier has moved much between the two images or the shadow has changed, makes trouble finding the correct match. Good spatial resolution and larger objects require a template with more pixels to cover the measuring area, point or object. Larger template requires larger search area. The size of the search area needs to be large enough to space the position displacement of the template.

A template size of 70 pixels and a search area of 100 pixels are used when matching images recorded with camera 1. The search area expands to 120 pixels when measuring in images with 8 days between. A template size of 70 pixels in a search area of 150 pixels is used to find match in the images from camera 2, because of larger spatial resolution and following motion of more pixels. The mentioned template size is very large compared to ordinary image matching. The reason is change in pattern of the measured objects. The object not only moves, but changes the pattern and gray scale distribution around the central point.

The matching is very sensitive to change in weather conditions. Sun amount and direction result in differences in light and shadow together with clouds and fog. All these factors cause in different gray scale and pattern in the different images. Good weather conditions are the most important factor for finding the correct match.

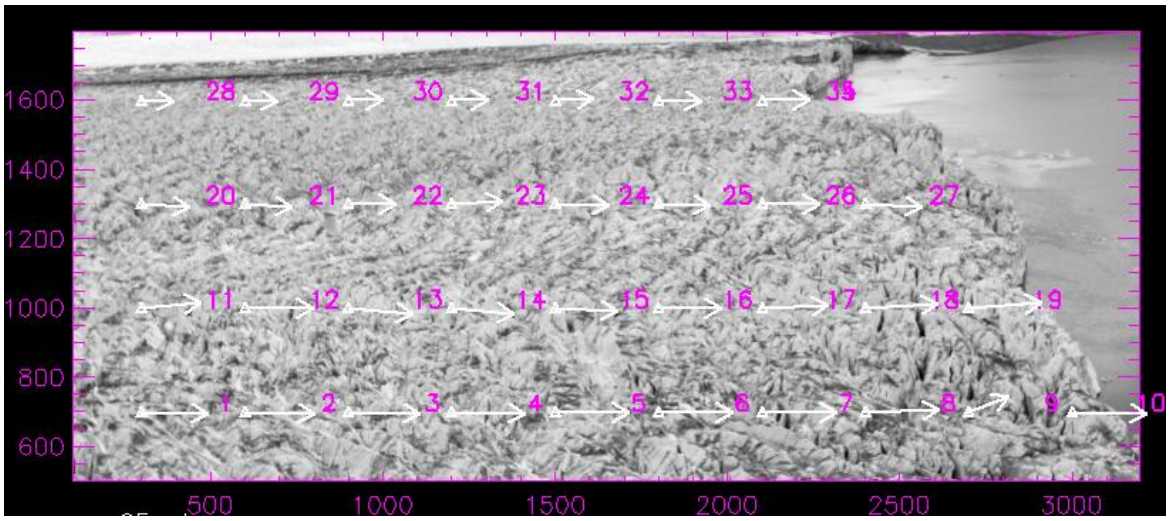

Figure 2-13: Displacement vector in image from 2007.

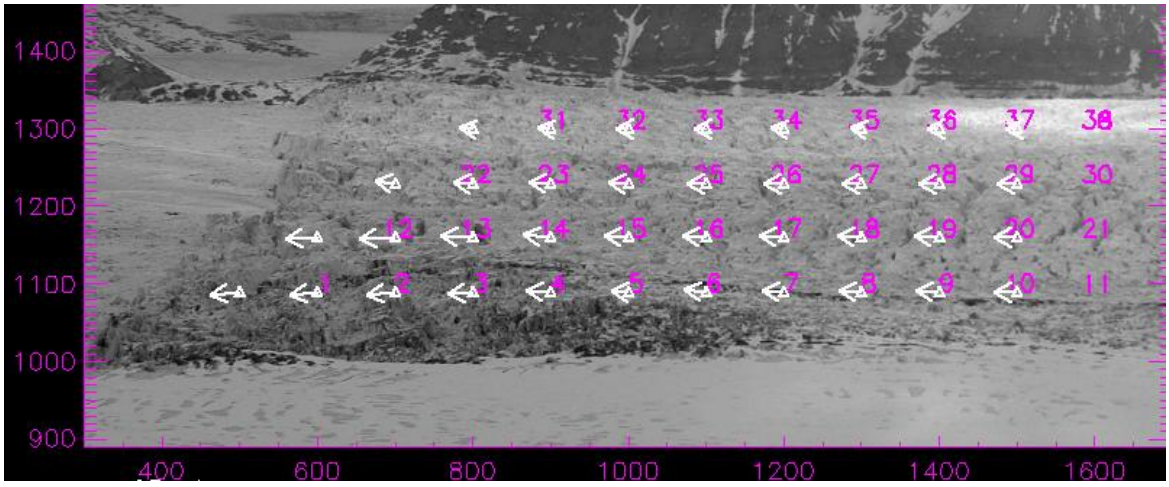

Figure 2-14: Displacement vector in image from 2009 and 2010.

The results are checked by showing image of the displacement vectors for all the points. (Fig. 2-13 & 2-14) The direction and length of the vectors should be close to similar because the glacier moves as a solid body; an outlier is probably an incorrect match of the point. The vectors closest to the view become larger any way because of the different scale in the oblique terrestrial image. If the result images not show vectors according to this, other size of template and/or search area can be tried. If totally different weather, change of image in time would help. The displacement of the points between two matched images is saved as a DAT file (Appendix D), which is the result file of the matching, and contains the image coordinates, displacement in x and y direction, total length, direction and correlation coefficient for each point. The heading needs to be removed before importing in Geophotoref, which is the following step in the totally measuring method. The name of the result file from Cias will also be the name of the result file from Geophotoref. A lot of time will be saved when importing these result files in MATLAB (Ch. 2.6.1) by choosing a smart name. Consecutive number is advisable, because it makes it possible to read in all the txt files in the chosen folder as a loop in MATLAB.

2.6 Georeferencing

The displacement found in Cias is in image coordinates. The computer program Geophotoref (Corripio, 2006), transform the displacement from image coordinates to terrain coordinates in meters. The velocity is then calculated by knowing the time between the matched images.

Geophotoref is a tool for georeferencing oblique images by using a digital elevation model, and need compiled IDL *.sav files to run. The program locates the geographical position of every pixel from the terrestrial image, which is useful when mapping land cover and assessing surface cover change. Ground control points, viewshed and camera parameters connect the image to the elevation model.

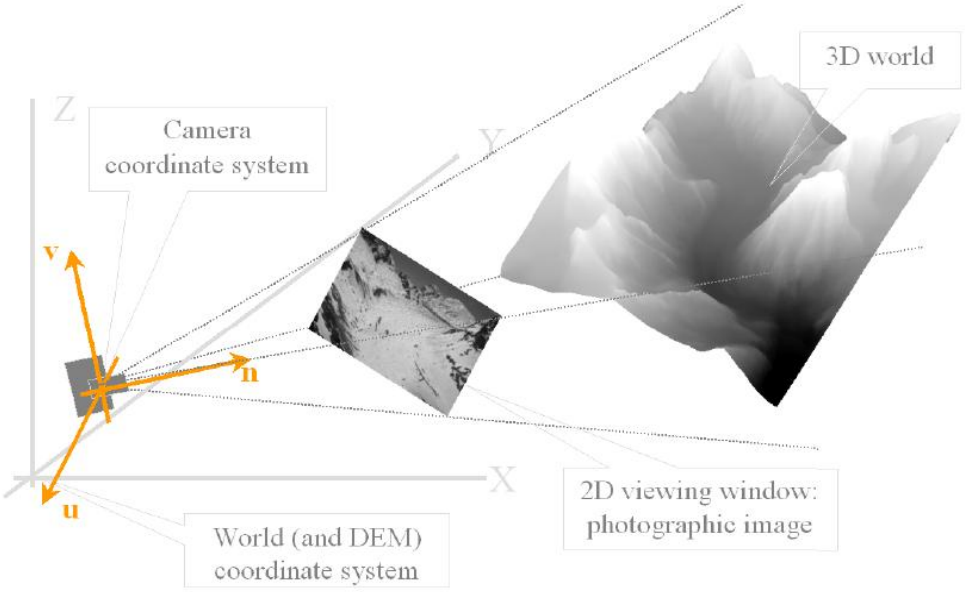

Figure 2-15: Georeferencing process. (Corripio, 2006)

The georeferencing process finds a function between 2-dimensional pixels in the image and 3-dimensional points in the elevation model. The coordinates of the original 3D landscape are transformed to the camera reference system and then projected onto a viewing window corresponding to a flat 2D. (Fig. 2-15) The geometry of the image formation inside the camera is replicated on the DEM by using viewing transformation and perspective projection. The first transformation in the georeferencing process translates every grid cell in the elevation model to refer them to a coordinate system with origin in the camera position. Then a transformation is applied according to the viewing direction and focal length of the camera. This results in a 3-dimensional set of points according to the cells in the DEM as seen from the camera point of view. The result viewing transformation is projected into 2-dimensional space. The 2-dimensional representation of the relief information in DEM is produced as a photograph seen from the camera point of view. Scaling of the camera view according to the image resolution establish the correspondence between pixels in the image, screen coordinates of the perspective projection of the elevation model and their location in terrain. A satisfactory result gives pixels from the image x, y and z values of the corresponding grid cells in the DEM. (Corripio, 2006) The result file from Geophotoref consists of x, y and z values of the measured image points (x, y), displacement of the same

points in x, y and z direction, direction and length of the horizontal displacement vector and correlation coefficient (Appendix E).

The viewshed mask is calculated by ArcGIS (ESRI, 2008). The same program is also used to decide the ground control points from the elevation model and a map of Svalbard. (Norwegian Polar Institute, 2010) All the necessary inputs in Geophotoref are stored in a *.set file, that includes the parameters in table 2-3.

Table 2-3: Input parameters to Geophotoref.

The result files from Cias without a header	The displacement and image coordinates which shall be georeferenced into terrain coordinates.
A colored image (Uncompressed TIFF)	For visualizing on the scream and result image, and to see if the terrain model fits the position of the images.
A digital elevation model of the area, DEM (GeoTiff)	Regular grid cells of points with x, y and z values in meters. A 2D array of elevation values.
GCPs (Ground control points)	To help connecting the image to the terrain model.
Visibility/viewshed	Visible region of DEM from camera point of view.
Camera coordinates	Camera point of view.
Target coordinates	Camera view direction.
Camera parameters: Focal length, size of image and sensor, resolution	Scale the camera view.

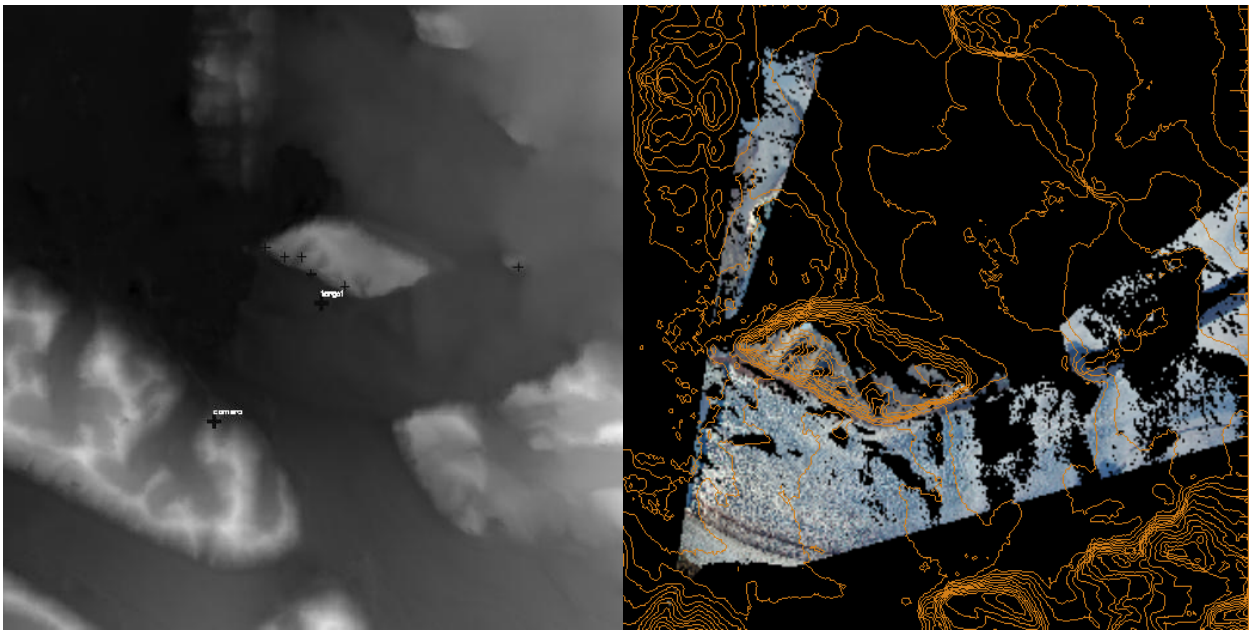

Figure 2-16: a) DEM with position of GCPs, camera and target. b) Camera view on a perspective projection of the DEM.

The whole DEM in camera coordinate system (Fig. 2-16a), the visible part of the DEM on a gray scale representation of the whole DEM, the visible part of the DEM in camera coordinate system, a perspective projection of the visible DEM with a superimposed rectangle indicating the camera view

frame (Fig. 2-16b) and the visible part of the DEM superimposed on the original image are displayed when running Geophotoref (Appendix F).

The work in Geophotoref is that part of the total method that takes shortest time, because the computations are done just once for all the images in same measuring period. The name of the Cias result file is the only change in input between the different matched image pairs. Each series of images requires preliminary work with adjustment of camera parameters to the elevation model. Changing of not exactly known camera parameters, target position and rotation of image is necessary to do once and decently for each reference frame, which is a large advantage of transforming the images into same reference frame before matching in Cias. The target position is in principle unknown. Easy mathematic gives the pixel coordinates of the target, but the challenge is to find the coincident point in terrain coordinates. Maps or DEM in ArcGIS makes it possible to pick out inexact terrain coordinates in the same way as GCPs. The visible part of the DEM superimposed on the original image display how successful the choice of target position, rotation and camera parameters has been together with the elevation model. The best adjustment is found by working literally. (Changing the target with consideration of the direction in x, y and z, forth and back, up and down, many times.)

The result files from Geophotoref consist of the terrain coordinates of all the points, the displacement in north, south and zenith direction, the length and size of the horizontal vector, correlation coefficient and image coordinates. (Appendix E) Some of the points in the result file only get numbers like “Not a number” or “infinite”. A reason could be that these terrain points are not according to the camera view. The points need to be in the real point of view to be measured, but the calculated camera view used in the georeferencing is not exactly correct because of imprecise adjustment between image and elevation model. (Ch. 4.1.5) The difference does not need to be large, but just enough to be covered behind a small hill. The best way to avoid this problem is to measure many points at once, and remove the points without terrain coordinates.

2.6.1 Usage of the velocity measurements

The result files from Geophotoref show how much the glacier has moved from the moment of the first image to the other. The length vector in the files shows the horizontal displacement in meters.

MATLAB is used for all the post-processing work of the measurement, that mainly consequence in different graphs. One of the many MATLAB script used for extracting velocity from the result files is found in appendix G. The displacement vectors included in the result files from Geophotoref are uploaded in MATLAB. Good notes tell the number of days between all the matched images, and make it possible to decide the velocity for each day by division. The everyday velocity is showed as graphs in chapter 3 and 5. The two vector components (dx and dy) need to be summarized separately before finding the summarized displacement over several matched images . (Eq. 2-8)

$$Vector\ length = \sqrt{dx^2 + dy^2} \tag{2-8}$$

3 Results

The velocity of Kronebreen is measured in 30-40 points distributed into four lines along the motion direction of the glacier. (Fig. 2-11 & 2-12) The lines do not necessarily be in straight lines in the terrain although they are in the images. Figure 3-1 displays the position of the matched points into the terrain after georeferencing. The topographical boundary (Norwegian Polar Institute, 2010) in the figure has not the correct position during the whole period of summer 2007 – summer 2010 because of seasonal changes of front position. (Ch. 1.1)

A sample of the matched points in figure 2-11 and 2-12 is used in graphs with velocity on the y-axis. Just a small percentage of the matched points are used in the results, but they are all included in the background study about accuracy (Ch. 4), general trend and comparison (Ch. 5). Measuring in the four different reference frames (Table 2-1 & ch. 2.4) cause in a small difference in terrain coordinates, although the attempt of matching same visually points in all the images. But the difference is small enough to be used as a point with same attributes according to the position. (See comparison between points with different color in fig. 3-1.)

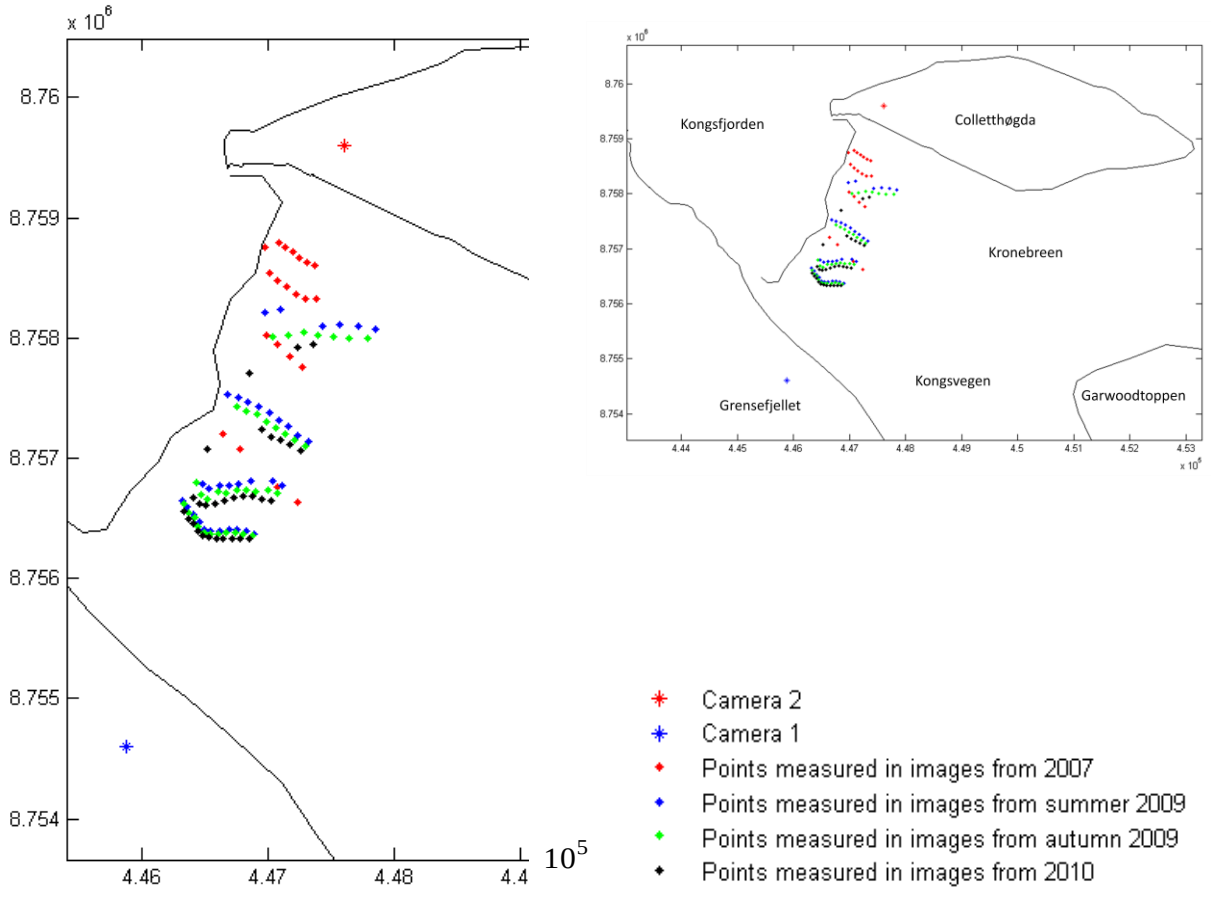

Figure 3-1: Map of the georeferenced points used for matching.

3.1 Temporal variation

The number of measurements over a given period decides the temporal resolution. A shorter period between two following measurements gives a better temporal resolution. The possibility of finding velocity between few days, in preference to 12-18 days found by satellite images, is one of the advantages of using terrestrial images. The method is tried out with 2, 4 and 8 days between the matched images. As a result of the testing (Ch. 5.1.1), 4 days between the images show up to be a suitable number of days, and consequentially used in most of the velocity graphs.

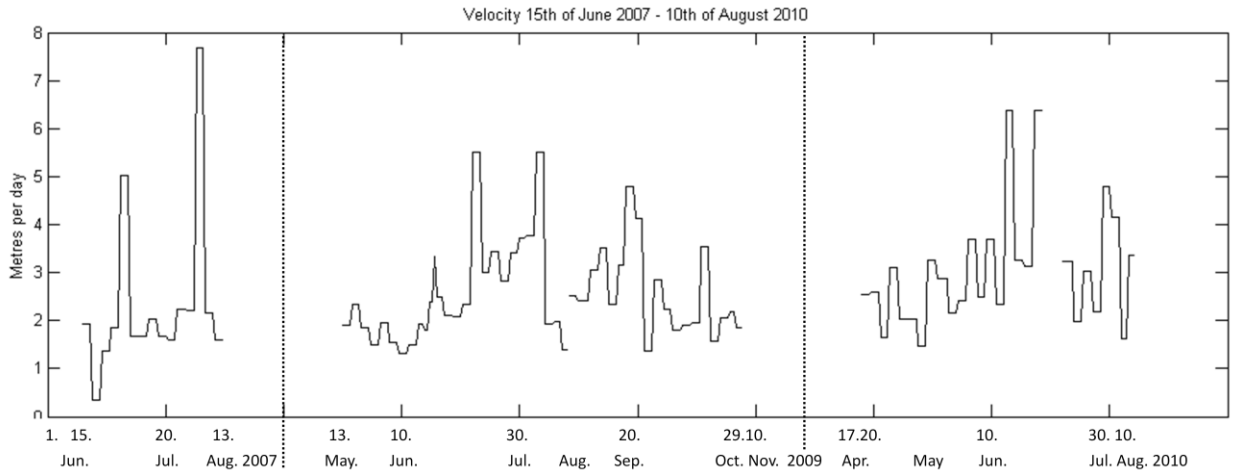

Figure 3-2: Temporal variations of the velocity from 13th of June 2007 to 10th of August 2010.

Figure 3-2 displays the temporal variation of the velocity during the measured period. The x axis represents how many meters the glacier moves through a point during a day. The daily velocity varies a lot according to the graph, and most of the big events happen in the middle of the summer. The displacement is measured between images with four days between, and daily velocity is got from division. The measurements are done in four different reference frames, which cause the difference in the terrain coordinates. The gaps in the graphs are caused by removing mistaken match of the point. More numerical explanation is found in table 3-1.

Table 3-1: Numerical information of figure 3-2.

Point	15.06-13.06, 2007	13.05-16.08, 2009	17.08-29.10, 2009	17.04-10.08, 2010
Coordinates of the point, (x, y)	(447275, 8757760)	(446774, 8756787)	(446754, 8756731)	(446731, 8756675)
Point in figure	22 in fig. 2-11	17 in fig. 2-12	17 in fig. 2-12	17 in fig. 2-12
Minimum velocity, m/day	0.35	1.32	1.37	1.48
Maximum velocity, m/day	7.69	5.51	4.79	6.39
Average velocity, m/day	2.34	2.56	2.60	3.05
Standard derivation, m/day	1.72	1.14	0.89	1.22
Distance to camera, m	1905	2376	2317	2257
Spatial resolution, m/pixel	0.42	0.81	0.78	0.76
Accuracy, m/day	0.37	0.30	0.29	0.29

3.2 Spatial variation

The velocity changes according to the position on the glacier. The velocity contribution on the glacier is explained across the glacier tongue (Ch. 3.2.1) and along the motion direction of the glacier (Ch. 3.2.2).

3.2.1 Cross profile

All the points, except from this chapter (3.2.1), are measured in lines in the tracking direction. There are too few points to show the velocity across the glacier tongue. Other points than showed in figure 3-1 are therefore measured in the same images with the aim of making a cross profile. Here, the points lie in lines across the glacier. (Fig. 3-3 & 3-4) Points in same line are almost in same distance from the front.

The cross profile graphs (Fig. 3-6, 3-7, 3-8 & 3-9) are made by using points in one and same line. The velocity close to the front is in main interest, but the points in these lines have a larger percentage of incorrect matches (Ch. 4.1.4). The closest line, with enough good points after matching, is chosen to make the cross profile. That is line number 5 from the front in all cases, except from summer 2009, where number 4 is selected. (Fig. 3-3 & 3-4) The x axis is in meters, as a distance to a chosen point. This reference point is chosen to be in line with all the measured points used to make the cross profile. Following glaciology norms, the measured point closest to south is the zero of x. That makes a cross profile where you look in the motion direction of the glacier, and the distance difference will be in a line. Outliers are not chosen, since the aim is to show the typical trend of velocity distribution across the glacier.

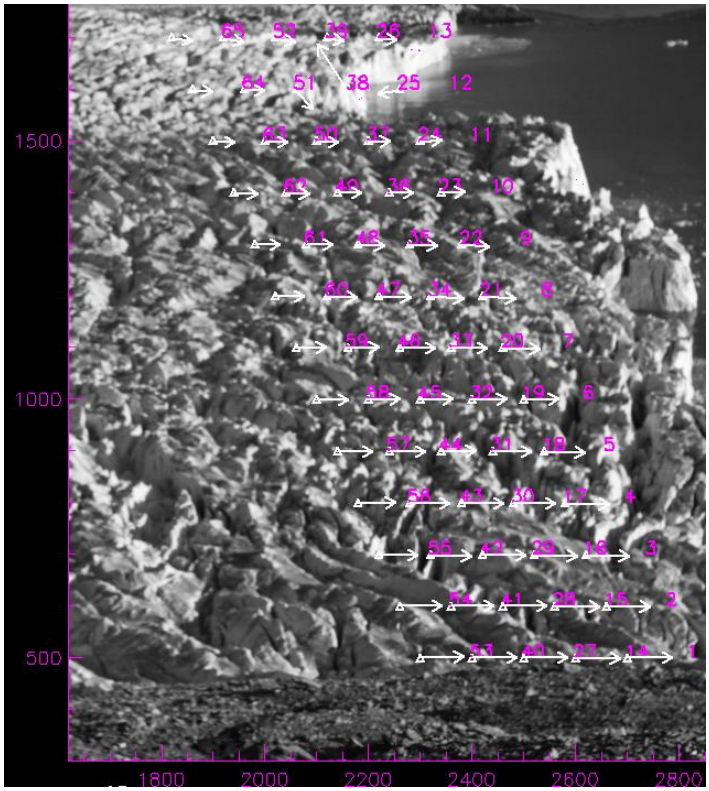

Figure 3-3: Points used in cross profile for 2007.

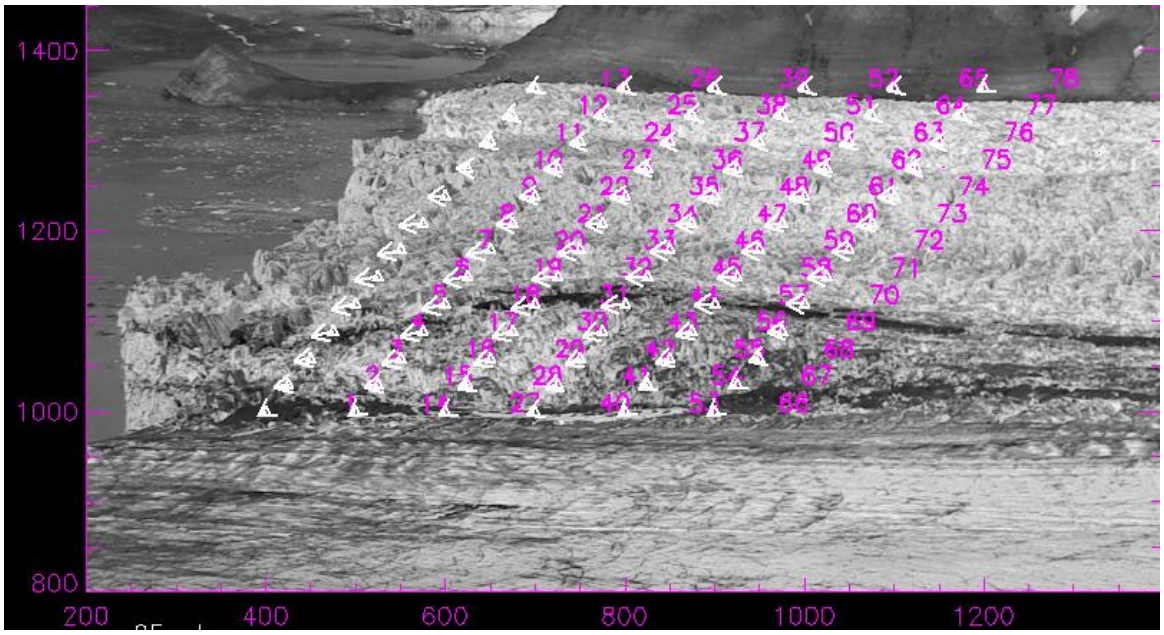

Figure 3-4: Points used in cross profile for 2009 and 2010.

Figure 3-5 shows the terrain distribution of the points in figure 3-3 and 3-4. The points closest to camera 1 are on the moraine.

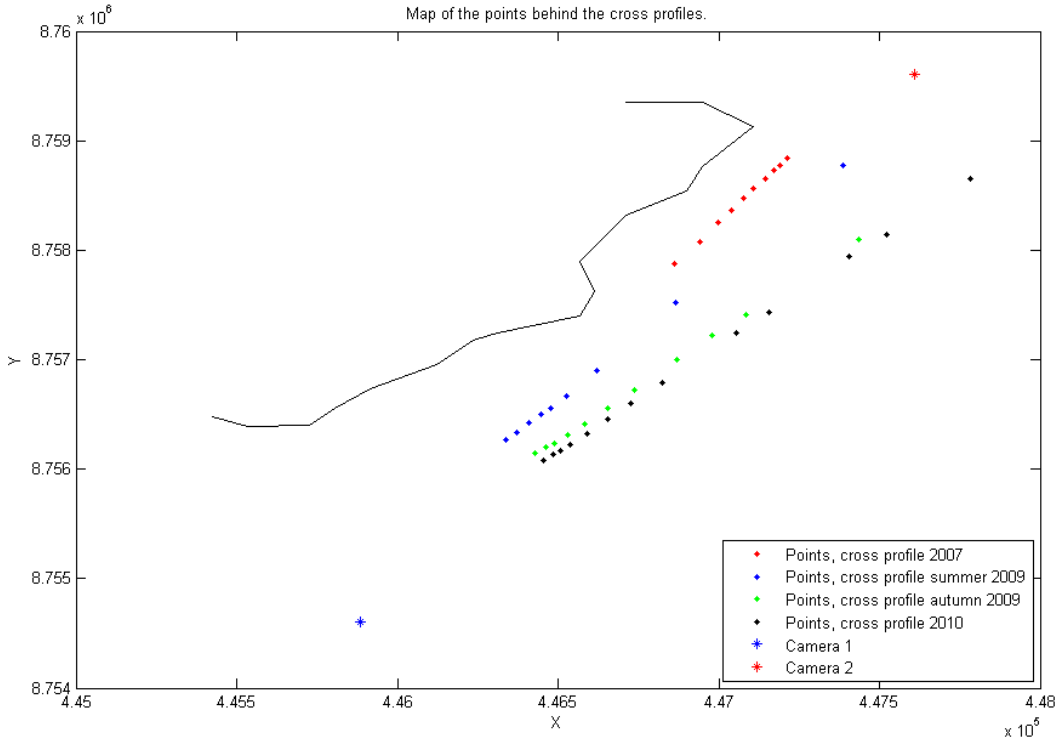

Figure 3-5: Map of the points used in cross profile for 2007, 2009 and 2010. The dots from 2007, autumn 2009 and 2010 represent point 53-65 in fig. 3-3 and 3-4. The dots from summer 2009 represent point 40-52 in fig. 3-4.

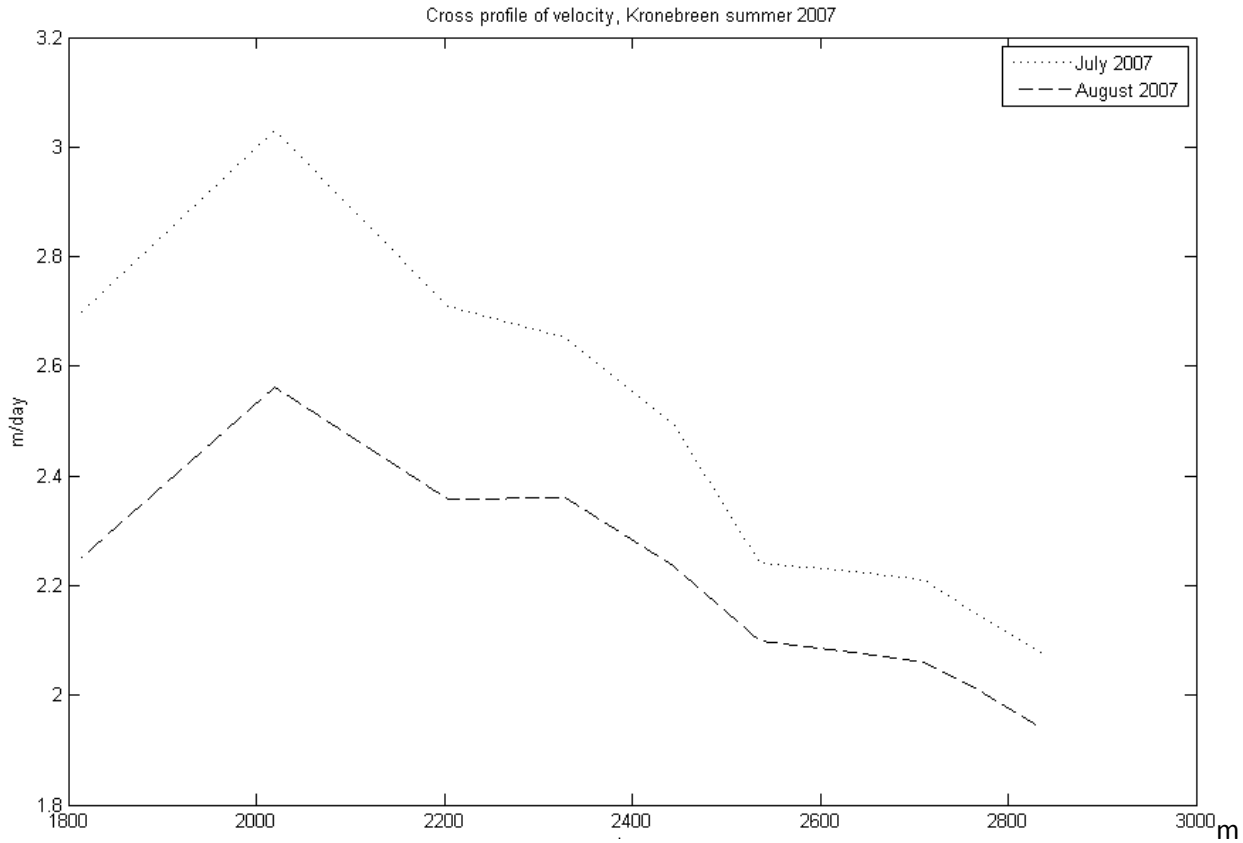

Figure 3-6: Cross profile 2007. The velocity is measured in the points displayed in fig. 3-3 and 3-5.

The velocities in 2007 are measured in images recorded 12th and 16th of July, 7th and 11th of August. Figure 3-6 shows the respective velocities. The best spatial resolution in the images will occurs in the points closest to the right side of the figure, since this will be closest to the camera and Colletthøgda. The left point is around 2 km from the camera, and the right one is around 1 km from the camera, according to table 3-2. The closest ones are very close to the mountain side of Colletthøgda, and the points to the right will be on the middle of the glacier. The distribution of velocity according to the position of the points seems to fit very well with the glacier motion. The glacier moves fastest in the middle, because of more friction on the sides. (Ch. 1.1)

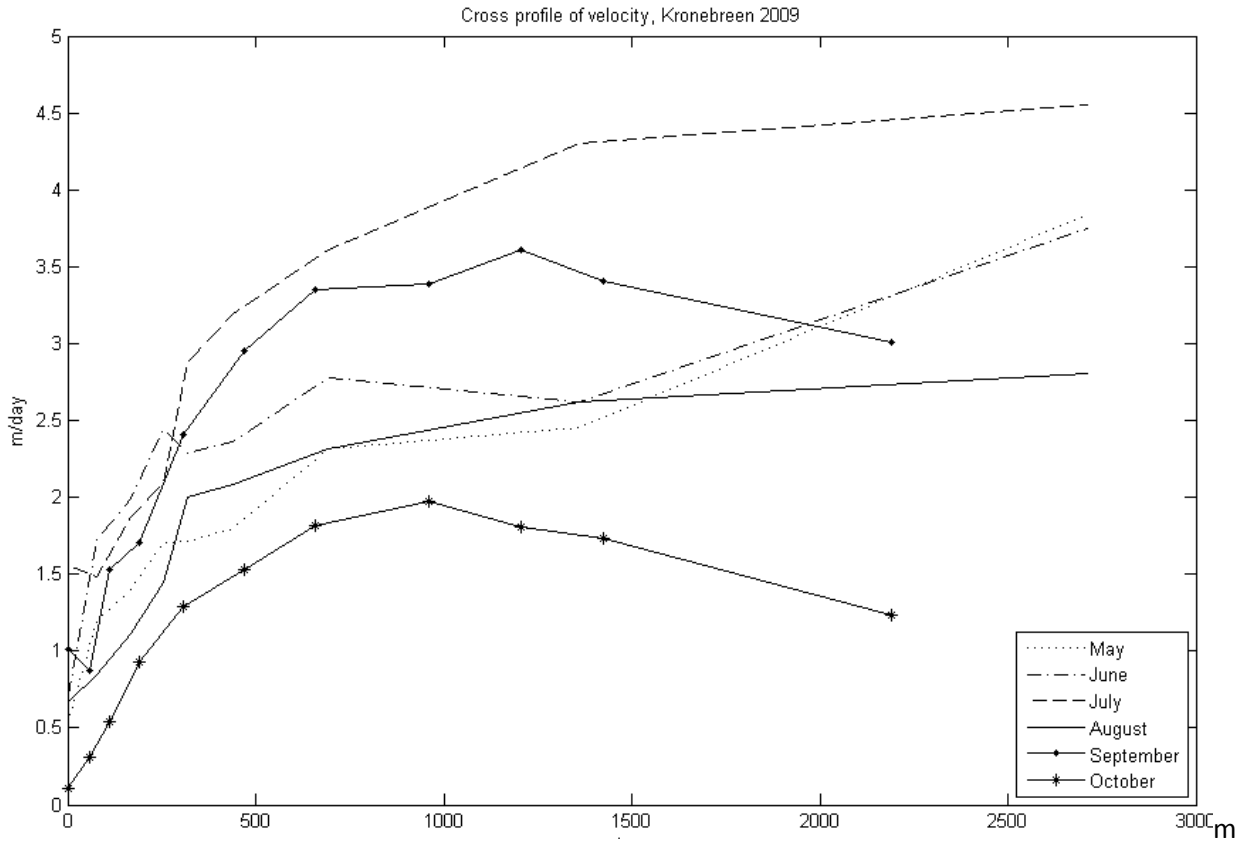

Figure 3-7: Cross profile 2009. The velocity is measured in the points displayed in fig. 3-4 and 3-5.

The velocities in figure 3-7 are measured in images from 16th and 20th of May, 23rd and 27th of June, 10th and 14th of July, 12th and 16th of August, 8th and 12th of September, 8th and 12th of October. The choice of dates is based on similarity of images with four days between. The most similar image pairs, based on weather conditions, are picked out for each month. Camera 1 stands 1800 meters to the left of the y axis. The right point is 3800 meters from the camera, according to table 3-2. The points closest to the camera are close to the moraine, and the other ones are closer to Colletthøgda and the middle of the glacier. The rising velocity towards the middle of the glaciers tongue makes sense, and it shall be almost no motion close to the moraine.

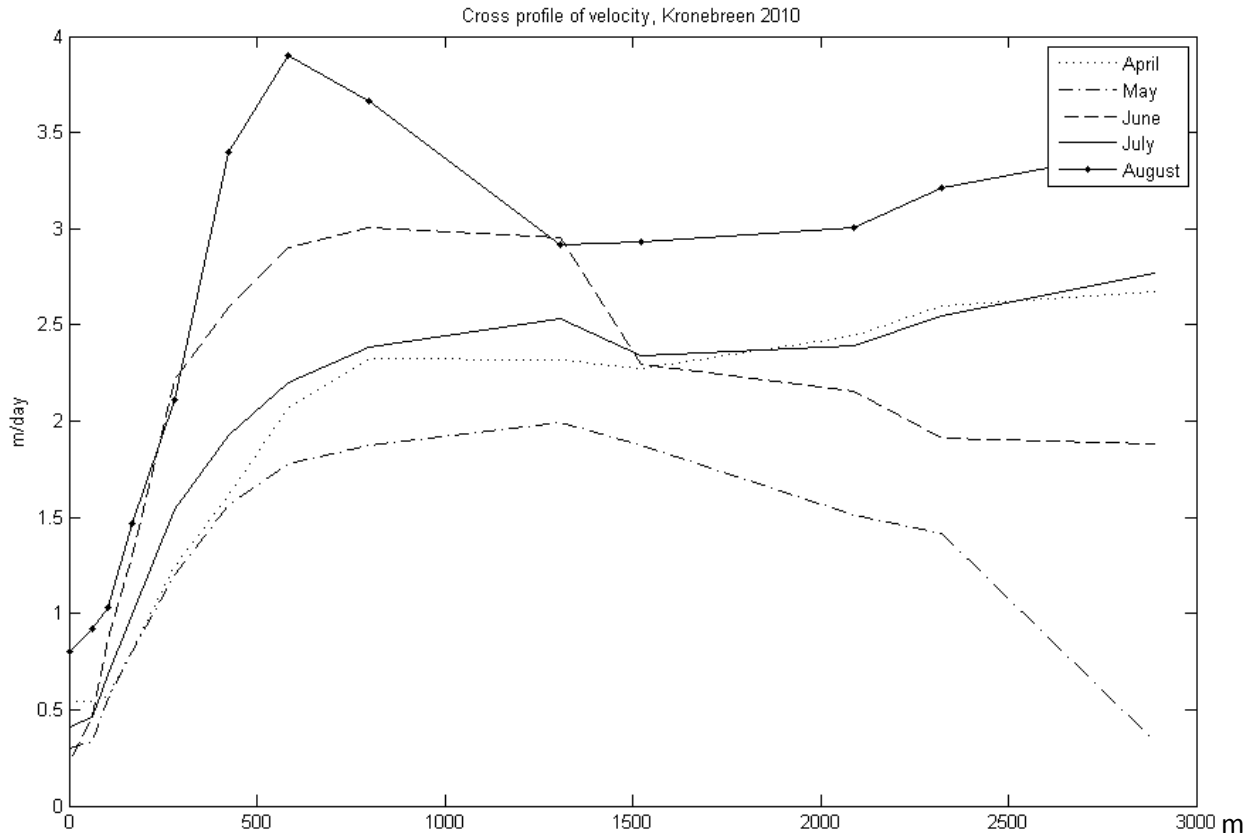

Figure 3-8: Cross profile 2010. The velocity is measured in the points displayed in fig. 3-4 and 3-5.

The distribution of the points with measured velocity are almost the same in figure 3-8 as in figure 3-7 since the images are taken from same camera position, and then almost have the same point of view. But as an improvement, the small difference in position, caused by different reference frames, makes it possible to get the correct match of the points that are farer away from camera. This cause in larger spatial distribution of the measurements, and following the graph covers larger area of the glacier front. The points spread from 1600 to 4500 meters from camera according to table 3-2. The zero position is the point in the line closest to the camera.

Figure 3-9 combines the velocity measurements from the three years of measuring; 2007, 2009 and 2010. The most representative graph is chosen from each year (Fig. 3-6, 3-7 & 3-8), instead of taking care of the same seasonal time. A direct comparison between years will therefore not be correct. But the relative velocity and differences in velocity across the glacier tongue should probably be the same.

The figure also shows the distribution of the measured points from the two different camera views, and the potential use of them. Camera 1 covers the area across the whole glacier. Camera 2 have too deep view angle to reach the whole line across the glacier. Measurements from both the cameras together give more detailed and trustful velocity measurements close to their position, and total distribution over the whole glacier. Table 3-2 shows information about the outer edges of points used for velocity measurements in figure 3-9.

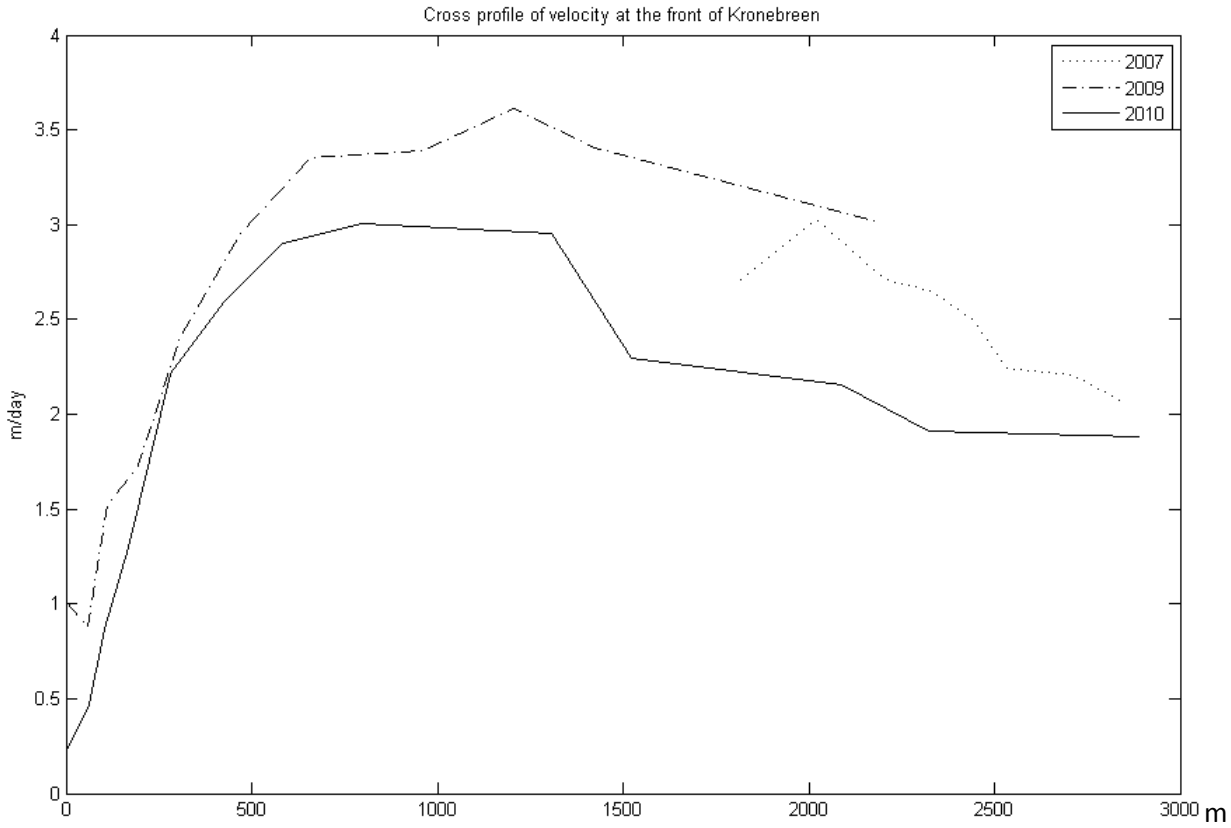

Figure 3-9: Cross profile 2007, 2009 and 2010. The velocity is measured in the points displayed in fig. 3-3, 3-4 and 3-5.

Table 3-2: Attached information about fig. 3-9.

Date	Point	Dist. camera	Dist. Front	Spatial res.	Accuracy
2007	(447214, 8758843) Closest to camera	924 m	150 m	0.20 pixel	0.18 m
2007	(446869, 8757881) Farthest from camera	1909 m	250 m	0.42 pixel	0.37 m
2009	(446489, 8756240) Closest to camera	1769 m	300 m	0.60 pixel	0.23 m
2009	(447435, 8758094) Farthest from camera	3831 m	500 m	1.29 pixel	0.48 m
2010	(446453, 8756083) Closest to camera	1615 m	300 m	0.54 pixel	0.20 m
2010	(447781, 8758650) Farthest from camera	4478 m	900 m	1.51 pixel	0.57

3.2.2 Acceleration towards the glacier front

The spatial distribution of the velocity varies dependent of the proximity of the front. Figure 3-10 shows the velocity in three positions along the glacier tongue during time. (13th of May – 16th of August 2009)

The points are chosen in same along tracking line with a relative distance of about 100 meters. The front position of the glacier changes during the measuring period because of forward motion caused by glacier motion and retreat caused by calving. (Ch. 1.1) The change in front position makes a different distance between the measured terrain position and terminus during time of measuring. The distance in table 3-3 is chosen from an average image in the middle of the season, but the relative distance between the three different points of velocity measurements is the same during the time of measuring. The different distance to the front appears as a result of measuring in same terrain point during time, instead of measuring velocity in a physical point moving on the glacier.

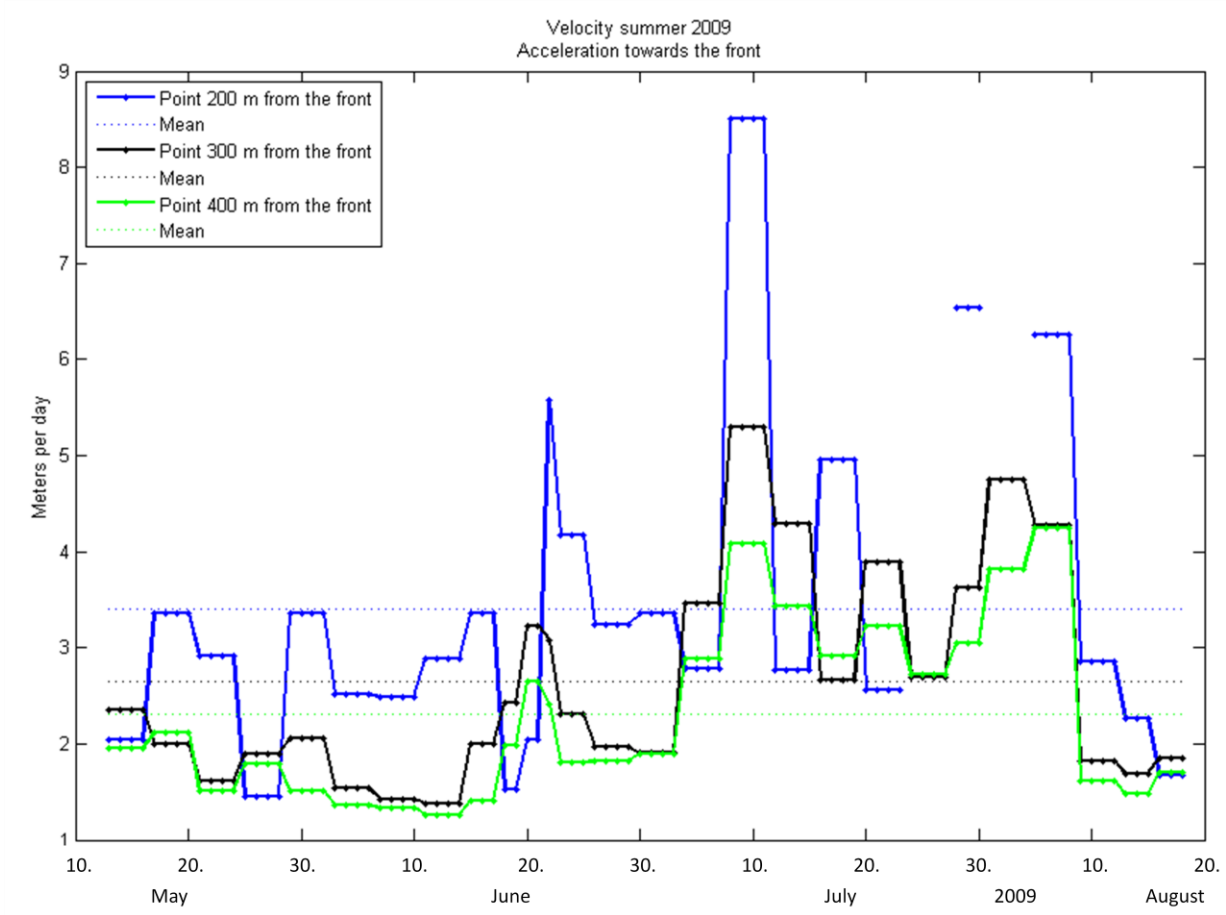

Figure 3-10: Acceleration towards the front.

The three different graphs in figure 3-10 represent different terrain positions with different distance to the glacier front. The figure shows highest velocity in the graph closest to the terminus, and lower farer away from it. The graph closest to the front also shows largest temporal variations. The observations

from the figure indicate acceleration towards the front. The glacier moves faster and varies most in velocity close to the terminus.

Table 3-3: Numerical information of figure 3-10.

Average distance from front	200 m	300 m	400 m
Coordinates of the point, (x, y)	(446537,8756753)	(446616,8756774)	(446690,8756775)
Point from fig. 2-12	14	15	16
Minimum velocity, m/day	1.45	1.38	1.26
Maximum velocity, m/day	8.50	5.29	4.25
Average velocity, m/day	3.41	2.64	2.31
Standard derivation, m/day	1.68	1.12	0.91
Distance to camera, m	2264	2308	2334
Spatial resolution, m/pixel	0.76	0.78	0.79
Accuracy, m/day	0.29	0.29	0.30

4 Accuracy of the results

4.1 Error contribution

It is useless to have a lot of results without knowing anything about the accuracy of them. A main part of analyzing the method is to find the uncertainty of the results, and go deeper into everything that can cause uncertainty in the results. This chapter tells about the different kinds of errors.

If one step increases the accuracy much more than the other, it is very important to give priority to this step. On the other hand, it could be needless to use a lot of time on a step that is too small to be mentioned in the results compared to the other, and then better to neglect it. Theoretically is it possible to avoid all these sources of uncertainty, but then it is necessary to do some of the steps different than in this thesis. (Ch. 6)

4.1.1 Interior orientation and camera calibration

The camera calibration includes finding the interior orientation parameters that reconstruct the moment of photographing, and then the bundle rays from sensor to terrain through the projection centre. It includes the geometric influence of the lens system, both mechanical and optical. The interior orientation parameters are described in table 4-1, figure 4-1 and figure 4-2.

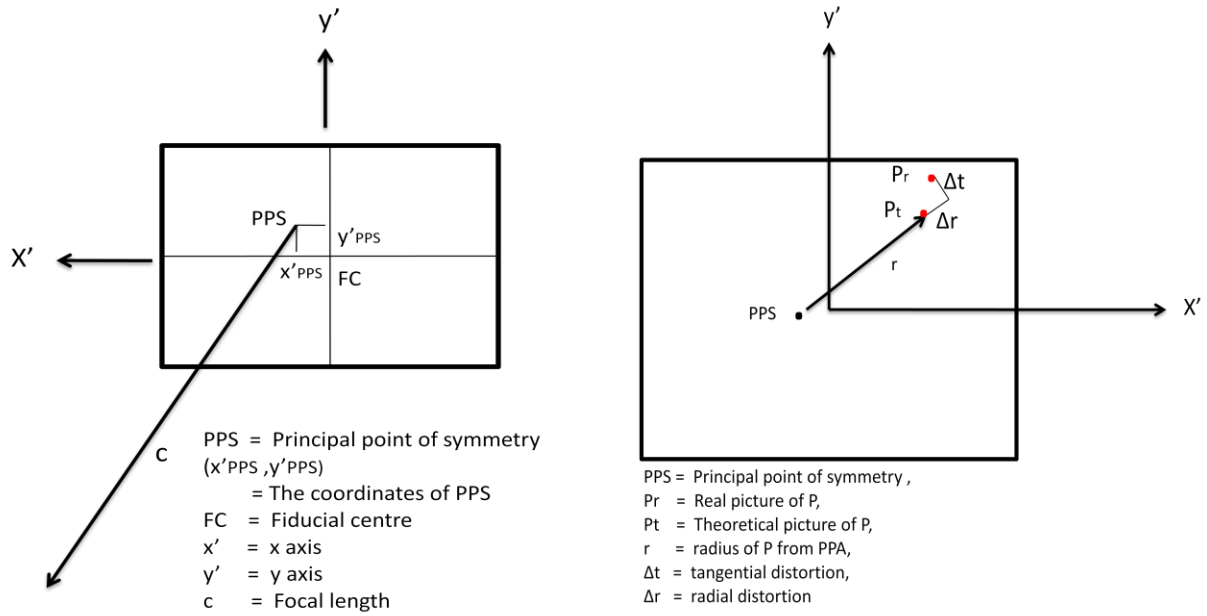

Figure 4-1: a) Principal point of symmetry (PPS). **b) Tangential and radial part of PPS.**

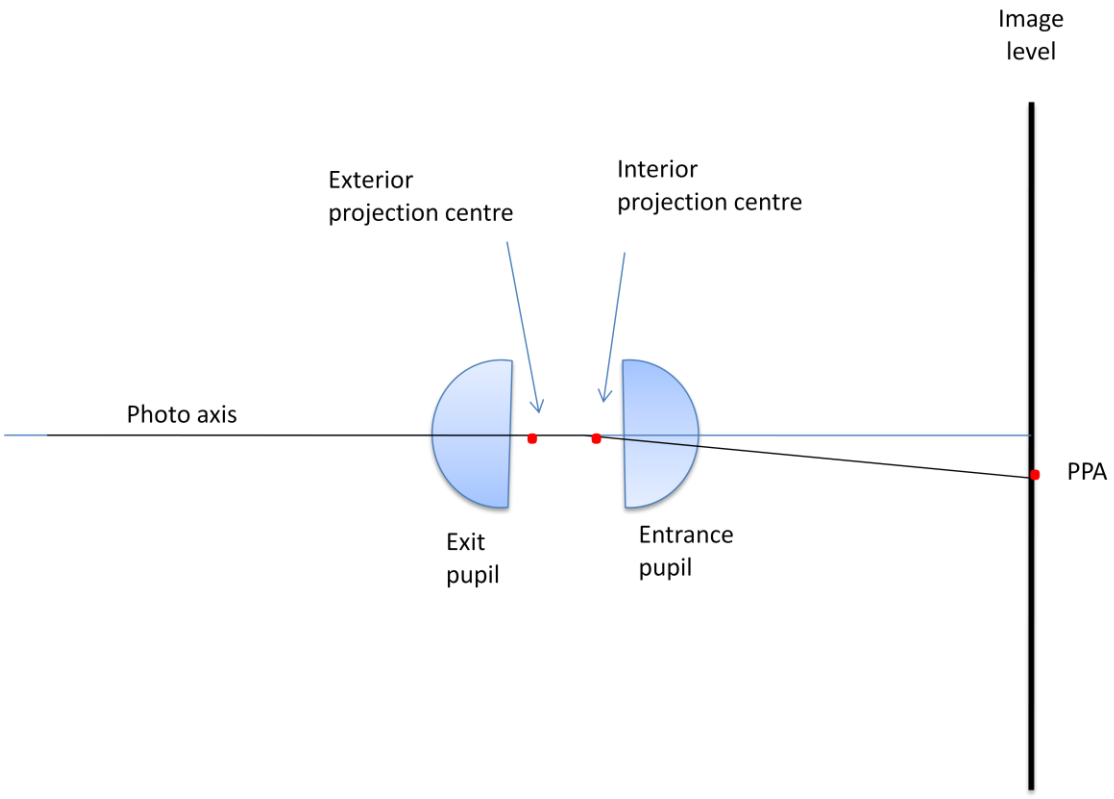

Figure 4-2: Principal Point of Autocollimation (PPA).

Table 4-1: Interior orientation parameters.

Orientation parameters	
Fiducial centre, FC (Basis for the orientation parameters)	The target of the image view. The geometric centre of the image. PPS and PPA are offsets from FC.
Principal point of symmetry, PPS	The section between orthogonally bundle rays and image level. The centre of distortion.
Principal point of Autocollimation, PPA	The section between deviate ray and image level. The deviation in the lens makes different exterior (Affect the rays) and interior (Used for counting) projection centre. The effect is rotation symmetric.
Lens distortion	Systematic distortion around PPS. Divided into radial and tangential lens distortion.
Calibrated focal length, c	Caused by change of air temperature, which results in a deformation in the image bundle of rays.

The mathematical model of central projection; with image point, projection center and ground points in collinear lines, orthogonally on the image level, is used if no calibration. The calibrated deformation is caused by the small deviations from the mathematical model. A self calibration is often done by bundle block adjustment, which gives the transformation parameters between mathematical model and intern image geometry as systematic errors. (Eq. 4.1)

The stable geometry of the CCD sensor makes usually up to date calibration unnecessary. The parameters are stable and do probably not change. But the calibration before use of the camera is still necessary. Measuring in images from not calibrated cameras can be a source of uncertainty. Use of not interior orientated images will cause in radial distortion, which is an error proportional to the distance between PPS and measured image point.

The measurements close to the glacier front mainly occur in the left edge of the images recorded with camera 1, and following in large distance from the image centre. A lens distortion will therefore affect measurements in this area of the image. But the lens distortion will influence the images in the same amount, because of the stability of the parameters. The relative error does not necessarily be high although the absolute error is high, since our measurements consist of measuring relative displacement between the images. Working with images in same reference frame involves measuring exactly the same image points. The points are close to similar since the reference frame is almost the same during the measuring periods. The interior orientation will influence the points in same image position in the same trimmed photo print in the same way. (Andersen, 2003; Jacobsen & Mostafa, 2001)

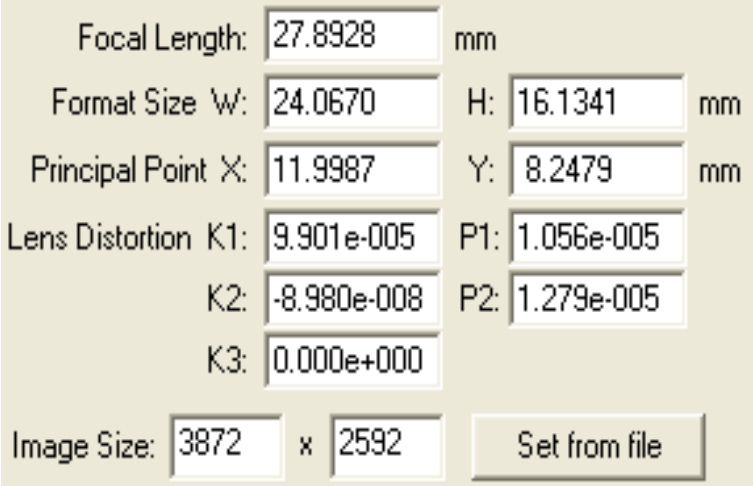

Figure 4-3: Calibration report of camera 2. (Sund, unpublished)

$$x_u = x_d + (x_d - x_c)(K_1 r^2 + K_2 r^4 + K_3 r^6) + P_1(r^2 + 2(x_d - x_c)^2) + 2P_2(x_d - x_c)(y_d - y_c)$$

$$y_u = y_d + (y_d - y_c)(K_1 r^2 + K_2 r^4 + K_3 r^6) + P_2(r^2 + 2(y_d - y_c)^2) + 2P_1(x_d - x_c)(y_d - y_c) \quad (4\text{-}1)$$

(x_d, y_d) is the distorted image point, (x_u, y_u) is the undistorted image point and (x_c, y_c) is the centre of distortion/principal point of symmetry.

The interior orientation parameters of camera 1 are unknown, since no calibration is done. It will cause in small or no decrease of accuracy in the results because of already mentioned small or no relative uncertainty. Camera 2 is calibrated by finding the interior orientation parameters in figure 4-3 and using them on all the pixels in the images according to equation (4-1). This resampling of the images need to be done before georeferencing, before or after matching. Ideally the cameras should have been calibrated inside of the camera box because of the influence from the window. (Sund, unpublished) Calibration of only the cameras will therefore just be a percentage of the ideally calibration. Therefore is none of the images from 2007 calibrated according to equation (4-1).

4.1.2 Image transformation

Theoretically, the images, which are recorded from same camera position and view, are in the same reference frame: The camera coordinate system. But in spite of a very steady camera, the images show camera motion, probably caused by mountain/ground motion. (Ch. 2.4) Transformation of the images into same reference frame is therefore necessary. Measuring of glacier displacement between images with different reference frames gives a larger measured value of displacement than it really is because of additional influence from displacement between the two different camera views (Reference frames).

The images from the same measuring period (Table 2-1) are transformed into the same reference frame as a chosen reference image from same period. The process of resampling can influence the uncertainty by giving worse accuracy. No transformation will be to the worse, but several steps of resampling increase the chance of including some more source of uncertainty. By assuming a conform

transformation (Eq. 2-3 & 2-4) between the images, translation, rotation and scale are taken into account.

Translation

Translation is the factor that influences the images most and is the only part ensured and rectified through the transformation. The offsets between (Appendix B) are used to translate the images from camera 1 into same reference frame for each measuring period. Offset in images from summer 2009 are found by automatically matching in MATLAB (The MathWorks, 2005). Offset in the images from autumn 2009 are found manually in GIMP (Kimball & Mattis, 2010) and translated in MATLAB. Images recorded in 2010 did not need to be transformed. Shortage of trustable conjugate points makes the images from camera 2 (2007) being untransformed.

The image quality, mainly caused by weather (Ch. 2.5 & 4.1.4), makes it difficult to decide offsets between the images. Evident, clear, physically points in a homogenous area without difference in snow or sea are not easy to find. This problem appears both in manually and automatically matching. Manually matching gives better control because of the continuous comparison with the images around by expecting realistic motion.

The manually deciding of the image coordinates for a physically point is given a standard derivation of 1 pixel because it is too easy to pick the neighbor pixel of the wanted one. This depends very much of the image quality. Fog makes the images unclear and less rich in contrast. Finding small offset in GIMP can make the translated images less similar than the reference image, instead of the wanted opposite.

Automatically matching also has problems with the choice of correct pixel when they are close to each other. The offsets in images from summer 2009 (Appendix B) are switching back and forth around 1 pixel instead of following a smoothly continuous motion in one direction. The script (Appendix C) deciding offsets with automatically matching works with integer. If the current displacement between the two images is a decimal numeral, the offset is decided as an integer in any case. Small difference in real offset will cause in a random choice between the two numerical alternatives. The maximum difference between real offset and decided offset from automatically matching is therefore 0.5 pixels.

The result of translation would not cause better images than up to one pixel in difference between two matched images. The metrical size of the uncertainty depends of the pixel size. (Ch. 4.1.6)

Rotation

Different offsets between the left and the right edge of an image indicates a need of rotation. A default of rotation leads to higher inaccuracy in the edges of the image compared to the images centre. The largest difference where observed in the first image from 2009, with a difference of 6 pixels in the edges, but 0 in the middle.

If necessary, the images should be rotated before translation offset is decided. The angle between measured points in the image is found by equation (2-5). Rotation is the difference between this angle and the one in the reference image. (Appendix B) Measuring of points far away from each other decrease the large influence of picking incorrect image coordinates of the physical point. Incorrect

image coordinates will still change the rotation angle more than the angle itself. Clearness and differences in weather conditions give high possibly of choosing the neighbor pixel in an image. The effect of picking incorrect image points is showed in table 4-2. The influence from y direction is larger because of few conjugate points with very large or very low y value to choose. The low y values are all in the sky, and the high ones in the glacier and snow.

Table 4-2: Effect of choosing the neighbor pixel.

Difference	1 pixel in x	1 pixel in y	2 pixels in x	2 pixels in y
Rotation angle (deg)	0.0001	0.023	0.0002	0.45

Except from the first image pair, the difference between rotations in our matched image pairs is not more than 0.05 degrees, and seldom more than 0.03 degrees. That is not much comparing to uncertainty of 0.02 (Or 0.05) degree caused by incorrect chosen image point with only one pixel. The incorrect calculated rotation angle can be as large as the rotation between the images. The results are therefore better by leaving out the rotation from the transformation formula.

Scale

The scale depends of the distance from camera and the focal length. The focal length is the same in all images recorded from same camera. The distance between camera and glacier is the same as long as the camera does not move forward or backward. The camera mainly moves down, either at one level, or more in one side. A very small backward or forward motion can appear if the camera moves down only in the front or the back. This motion is very small compared to the distance. (Eq. 4-2) The change will cause in 2 mm incorrect measurement in areas 2 km away from the camera, which is uninteresting in this case.

$$Fractional\ change = \frac{Change}{Distance} = \frac{2\ cm}{2\ km} = 10^{-5} = 0.00001 * distance \quad (4\text{-}2)$$

The scale is not taken care of in the transformation because it is very difficult to find. (Of same reasons as mentioned about rotation and translation) A possible scale difference will not cause any uncertainty of the measurement results. My transformation therefore only includes translation.

Checking the transformation with Helmert transformation in Cias

$$\vec{X'} = \vec{T} + s \quad \vec{R} \quad \vec{X} \quad (4\text{-}3)$$

$$\begin{bmatrix} x' \\ y' \end{bmatrix} = \begin{bmatrix} t_x \\ t_y \end{bmatrix} + s * \begin{bmatrix} 1 & -\sin\propto \\ \cos\propto & 1 \end{bmatrix} * \begin{bmatrix} x \\ y \end{bmatrix} \quad (4\text{-}4)$$

x', y' are the transformed image coordinates of ***x, y*** with the he different offset ***t*** in each direction, a rotation α and a scale ***s*** of the whole image.

The matching in Cias is done in the predefined reference frame without choosing the in build conform Helmert transformation. (Eq. 4-3 & 4-4) Helmert transformation requires a sample of conjugate points to decide the transformation parameters to transform the second image into the first one. A new

transformation is decided for every match. The two matched images are in same reference frame after transformation, but each matched image pair can be in different reference frame. The points need to be picked out manually one by one because the position sensitivity requires a point with large contrast and no motion between the images. Iterative removing chosen conjugate points from the transformation decision is necessary for avoiding large outliers caused by sensitivity. Result in different reference frame and large time-consuming process is the main reasons for using images in predefined reference frames. But the in build transformation can be used to check if our already transformed images have ended up in same reference frame.

The transformation is checked between samples of images; three image pairs from each period. (Table 4-3) Image pairs with large translation offset between them are chosen to find the largest error caused by not satisfied transformation. (Appendix B)It is about 4 days between the images, which is most representative, because it is the same number of days as in the measurement. Images with similar weather are used to make it easier finding conjugate points. The same image pairs are also used to check the displacement of points without motion, by making result file in the same way as earlier. Table 4-3 consists of the smallest value of each transformation parameter, together with a mean of at least 10 points.

Table 4-3: Differences in reference frame in already transformed images.

Date of image pairs	t_x, pixel	t_y, pixel	α, deg	S	dx min/ mean	dy min/ mean	length min/ mean	Direction
14.06-18.06, 2007	0.16	-1.90	359.988	1.00037	0/0.40	-0.38/-1.65	1.13/1.79	166
04.07-09.07, 2007	-0.14	-1.48	359.990	1.00006	0/0.14	-0.75/-1.46	1.06/1.61	187
02.08-06.08, 2007	-0.43	-0.30	359.992	0.99966	0/-0.3	0/-0.23	0.25/0.57	233
12.05-16.05, 2009	-0.68	-1.27	359.954	1.00065	0/-0.66	-0.75/-0.89	1.03/1.15	217
16.05-20.05, 2009	0.19	0.66	359.991	0.99976	0/0.21	0.25/0.65	0.35/0.69	31
07.08-11.08, 2009	-0.14	0.59	359.971	0.99978	0/-0.08	0/0.23	0.25/0.39	163
16.08-21.08, 2009	0.10	0.63	0.022	0.99995	0/-0.02	0/0.5	0/0.62	128
25.08-29.08, 2009	0.67	0.48	0.042	0.99984	0/0.53	0/0.4	0.5/0.93	76
30.09-04.10, 2009	0.07	0.13	359.991	0.99962	0/-0.03	0/-0.05	0/0.18	113
16.04-20.04, 2010	0.75	-0.16	0.021	1.00016	0.25/0.48	0/-0.33	0.35/0.69	132
09.05-13.05, 2010	0.68	1.33	0.020	1.00062	0/0.25	0,5/0.88	0.75/0.97	87
04.08-07.08, 2010	-0.60	0.23	359.977	0.99995	0/-0.18	0/0.18	0/0.38	162

None of the transformation parameters in table 4-3 are zero or one (scale) as wanted, which is no surprise. The translation has a value between zero and one because of large pixel size and because it is impossible to find offset in anything else than integer numbers when using MATLAB script. All the rotation and scale in table 4-3 is between the raw images because there is no rotation or scale included in the predefined transformation. The largest value of scale will make a 1 m large pixel less than 1 mm bigger.

Points where no motion in real life is expected are used as conjugate points. That involves contrast between sky and mountain. Points in snow edges are also included failing clear and remarkable points. The snow amount is changing during the days in the image pairs and will also influence the comparison. A large percentage of mistaken matches appears because of gray scale sensitivity in the matching software, but can easily be removed in the result file (Column 6-9 in table 4-3). An iterative removing of chosen conjugate points from the transformation decision results in same effect. (Column 2-5) The majority of remaining points then move less than 1 pixel in each direction. Some of the points move more because of different snow amount. The most similar reference frame between images show up to be in autumn 2009, were the images are translated manually.

The largest difference appears in images from 2007, which show offsets from 1-3 pixels in y direction. Different snow amount could be the reason, but this is probably not the only reason because very few of the displacements of y are less than 1 pixel. However, the displacement is on the Grensefjellet, very far behind the measured points on the glacier. Together with smaller ground pixel size, as are less than half of the images recorded from camera 1, the uncertainty will be mostly in same amount in all images.

An uncertainty of 1 pixel for images recorded with camera 1, and 3 pixels in images from camera 2, is decided on the background of this research and the displacement of points with “no” motion in the result files. This is only the uncertainty caused by difference in reference frame.

Since almost the same order of magnitude occurs in both Helmert transformation, and in the result files of individually point without motion, is it trustful data.

4.1.3 Oblique images

Orthophoto are images with same attributes as a map. The images are geometrical corrected of lens distortion, topography and camera tilt to make uniform scale.

In opposite, terrestrial images are oblique images. The scale is not the same in the whole image because of a vertical view angle being something else than zero. The difference in angle makes difference in the distance between the camera and measured points in the image. Difference distance and angle appears in the background, foreground, middle and edges of the image.

The effect of the oblique photography situation will cause a geometrical effect with radial displacement. Placing of cameras is made to avoid it, with direction of displacement vector across the camera view direction. Same scale occurs in images with normal recording and flat terrain. The glacier is the measured and interesting area, and can be treated as a flat terrain, where affine transformation is satisfied.

The direction and distance are already taken care of in equation (2-2), and would not cause any uncertainness in the measuring result.

4.1.4 Image matching

Cias choose the area with highest correlation coefficient to decide the image position of the match. The most similar position in the image is not necessarily the same physically point. Weather conditions are the main cause of disparity by change in light, shadow and clearness caused by sun and fog. The crevasses make the visually pattern of the glacier that makes matching possible. Few days and small motion between the matched images makes it easier to recognize the same area. The opposite case changes the pattern through motion, which makes it difficult to find a match of the point. The large velocity close to the front, which also is more influenced by calving, causes in more pattern change and bigger percentage of not successful matching in points close to the terminus.

The match is either correct or incorrect point. The image of displacement vectors makes it possible to see which matches have become incorrect. The vectors ought to be in almost same direction and length since the glacier moves like an elastic, solid body. Is it easy to see possible outliers if the motion or time between the two images is large enough. Change to images with more similar weather instead of taking care of the temporal resolution can increase the percentage of correct matched points.

Different size of template and/or search area can produce different results of displacement vector. The choice decides the automatically matching process in Cias. The search area needs to be large enough to space the template moving to the correct point in the second image. Larger template requires therefore larger search area too. An unnecessary large search area includes larger area without the current match inside, which increase the time and chance of getting incorrect match. The template size depends of the pattern around the matching point. A small template indicates the exactly chosen point, and a bigger one indicates more of the area around. Larger template gives a more unique solution, but usually smaller correlation coefficient.

A large average correlation coefficient does therefore not necessarily indicate a good choice of template size and search area. The default values in Cias are a template of 15 pixel and search area of 100 pixels. The size of both template and search area are changed to check which size give best results. The percentage of correct matched points increases when increasing the template up to a saturation point. (Fig. 4-4a & fig. 4-4b) The search area will be too small when continue increasing of the template because of less space. (Fig. 4-4c & 4-4d)

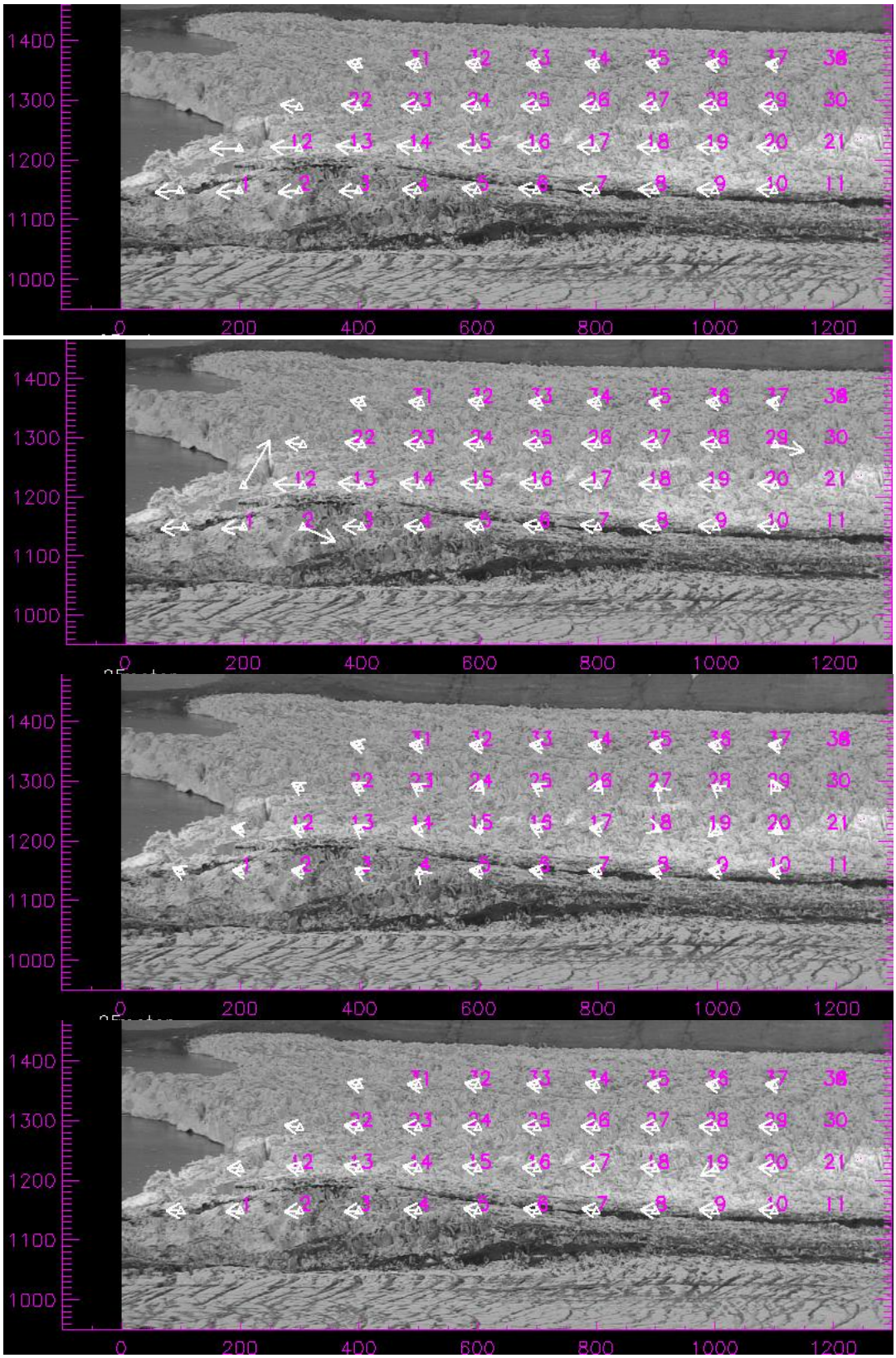

Figure 4-4: Different size of template and search area gives different match: a) 15&100 b) 30&100 c) 90&100 d) 90&110

Table 4-4, 4-5 and 4-6 show the difference in length, direction and correlation coefficient of the displacement vector when changing the size of the template and search area. The good choice of size are written with bold letters and the worse once in italic. 30/100, 50/100 and 70/100 correspond best with each other, together with 90/120 and 90/130, according to the three tables.

Table 4-4: Difference in mean length of all the 38 points, when changing size of template and search area in Cias.

Difference in length	15/100	**30/100**	**50/100**	**70/100**	*90/100*	*90/110*	**90/120**	**90/130**
15/100	0							
30/100	1.32	0						
50/100	1.35	**0.03**	0					
70/100	2.19	**0.87**	**0.84**	0				
90/100	*9.31*	*8.00*	*7.97*	*7.12*	0			
90/110	4.39	3.07	3.04	2.20	*4.92*	0		
90/120	2.11	**0.79**	**0.76**	**0.08**	*7.21*	2.28	0	
90/130	1.40	**0.08**	**0.05**	**0.79**	*7.92*	2.99	**0.70**	0

Table 4-5: Difference in mean direction of all the 38 points, when changing size of template and search area in Cias.

Difference in direction	*15/100*	**30/100**	**50/100**	**70/100**	*90/100*	**90/110**	**90/120**	**90/130**
15/100	0							
30/100	*14.83*	0						
50/100	*14.89*	**0.05**	0					
70/100	*15.19*	**0.35**	**0.30**	0				
90/100	1.35	*13.48*	*13.54*	*13.83*	0			
90/110	*15.20*	**0.37**	**0.31**	**0.02**	*13.85*	0		
90/120	*15.60*	**0.76**	**0.71**	**0.41**	*14.24*	**0.39**	0	
90/130	*15.26*	**0.43**	**0.37**	**0.08**	*13.91*	**0.06**	**0.33**	0

Table 4-6: Difference in mean correlation coefficient of all the 38 points, when changing size of template and search area in Cias.

Diff. in correlation	**Corr. min**	**Corr. max**	**Corr. Mean**	15/100	**30/100**	**50/100**	70/100	*90/100*	90/110	90/120	90/130
15/100	0.51	0.97	0.83	0							
30/100	0.49	0.95	0.79	**0.04**	0						
50/100	0.54	0.95	0.73	**0.10**	**0.06**	0					
70/100	0.33	0.91	0.66	0.17	**0.13**	**0.08**	0				
90/100	*0.01*	*0.73*	*0.31*	0.52	0.48	0.43	0.35	0			
90/110	0.18	0.82	*0.48*	0.35	0.31	0.25	0.18	0.17	0		
90/120	0.30	0.88	0.62	0.21	**0.17**	**0.11**	**0.03**	0.32	0.15	0	
90/130	0.39	0.88	0.64	0.19	**0.15**	**0.09**	**0.02**	0.33	0.16	**0.02**	0

The length and the direction of the displacement vector change when increasing the template to 30 pixels instead of using the default value of 15 in a 100 pixels search area. (Figure 4-4a & 4-4b, table 4-4 & 4-5)Almost the same result occurs when increasing the template to 50 and 70 pixels. The result would not be exactly the same without using exactly same size of template, although all of them look correct. Increasing the template to 90 pixels in a search area of 100 pixels changes the results to include just incorrect matched points. (Fig. 4-4c) The small difference between template and search area makes is impossible to reach the point that is the correct match. Increasing search area according to the template increase solves the problem. A search area of 110 pixels is not enough (Fig. 4-4d), but a search area of 120 pixels is enough to space the correct displacement of the 90 pixels large template.

A template of 30 pixels in a search area of 100 pixels seems to be a good start choice based on the research above. A change to respectively 70 pixels and 120 is useful when it is more than the 4 days between the images in the research. Several days require larger search area because of more glacier motion, but also larger template because of change in the pattern. This testing adjusts for images from camera 1, but need to be changed when working with other images. Images from camera 2 have larger scale which cause in displacement in more pixels. A template of 70 pixels is used in a search area of 150 pixels when measuring in images with 2 or 4 days between. Measuring for comparing with velocity from satellite images makes a displacement between images of 12-19 days. Template size of 150 pixels in a search area of 250 pixels works best in this case. The choices need to be used for all the points in a matched image pair (Or the match can be done twice, with half of the points in each) although it requires larger search area closer to the camera because of scale differences in the image.

The correlation coefficients are larger when using small template because it is easier to find a similar area. A larger template insists a more unique area. A match with larger template is more trustworthy, but can give a small correlation coefficient. Too small search area to reach the correct match gives very small correlation coefficient which indicates mistaken matched point. (Table 4-6)

Anyway what is changed, incorrect matching will appear because of differences in the images caused by weather conditions and glacier motion. Use of gray scale images can result in fewer differences but also avoids unwanted differences like weather changes. A shadow can destroy the whole image comparison.

4.1.5 Elevation model

Georeferencing of the displacement into terrain coordinates in Geophotoref requires a digital elevation model. Motion of glacier and mountains change the elevation of the terrain during the time. The DEM used for measurement represent the elevation in 2007, made from satellite images. (Spot Image, 2007)The used DEM will never be totally correct except from the moment of photographing.

The accuracy of the terrain model cause in two types: Velocity accuracy and position accuracy. The first one is the interesting one in this case, by measuring the difference through seasons. Position accuracy is important when comparing the result with other kind of measuring in the same points, for example velocity from satellite images.

Velocity uncertainly appears when the two ends of the displacement vector from Cias have different height. The resolution of 40 m and absolute precision of 30 m RMS (Spot Image, 2007) makes velocity uncertainly caused by elevation model very seldom happen. Nevertheless, the horizontal effect of a 20 cm elevation, which can imagine a high difference in a vector, is checked in table 4-7.

The precision of the DEM is 8 m in elevation, together with the elevation change of 2 m for each year, since the elevation change through the time. (Nuth, unpublished) This cause in a precision of 8 m in images recorded in 2007 and maximum 14 m in images recorded in 2010. The elevation difference results in incorrect position because of wrong intersection between camera rays and glacier. (Fig. 4-5) The horizontal position error depends of the relative position of camera and measured points according to equation (4-5) and (4-6). View angle, time, accuracy of DEM and adjustment between DEM and image influence the position accuracy.

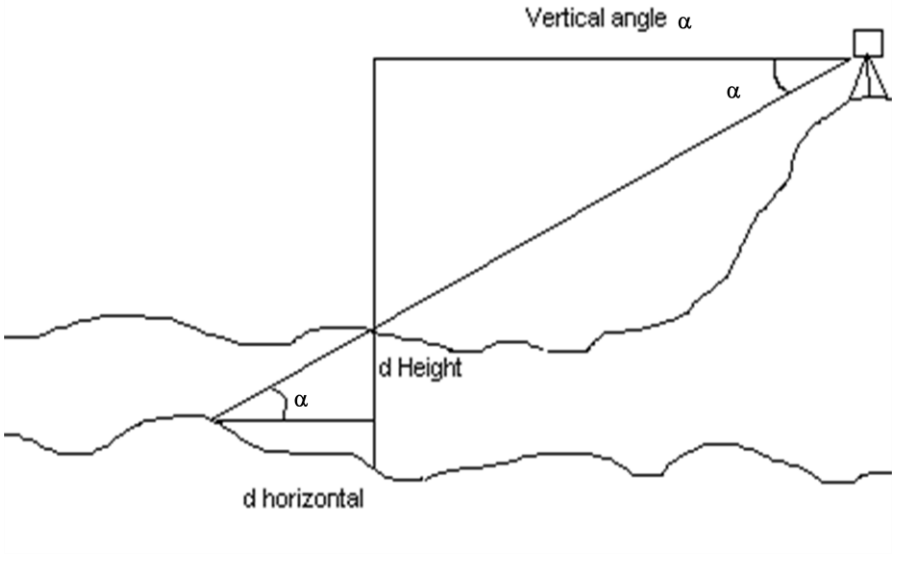

Figure 4-5: View angle and distance decides the horizontal accuracy

$$d\ Horizontal = \frac{dH}{\tan\propto} \tag{4-5}$$

$$\tan \propto = \frac{dZ}{\sqrt{dX^2 + dY^2}} \tag{4-6}$$

Table 4-7 displays the horizontal accuracy caused by different accuracy of the elevation model. The table is an extract of appendix H, which include the measured terrain points measured in 2007 and summer 2009 from figure 2-11.The points measured autumn 2009 and summer 2010 are leaved out because they are almost the same as summer 2009. Table 4-7 show a remarkable difference in position accuracy between images recorded with camera 1 and 2. The accuracy is almost double as good in images from camera 2 compared to camera 1. The oblique distance to the point most far away from camera is more than twice as to the closest point, and then also the horizontal accuracy. But this effect decrease for

points which are farer away from the camera. The close position between camera and measured points is very important because of the deep vertical view angle to them.

Table 4-7: Horizontal accuracy influenced by the digital elevation model, an extract of appendix H.

Point	Distance, m	dH = 14 m, m	dH = 8 m, m	dH = 20 cm, m
Camera 2				
Minimum value	1027	39.76	22.72	0.57
Mean	1610	65.39	37.37	0.93
Maximum value	3018	130.06	74.32	1.86
Camera 1				
Minimum value	1924	95.34	54.48	1.36
Mean	2690	128.51	73.44	1.84
Maximum value	3999	197.34	112.77	2.82

The position accuracy will in additional be influenced the relative adjustment of image and elevation model. (Ch. 2.6) It is difficult to make all the points from the elevation model coincide with all position in the image. Ground control points is helpful in this process, but are decided from ArcGIS which results in an accuracy in the order of 100 m, instead of having known terrain coordinates measured in the field. The target position has largest influence of the fitting process, and is found in same way as the GCPs. Rotation of image and changing the scale by the focal length results in different adjustment. The consequences of numerical change in target position, scale of rotation are tried out, and displayed in table 4-8.

Table 4-8: Consequences of changing parameters in Geophotoref

Parameter	Consequence
Changing target X with 10 m	X coordinate change with less than 10 m, Y coordinate with around 1 m
Changing target Y with 10 m	X coordinate change with around 10 m, Y coordinate with around 20 m
Changing target Z with 10 m	X coordinate change with around 100 m, Y coordinate with around 300 m,
Changing rotation with 1 deg	X coordinate change with around 5 m, Y with around 10 m
Changing scale with 1 mm	X coordinate change with around 10 m, Y with around 10 m

The velocity change very much dependent of the terrain coordinates. The highest individually difference is in the area near the glacier front. Change of z value is the only change in the table around which cause in remarkable change in velocity. The other changes cause less than 1 m in velocity difference. But the velocity difference is not interesting, since it is measured in different terrain points.

The position difference is not the same for all the measured points in the result file, but mainly changing of 10 m in x or y value of the target position results in around 10 m difference in both x and y direction of the points. Changing z value of the target cause in large terrain displacement in x and y of the point

(Coincide with large difference in velocity), but very little in z. Changing of 1 deg in rotation or 1 mm in scale give less change in both x and y coordinates of the point.

The testing shows change of the coordinate value, but small and irrelevant change in velocity.

4.1.6 Spatial resolution

The ground pixel size explains the spatial resolution of the image and the measured points in the image. Different vertical view angle and distance to the measured points is an effect of oblique images. The size of the images sensor and the distance to the point decide the scale and ground pixel size of the point. (Eq. 2-1 & 2-2)

The result will not be better than half of the pixel size when working with integer number. Many of the earlier explanations about accuracy are in the magnitude of pixels, but the metrical value is more comparison and interesting. The accuracy in meter depends of the image position. The points closest to camera 2 will have best and smallest spatial resolution (Ground pixel size) with 23 cm according to table 4-9. (Appendix H) The points closest to the front have larger resolution because they are closer to the image edges.

Table 4-9: Spatial resolution of the measured points, extracted from appendix H.

Point	Distance, m	Vertical angle, deg	Horizontal angle, deg	Ground pixel size, m
Camera 2				
Minimum value	1027	-19.40	233.30	0.23
Mean	1610	-13.86	250.38	0.36
Maximum value	3018	-6.14	262.83	0.67
Camera 1				
Minimum value	1924	-8.35	60.35	0.65
Mean	2690	-6.57	68.15	0.91
Maximum value	3999	-4.06	78.00	1.35

Table 4-9 show the planimetric resolution (Parallel to the image sensor), but it will is larger along the view direction, dependent of the view angle. The glacier is sloping parallel to the image sensor, and makes this planimetric resolution be the spatial resolution of interest.

The ground pixel size compared with the result files from Cias and Geophotoref. The displacement in the result files from Cias is in pixels, and the one from Geophotoref is in meters. Multiplying the result from Cias with the pixel size gives metrical value of the displacement. (Eq. 4-7) This value is similar with the one in the result file from Geophotoref. The comparison show up to coincide.

$$Displacement\ in\ pixel, Cias * pixel\ size = Displacement\ in\ m, Geophotoref \quad (4\text{-}7)$$

4.2 Total error

The incorrect counted velocity for one point in a chosen period is the sum of all the errors. (Ch. 4.1) The errors cannot be summarized directly, since the error contribution influence the measured velocity in different direction and amount, the errors affect each other and the size of an individual error is unknown. Comparison of the velocity result to a trustable number is the easiest way to find the accuracy.

This uncertainty in the velocity measurement can be decided as the standard derivation (Eq. 4-8), which explain how much the velocity variety around the given velocity. All the counted standard derivations in this thesis are divided on the days to get the uncertainty for each daily velocity.

$$\sigma = \sqrt{\frac{1}{n-1}\sum_{i=1}^{n}\left(x_{a,i} - x_{b,i}\right)^2} \tag{4-8}$$

$\sum_{i=1}^{n}\left(x_{a,i} - x_{b,i}\right)^2$ is replaced by the differential vector multiplied with the translated edition, when doing the calculations on matrix form.

$x_{a,i}$ is the unknown daily velocity found by measuring in terrestrial measurement, $x_{b,i}$ is the known daily velocity the our results is compared with. The uncertainty of our measurement can be found if we have $x_{b,i}$ to compare our results with, but no solution exists.

4.2.1 Comparison between different matching interval

All the images are matched with 2, 4 and 8 days between. One and 16 days are also tried, but without success. Comparison of the results from same dates but different matching interval could be a useful way of checking results.

As first sight, the sum of the measured velocities (By eq. 2-8) during one period should be the same independent of the number of days between the matched images pairs, and then also the average velocity of the different matching interval. This theory does not work out, since the direction of the vectors are not the same during the time. The velocity shall not be the same, but can still be compared; since the velocity measured every 2nd day shall not be smaller than the velocity measured every 8th day. A standard derivation calculated from the different matching intervals will not be valuable as telling the accuracy.

Comparing the graphs of the different matching interval is helpful to say if there is some mistaken matched points in the series, since the relative temporal variation shall be similar. Anyhow the sum of them are different, the graphs from measuring every 4th day shall fall within graphs from measurement every 2nd day. The same is expected with graphs of respectably 4 and 8 days between. (Ch. 5.1.1)

Different matching interval suits for different requirement. The sum of several velocities is not the same as the direct measuring of the same period. If every day velocity is wanted, matching of images with one day between is best to use. But if velocity every 8th day is wanted, is it better to measure in images with 8 days between, instead of summarizing 7 match. The same velocity does not appear because of

different direction of the velocity and the percentage uncertainty increase with fewer days. The uncertainty of the transformation is related to each match. Velocity measurement with small time interval cause a smaller movement, but the errors are nearly the same, which makes a bigger fractional uncertainly.

4.2.2 Estimate of total accuracy

All the elements in chapter 4.1 influence the accuracy and decide the total uncertainty together. Table 4-10 tries to summarize them in a well balanced way.

Table 4-10: Sources of uncertainty.

Source of uncertainty	Amount of influence, pixel
No updated camera calibration	~ 0
No perfect transformation	≤ 1 for camera 1, and ≤ 3 for camera 2
Matching	~ 0, since the most incorrect ones are deleted
Georeferencing and elevation model	~ 0
Total uncertainly	1.5 for camera 1, and 3.5 for camera 2

The uncertainty of the transformation is the largest and following the most dominant source. (Ch. 4.1.2) Calibration, matching, elevation model and georeferencing also influence the accuracy, but their contributions become very small compared to the uncertainty caused by transformation. None of the sources are zero, but they are close to zero (~ 0), and very small compared to the domain source. But since they have a small effect, are several and have unknown size, the total influence of them will be something else than zero. 0.5 pixels are decided to be the sum of the uncertainty caused by accuracy influence from all the other sources than the transformation in each match. This small number shows that their influence is closer to zero than one, but still it is something. It is better to under estimate than over estimate when talking about accuracy.

Together with the known accuracy of 1 and 3 pixels in not optimal transformation (Ch. 4.1.2), the total uncertainly will be 1.5 pixels for images from camera 1, and 3.5 pixels for camera 2. The metric accuracy depends of the pixel size, and can be found by equation (4-9).

$$Accuracy = accuracy\ in\ pixel * pixel\ size \tag{4-9}$$

The spatial resolution (Ground pixel size) of each point is found in appendix H and table 4-9. Table 4-11 displays the numerical accuracy of a sample of points (The points used in graphs in ch. 3 and 5). The distance influences the spatial resolution, the spatial resolution influences the accuracy, and the days between matched images decide the accuracy per day.

Table 4-11: Accuracy in meters

Point	Camera distance, m	Ground pixel size, M	Accuracy, pixel/ match	Accuracy, m/match	Accuracy, m/day
Fig. 4.2: Spatial resolution					
(447275,8757760), 2007	1905	0.42	3.5	1.47	0.37
(446774,8756787), summer 2009	2376	0.81	1.5	1.22	0.30
(446754,8756731), autumn 2009	2317	0.78	1.5	1.17	0.29
(446731,8756675), 2010	2257	0.76	1.5	1.14	0.29
Fig. 4-6: Cross profile					
(447214, 8758843), 2007	924	0.20	3.5	0.70	0.18
(446869, 8757881), 2007	1909	0.42	3.5	1.47	0.37
(446489, 8756240), 2009	1769	0.60	1.5	0.90	0.23
(447435, 8758094), 2009	3831	1.29	1.5	1.94	0.48
(446453, 8756083), 2010	1615	0.54	1.5	0.81	0.20
(447781, 8758650), 2010	4478	1.51	1.5	2.27	0.57
Fig. 4-9: Acc., summer 2009					
(446537,8756753)	2264	0.76	1.5	1.14	0.29
(446616,8756774)	2308	0.78	1.5	1.17	0.29
(446690,8756775)	2334	0.79	1.5	1.19	0.30
Fig. 5-2: Climate, 2007					
(447235, 8756628)	3018	0.69	3.5	2.42	0.60
Fig. 5-3: Climate 09/10					
(446616,8756774), Summer 2009	2308	0.78	1.5	1.17	0.29
(446606,8756716), Autumn 2009	2251	0.76	1.5	1.14	0.29
(446579,8756624), 2010	2155	0.73	1.5	1.10	0.27

Points 1.5 km from camera 2 have a ground pixel size of 0.33 m, which gives an accuracy of 0.29 m/day if 4 days between the matched images. Points 2.5 km from camera 1 make a pixel size of 0.84 m, which gives an accuracy of 0.32 m. The different accuracy from the two cameras arises from larger distance between points and camera 1, smaller focal length in camera 1 and less uncertainly caused by different reference frame. The accuracies from this table are used to explain the graphs in chapter 3 and 5.

The uncertainly caused by spatial resolution show up in all matched pairs. The daily uncertainty will decrease with more days between the images. The challenge will then be to find the best balance between the temporal and spatial resolution.

5 Discussion

5.1 Temporal resolution

5.1.1 Different matching interval

The velocity measurement is done with matching in image pairs with 2, 4 and 8 days between. Figure 5-1 shows the comparison of the different matching intervals of measurements from summer 2009. One and 16 days are also tried as an alternative temporal resolution, but without success. The graph is getting smoother as more days it is between the images in one pair. At the same time the temporal information becomes poorer. The accuracy of daily velocity increases with number of days between the images. That is because the uncertainty depends on each match. (Ch. 4.2.2)

The graph with 4 days between the matched images indicates the temporal velocity change in the easiest way. It smoothes the graph with 2 days between, but still get the interesting temporal variations as wanted. Matching with 8 days between is useless in this case, since the temporal variations are some of the main wanted information from this method. The idea of the comparison was to check how good temporal resolution is possible to get without disturbing the accuracy of the results.

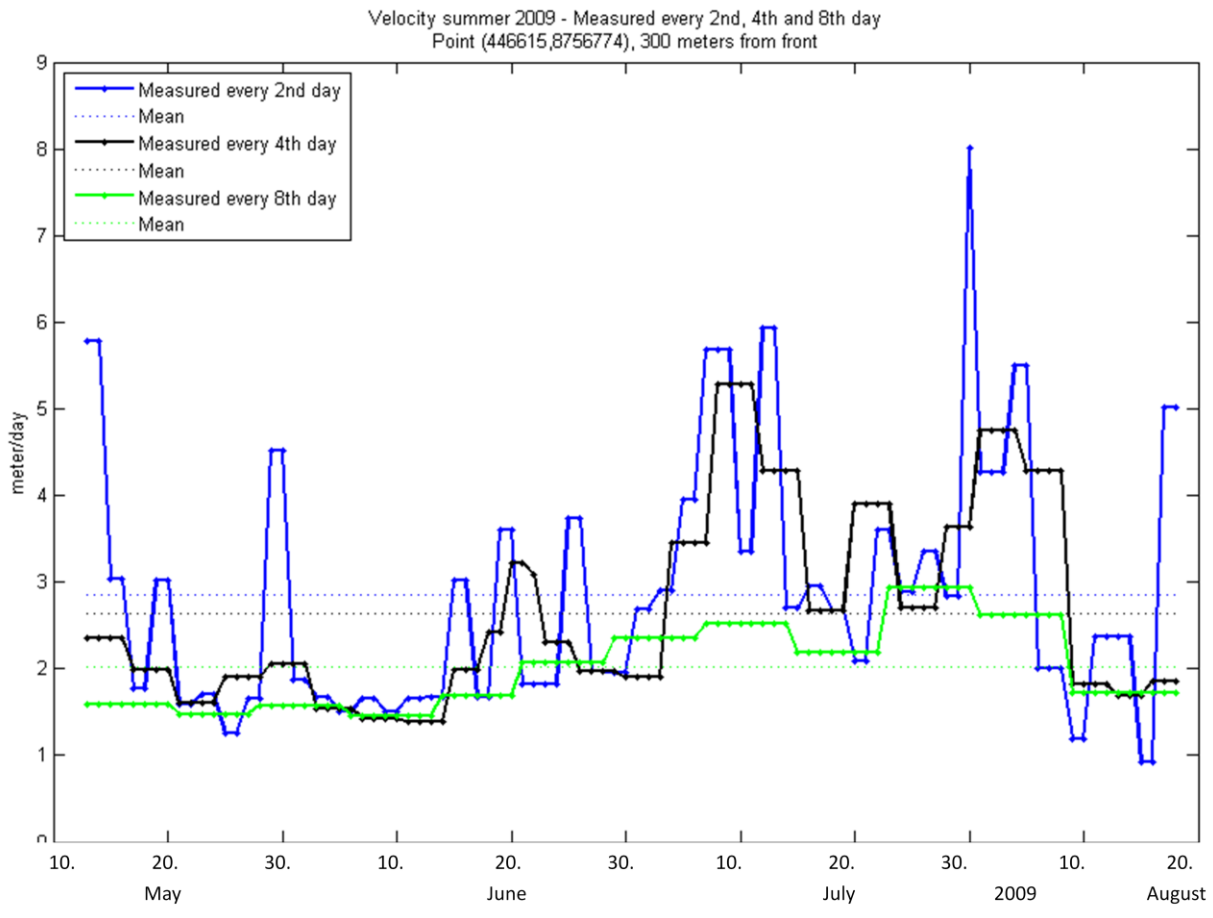

Figure 5-1: Different matching intervals for point (446616, 8756774) nr. 15 in fig. 2-12.

The graph with 4 days between each match, is exactly the same as the one 300 m from front in figure 3-10. The numerical information which is not in table 5-1 can therefore be found in table 3-3. The accuracy is picked out from chapter 4.2.2, and the rest are extracted from the graphs themselves.

Table 5-1: Numerical information about figure 5-1

Days between matched images	Average velocity, m/day	Minimum Velocity, m/day	Maximum velocity, m/day	Standard derivation, m/day	Accuracy, m/day
2	2.85	0.92	8.00	1.43	0.58
4	2.64	1.38	5.29	1.12	0.29
8	2.02	1.46	2.94	0.48	0.15

5.1.2 Choice of temporal resolution

Figure 3-2 shows the temporal variations of the velocity. With background in chapter 5.1.1, is 4 days chosen as the matching interval between images. This number is used in all the graphs above. The possibility to find velocity between few days is the main advantages of using terrestrial images. The satellite images are restricted by the orbit and geometrical conditions to have for more than 12-19 days between the images of same area.

Figure 3-2 shows the difference in velocity between days. The velocity in 2007 varies from 0.35 m to 7.69 m with an average of 2.34 m/day (Table 3-1). The largest value can be explained by a raining event in chapter 5.3. The big variations appear evident in 2007 because of larger ground pixel size. The velocities measured from camera 1, in 2009 – 2010, appears more similar to each other. The velocities vary from 1.32 m to 6.39 m with a mean of 2.74 m. The biggest velocities appear in June and July for all the three years.

Most of these temporal variations are lost by only using satellite images for velocity measurement. Matching terrestrial images with too few days between includes too much noise to get good information of the measurements. A good balance of small noise, enough measurement during a period and good enough accuracy decide how god temporal resolution which are possible and interesting to use.

5.2 Spatial variation

All the graphs in chapter 3.2 show the spatial resolution of the velocity. The velocity distribution on the glacier change a lot, both systematically and random. One of the systematic parts of the distribution is the acceleration towards the front. Figure 3-10 shows a faster velocity of the point closest to the front, compared to the points that are farer away in the same line. The calving events appear at the front, and the points closest to an event will be influenced most. When the closest point get velocity from the calving event, the next point will get velocity from the point forward going faster and the next one will be influenced by the one in front of it, and so it goes. This results in acceleration towards the front.

Velocity measurements further away from the front will not satisfy the velocity needed close to the terminus, since the velocity change much according to the distance from the front. The velocity close to the front is of main interest in relation with calving events. Stake and GPS measurement gives good results, but are too dangerous to use close to the front. Photogrammetric measurements make it possible to find velocity from a safe distance to the front. Terrestrial photogrammetry exploits good temporal resolution from ground measurement and safe distance from photogrammetry.

The velocity depends of the position across the glacier tongue, in additional to the along tracking velocity. Figure 3-6, 3-7, 3-8 and 3-9 show the cross profile of the glacier in 2007, 2009, 2010 and all years together. The glacier moves fastest in the middle position and more slowly close to Colletthøgda and the moraine between Kongsvegen and Kronebreen. (Fig. 2-2 & 2-4)

Using images with a ground pixel size of 0.23 m (Ch. 4.1.6) in terrestrial images instead of 2 m (Spot Image, 2010) in satellite images gives a large advantage when finding spatial resolution of the velocity. The spatial resolution of the images used for velocity measurement decides the possibility of extracting the spatial distribution of the object itself. (Kronebreen) Small ground pixel size makes it possible to measure different velocity within a smaller area, which gives a more detailed spatial distribution of the velocity of the glacier.

5.3 Weather effect on the velocity

Glacier motion is explained together with calving and seasonal variations in chapter 1.1. All the conditions around the glacier have influence on the velocity. The landscape and area decide the slope, gravity forces, pressure, accumulation and ablation. Velocity variations appear because of varying climate and weather conditions during time. Seasonal variations in climate cause the main differences, in additional to short-time variations. All elements of climate (pressure, wind, sun, temperature and precipitation) and connection between them have influence on the velocity variations. Precipitation and temperature have the largest effect because of the big water amount effect.

Sub glacier water from the surface makes the glacier slide on the glacier bed. The water comes from raining and melting surface by increasing temperature. The temperature usually changes through the seasons, while the rain amount together with large temperature variation has more short-term variation. The glacier tongue moves fastest during the first few days of a rainy period before the water percolate through the accumulation zone, and slowest just after the rain stops. The pushing from the accumulation zone above decreases after the rain stops. (Fountain & Walder, 1998)

The temporal variations in other points than in figure 3-2 are showed in figure 5-2a (2007) and figure 5-3a (2009-2010). Both the two graphs are compared with climate data; temperature (Fig. 5-2b & 5-3b) and precipitation (Fig. 5-2c & 5-3c). (Norwegian Meteorological Institute, 2010)

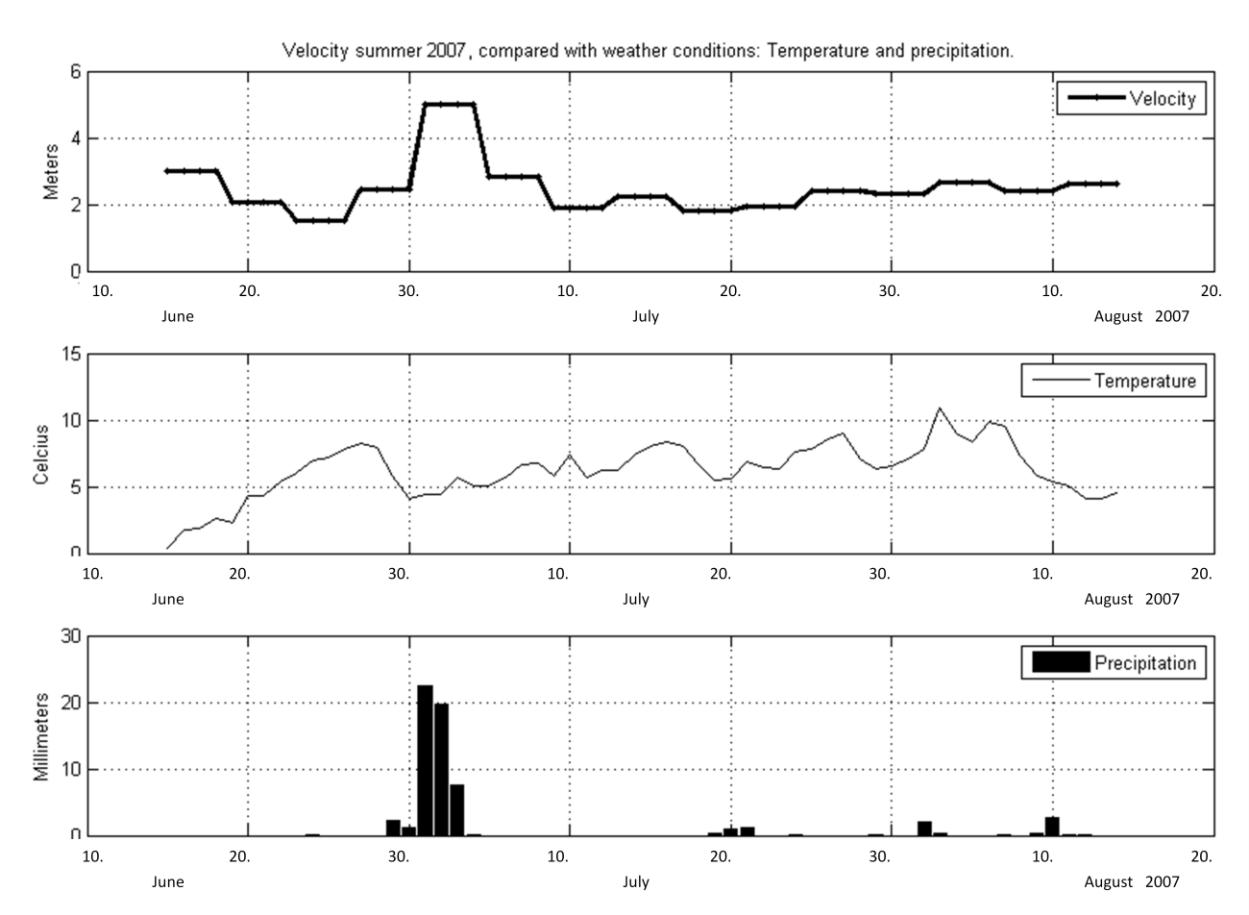

Figure 5-2: a) Velocity 2007 **b) Temperature 2007** **c) Precipitation 2007**

The velocity in figure 5-2 are measured in point (447235, 8756628), which lies 3000 m from camera and 700 m from the glacier front. Table 5-2 shows a velocity variation between 1.52 m and 5.01 m, with an average of 2.47. The graphs show that the velocity for the given point increased during the period with much rain in the beginning of July. The other tops of velocity fit together with increase in temperature. The cause is that higher temperature produce more melt water, which lets the glacier slides more.

Table 5-2: Numerical information about figure 5-2a.

Coordinates of the point, (x, y)	(447235, 8756628)
Point from figure 2-11	29
Average velocity, m/day	2.47
Minimum velocity, m/day	1.52
Maximum velocity, m/day	5.01
Standard derivation, m/day	0.79
Distance to front, m	700
Distance to camera, m	3018
Spatial resolution, m/pixel	0.69
Accuracy, m/day	0.60

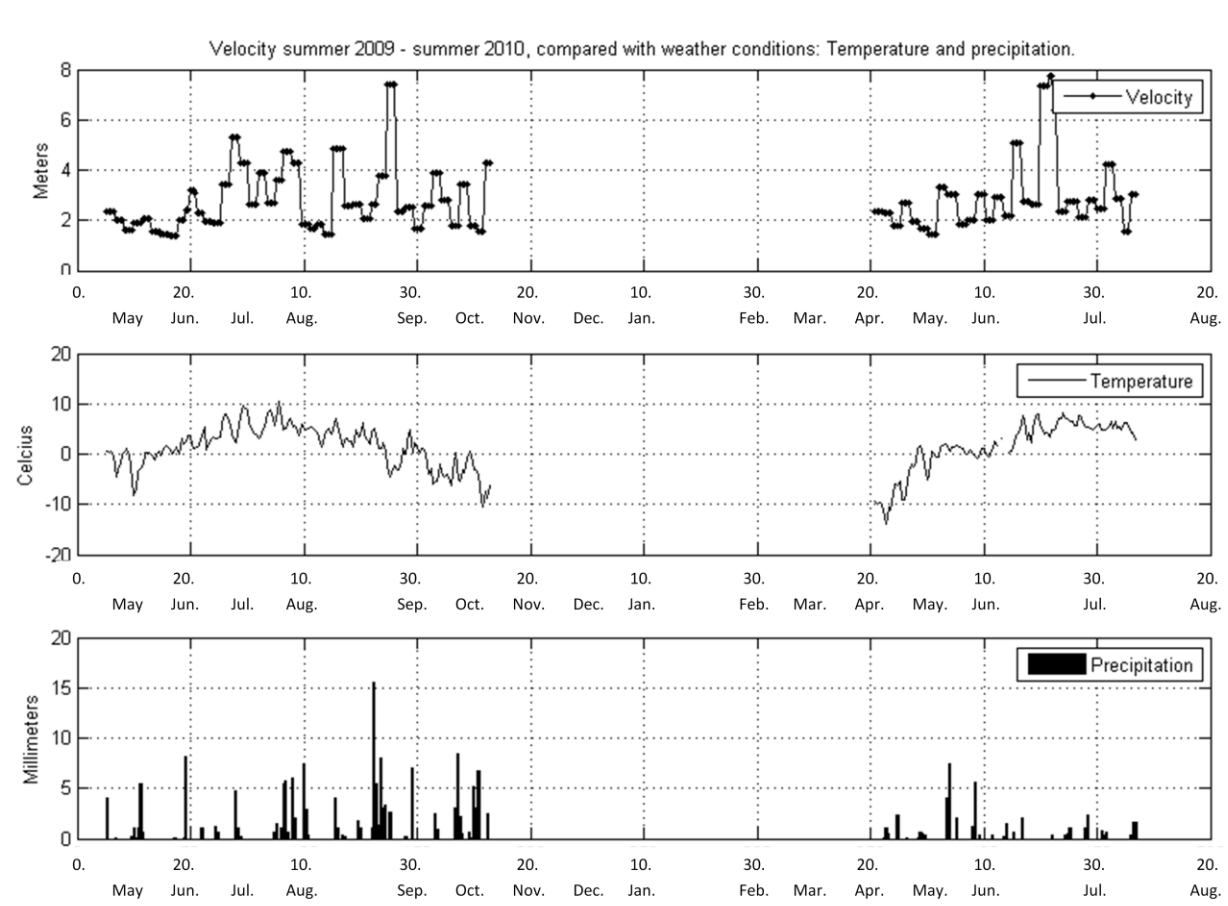

Figure 5-3: a) Velocity 2009-2010 b) Temperature 2009-2010 c) Precipitation 2009-2010

The velocity in figure 5-3 is measured in point (446616, 8756774), 2300 m from camera and 300 m from glacier front. The velocities vary from 1.38 to 7.75 m, with an average of 2.84 m, according to table 5-3. The highest velocity in 2009 falls together with the biggest rain event in august. The other high velocities come few days after raining too. The velocities in July 2009 increase without increasing precipitation, but the temperature seems to be the reason in these cases. The same happens in 2010: Increasing precipitation results in higher velocities the following days. It is enough with higher temperature to increase the velocity in July and June.

Table 5-3: Numerical information about figure 5-3a.

Date	13.05 – 16.08, 2009	17.08 – 29.10, 2009	16.04 – 10.08, 2010
Coordinates of the point, (x, y)	(446616,8756774)	(446606,8756716)	(446579,8756624)
Point from figure 2-12	15	15	15
Minimum velocity, m/day	1.38	1.42	1.44
Maximum velocity, m/day	5.29	7.42	7.75
Average velocity, m/day	2.64	2.98	2.90
Standard derivation, m/day	1.12	1.43	1.40
Distance from front, m	200	200	200

Distance to camera, m	2308	2251	2155
Spatial resolution, m/pixel	0.78	0.76	0.73
Accuracy, m/day	0.29	0.29	0.27

5.4 Comparison with other datasets

5.4.1 Analog terrestrial photogrammetry in same area

Kronebreen is an interesting glacier for study because of the fast and varying motion. There are several old measurements of the glacier velocity that can be used for comparing with the measurements in this study. Stake measurement, airborne photogrammetry, remote sensing with satellite images and even terrestrial photogrammetry have already been used in the same area as this study.

The velocity is measured on Kronebreen with analog terrestrial photogrammetry by Pillewize in 1938 and 1962. Voigt has measured the velocity in 1962 and 1964-65. The last one gives overall information about velocity across the glacier front, along the glacier and the change through the year. A special attention drawn to this measurement because of the position of the camera: One of the bases is almost similar to images taken with camera 1, but seems to measure further away from the front. Figure 5-4 show the cross profile measured from this position in August and July 1964. (Melvold, 1992)

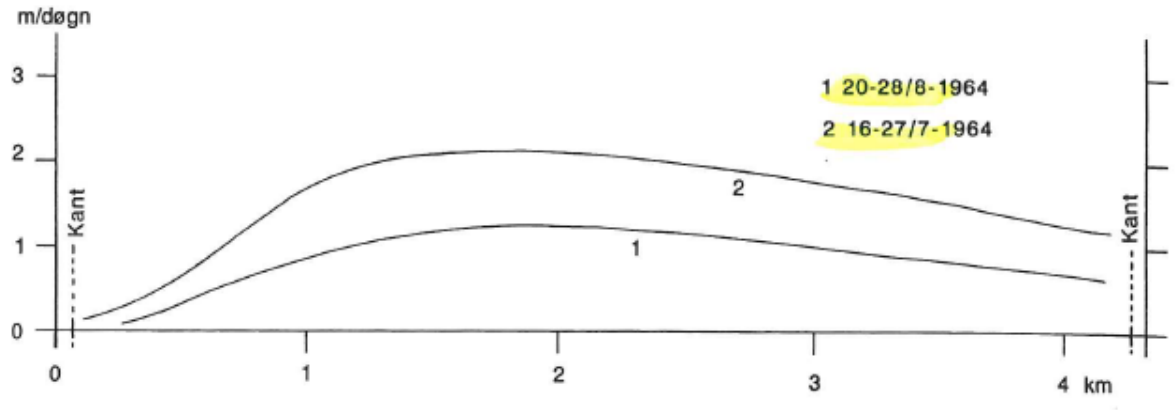

Figure 5-4: Cross profile of Kronebreen measured of Voigt in 1964. (Melvold, 1992)

Melvold (Melvold, 1992) measured the same area in 1989-90 (Spring and autumn both years.) as Voigt did in 1964-65. He has used analog, terrestrial photogrammetry with 10-11 days between the images, to get the velocity of the same area. A cross profile (Fig. 5-5) is made by measuring a line across the glacier tongue of both Kongsvegen and Kronebreen in 4 different dates. Figure 5-5 displays a velocity of 1.3-1.4 m/day 250 m north of the moraine, and 0.2-0.3 m/day 50-80 m north of the moraine. The moraine itself has very small motion compared to Kronebreen.

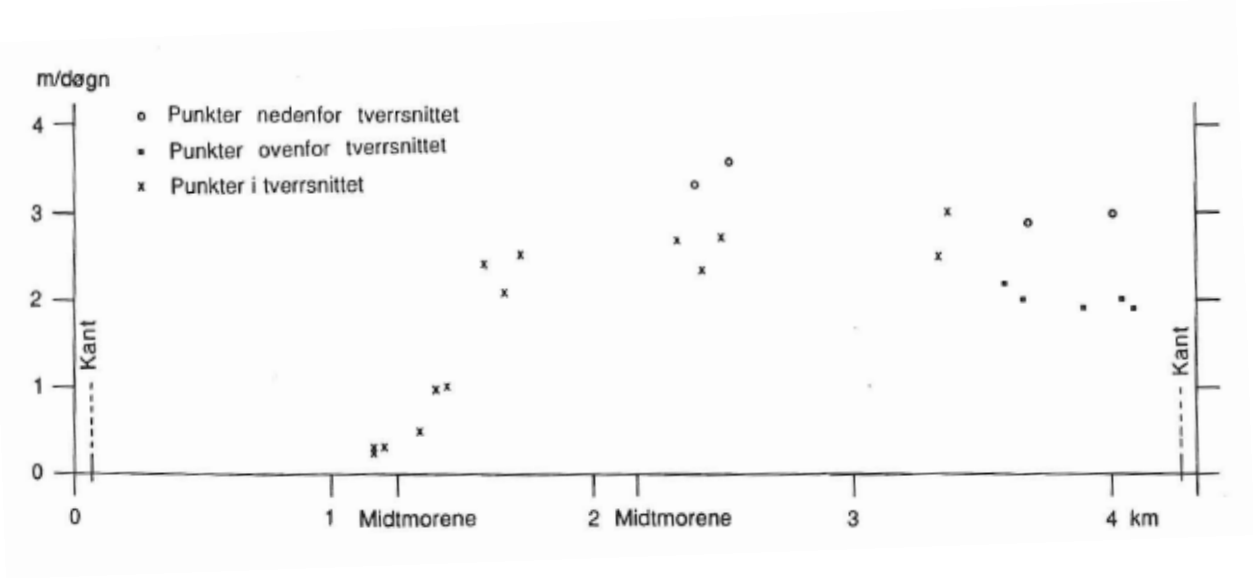

Figure 5-5: Cross profile from 1990 (Melvold, 1992) South to the left and north to the right.

The absolute values of the velocities are not representative because of different distance to the glacier front and different terrain coordinates. But the distribution of the velocity across the glacier is probably not changing too much, although these velocities are found my measurement up to 20 years ago. The velocity distribution can be recognized with the cross profiles found in 2009 and 2010. (Fig. 3-7 & 3-8)

5.4.2 GPS measurement at the same time

There are other measurements of Kronebreen ongoing today. The big activity of the glacier and the position close to civilization makes Kronebreen a popular object for science. Stake measurements are restricted to amount of data since you need safe access to every measured position. The areas where stake measurements are used are often safer to visit because of little motion and fewer crevasses. GPS measurements give better temporal resolution because the measurements are of continuing. The GPS only need to be visited for changing memory card and battery, just like the time-lapse cameras.

Nuth (Nuth, unpublished) has GPS measurement from May 2008 to May 2010. Figure 5-6 shows the length and the direction of the displacement in m/day and degrees. The position of the measurements is around 4 km above the glacier front. The absolute velocity will be higher in measurements closer to the front because of the acceleration. But still Nuth's measurements are very valuable for comparison. The relative variations are probably the same since the same weather conditions has been the same on the whole glacier at same time.

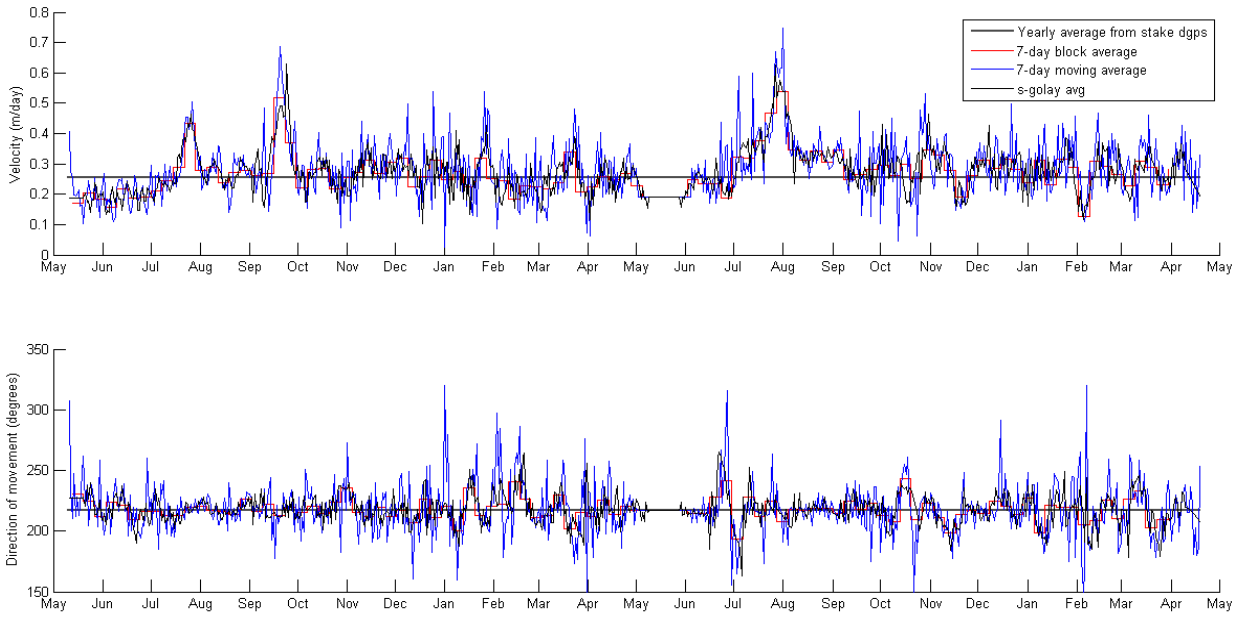

Figure 5-6: GPS Measurement from 2008 to 2010 (Nuth, unpublished)

Figure 5-6 show a big increase in velocity in end of July/beginning of August 2009. The velocity grows from June, but slow done towards September. The increasing and decreasing through the summer seems to fit with the temperature variations in figure 5-3. Some of the peaks that look like outliers in figure 5-6, also appear in the photogrammetry measurement in figure 5-3a. These peaks coincide with increasing precipitation (Fig. 5-3c), but look stronger in figure 5-3a. It looks like all the conditions strengthen the velocity in the front more than further away from it.

5.4.3 Velocity measurement from satellite images at same time

Satellite images have been used for measuring velocity for a long time. High resolution satellite images are here used to extract velocity from the images. (Spot Image, 2007)

The velocities are extracted directly from a velocity matrix by choosing squares which are in accordance with the terrain coordinates of the measured points. The velocity matrix are received from Etienne Berthier (Berthier, unpublished), who has made velocity matrix from time following satellite images. The satellite images has a spatial resolution of 2 m, and the velocity matrix have a grid of 32 m. (Spot Image, 2010)

The velocity from the matrix is no solution, but a good comparison to the velocity from our terrestrial images. The given accuracy is 0.20 m. (Spot Image, 2010) Another way to find the accuracy is to extract the velocity of the squares around the wanted one. Three different velocities are found for the same terrain point: The velocity in the square which corresponds to the terrain point, the average of the velocities in 9 surrounding squares and an average of 25 squares. Table 5-4 shows the standard derivation (Eq. 4-8) between finding the velocities in these three ways.

Table 5-4: Standard derivation when using different numbers of square to extract velocity from satellite images.

Between	1 and 3*3 squares	1 and 5*5 squares	3*3 and 5*5 squares
Standard derivation	0.06 m	0.08 m	0.05 m

The velocity found by 5*5 surrounding squares is used to compare with the velocity from terrestrial images. It is more useful and safer to choose more squares because of the uncertainty in the terrain coordinates of the measured point.

The velocities from Formosat satellite images are measured with 12, 19 and 18 days between. (14th and 26th of June, 15th of July and 2nd of August) Comparing these velocities with velocity from terrestrial images from the same days is most correct. But many days between the images make the automatically matching in Cias struggle to find correct match. Only 2 of 34 points in the result find correct match in all the three pairs. Comparison between velocity from terrestrial and satellite images works badly since these two methods have different area of application. Terrestrial photogrammetry works best with good temporal resolution which is not possible to get from satellite images.

Comparison of the velocity from satellite images with our every 2nd day measurement from the same period is more correct. Figure 5-7 shows that the velocity from the satellite images falls within the variability in the velocity from terrestrial measurement. The graph shows the temporal variation of two different terrain points. The velocities from the satellite images are extracted from the same two terrain points.

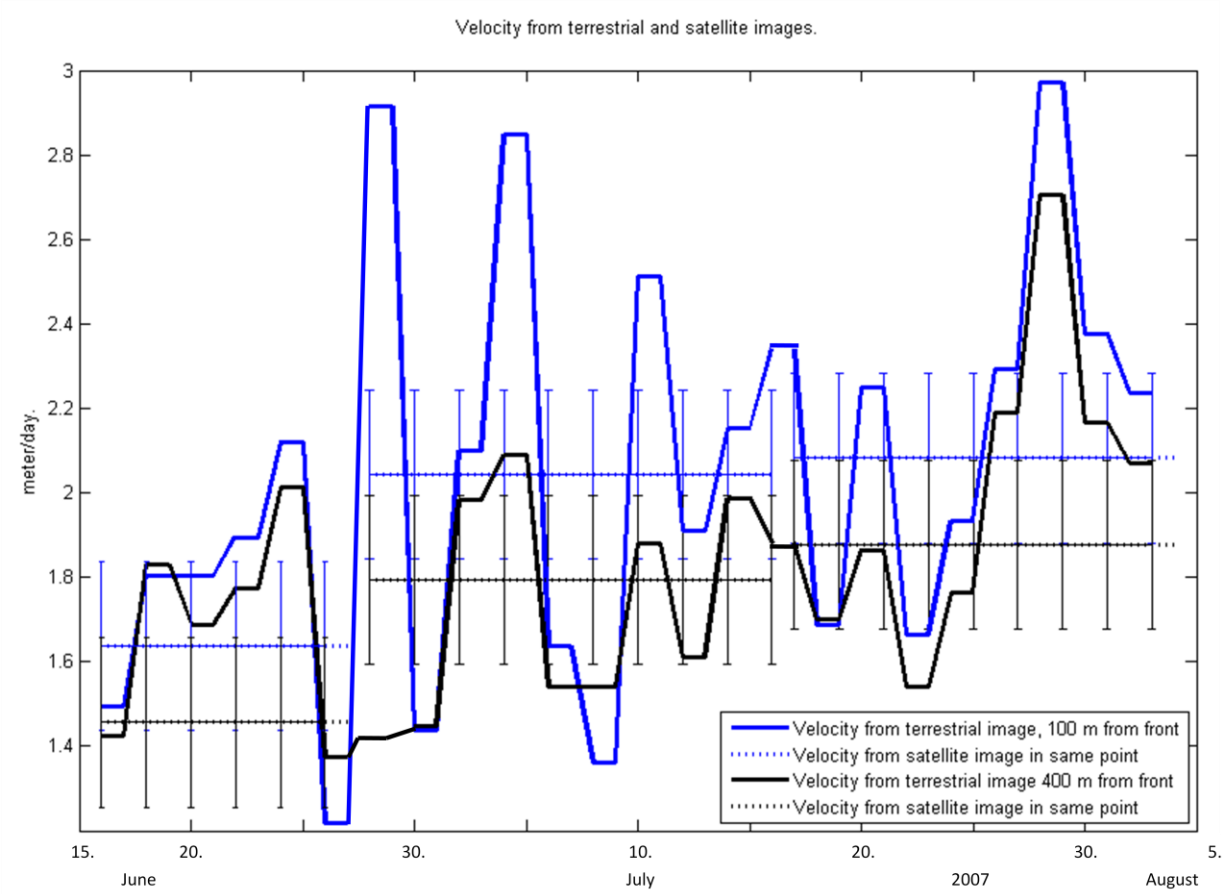

5-7: Velocity measured with terrestrial and satellite image, 14th of June to 2nd of August 2007.

Table 5-5: Numerical information of figure 5-7.

Graph	Terrestrial, 400 m from front	Terrestrial, 100 m from front	Formosat, 400 m from font	Formosat, 100 m from front
Coordinates of the point, (x, y)	(447311,8758631) Point 5, fig. 2-11	(447137,8758749) Point 8, fig. 2-11	(447311,8758631) Point 5, fig. 2-11	(447137,8758749) Point 8, fig. 2-11
Minimum velocity, m/day	1.38	1.22	1.46	1.92
Maximum velocity, m/day	2.71	2.97	1.88	1.63
Average velocity, m/day	1.87	2.06	1.71	2.08
Standard derivation, m/day	0.34	0.47	0.22	0.25
Distance to camera, m	1073	1036	888513	888513
Spatial resolution, m/pixel	0.24	0.23	2.00	2.00
Accuracy, m/day	0.42	0.40	0.20	0.20

Figure 5-7 shows an increasing velocity from June to August 2007. The same happen in the velocity measurement from both the terrestrial images and the satellite images. The point closest to the front has largest velocity in both cases. Two days between the measurements from terrestrial images make larger uncertainly in the result, but better display the different in the temporal resolution between the two methods.

6 Further work

6.1 Use of the results

Velocities measured by matching of images with 4 days between are the most usable ones, and as consequence used in the velocity graphs. The velocity graphs will be used in Anne Chapuis doctoral dissertation about calving. (Ch. 1.1) Own observations about calving amount, together with glacier velocity from these terrestrial measurements gives the calving rate by equation (1-1).

The graphs with velocity together with climate data (Fig. 5-2 & 5-3) are of main interest, but all the graphs gives a totally picture of the velocity together. Figure 3-8 show that the points measured from camera 1 and camera 2 coincide on the glacier, which makes it possible to make a more complete velocity distribution across the glacier. By using images of both the two cameras at same periods also gives a new way of comparison of the results.

6.2 Improvement of the method

The method with terrestrial photogrammetry is based in many good ideas. Time-lapse cameras with solar panel easily give big amounts of data, the computer program Cias makes it possible to automatically match many points at once to see displacement, and Geophotoref only needs an elevation model to transform the pixel displacement into velocity in meters. But during work the method, there is still more than one thing that has showed up to be not satisfactory.

The main uncertainty of the results is a consequence of images in not exactly the same reference frame caused of missing trustable, stable and same-looking area and conjugate points to decide the transformation. An improvement of finding good transformation parameters between the images will make better accuracy. The raw images are the limitary factor for finding good reference area with useable conjugate points. Attributes of the ground and weather conditions will probably still make motion of the camera during the time, and following requirement of finding transformation between images recorded from same position. The decision of finding transformation parameters need to be done in a smarter way.

Clear, trustable, well defined and not changing physical conjugate points with no motion are necessary and short supply in the images. Having enough such points to find the image coordinates of, gives the correct transformation. The points can be colored marks spread around the mountains in the trimmed print. But it is illegal to paint and change the landscape inside a natural reserve.

The adjustment between image and elevation model has the main influences on the position accuracy. Measuring terrain coordinates of the painted marks will make the adjustment easier and more correct. Field measurement will help without painting too, as long as the measured point is possible to find in the image view.

Test photographing with the same camera before or after data collecting can decide the accuracy of the results. Measuring stakes on the glacier in both camera and total station makes a good workable measurement comparison that can be done at the same time as the images are taken.

The accuracy is indirectly dependent of the spatial resolution of the images. Longer focal length increases the ground pixel size in the image by equation (2-2). The view angle is important for the adjustment between elevation model and image, but is best by camera still being at the same position.

Clear and no change in the weather make the matching process in Cias working better, but it is not possible to influence the weather conditions. The matching in Cias works, but the percentage of correct matched points is not good enough. Edge detection, for instance, has worked successfully in a similar method for velocity measurement in Greenland. (Yushin & Box, 2010), and can easily be implemented in MATLAB. Our solution has been to choose more points than needed, and then just remove all the points with known incorrect match from the result files.

7 Conclusion

The method of georeferencing displacement found by image matching works very well with terrestrial images. Choosing a suitable size of template and search area, few enough days regarding the size of the displacement and images with similar weather, increases the percentage of correct matches. Using images from the same reference frame, makes it possible to do the adjustment between elevation model and image just once in the georeferencing process, and gives the same image points the same terrain coordinates in all the result files.

Camera motion makes it necessary to transform the images into the same reference frame. Although this is the most time-consuming part of the work, the used transformation formula only includes the translation in x and y direction. To include the effects of rotation it is necessary with enough conjugate points well distributed in the whole images, in contrast to the few usable points in the middle of the background in our images. A more complete transformation of the images would improve the total matching method considerably.

The small and unwanted difference in reference frames between the images, is the main source of the uncertainness in the results. Difference in reference frame between already transformed images is found by measuring displacement of still points and by the implemented Conform transformation in the matching program, Cias. The maximum difference is 1 pixel in images from camera 1, and 3 pixels in images from camera 2. When including the uncertainness of non updated camera calibration, elevation

model, matching and georeferencing process, it makes respectively 1.5 and 3.5 pixels in uncertainty. The total uncertainty can also be found by field measurements in concurrent area as the camera view, by giving a solution to compare the results from terrestrial images with.

The distance between the position of the camera and measured points decides the numerical uncertainty in meter. The displacement accuracy of image pairs is 0.81 m in each match, with a ground pixel size of 0.23 m of points 1 km away from camera 2. A temporal resolution of 4 days makes an absolute velocity accuracy of 0.20 m per day. Points 2 km away from camera 1 has ground pixel size of 0.67 m, which result in a uncertainty of 1.01 m per match and 0.25 m per day with 4 days between the matched images. In addition, the position accuracy will be approximately 100 meter, but depends of elevation model, time and view angle.

The accuracy of the absolute velocity can be improved by larger focal length and better preprocessing of the raw image data. Implementing of clear and obvious artificial points in field will be helpful conjugate points that make it possible to decide a better transformation between images in different reference frame. With known terrain coordinates of the points, they will be useful when adjusting the image to elevation model in the georeferencing process. An updated elevation model will improve the position accuracy.

Recording images every hour and every sixth hour makes it possible to use good images from every day which gives a good temporal resolution of the velocity. A frequency of 4 days between the matched images appears to be the best temporal resolution based on the uncertainty of the results.

The results are presented in graphs as temporal and spatial variations in velocity. The temporal variations in velocity attend the seasonal variations caused by temperature, and the short-time variations follow rain events and rapidly increase in temperature. The spatial variations appear along and across the glacier tongue. The velocity increases towards the front, where the variations also have largest range. The velocity across the glacier tongue is largest in the middle and smaller in the margin of moraine and Colletthøgda. Comparison with earlier measurements show that the cross profile has almost similar pattern.

Measuring velocity with terrestrial photogrammetry is a good alternative to satellite images. The temporal resolution has indefinite frequency, but the use is restricted by the uncertainty in matched image pairs. The smaller ground pixel size improves the spatial resolution. The absolute velocity accuracy is almost the same as in satellite images. The equipment used during the steps between recording images and making velocity graphs are cheap and easy to use. An implementation of a good transformation of images into same reference frame will improve the method considerable. The possible improvement can increase the accuracy and open for the use of even better temporal resolution of the measurements.

8 References

Andersen, Ø. (2003). *Orientering i stereoinstrument*. 2. ed., vol. 1. Ås, Norway: Institutt for kartfag, NLH. 205 pp.

Apogee Imaging Systems. (2010). *Telescope Optics & Pixel Size*. Roseville, California: Apogee Imaging Systems. Available at: http://www.ccd.com/ccd113.html (accessed: 19.10.10).

Benn, D. I., Warren, C. R. & Mottram, R. H. (2007). Calving processes and the dynamics of calving glaciers. *Earth-Sciense Reviews*, 82 (3-4): 143-179.

Berthier, E. (unpublished). *Velocity from satellite images*. Toulouse, France: LEGOS.

Chapuis, A., Rolstad, C. & Norland, R. (2010). Interpretation of amplitude data from a ground-based radar in combination with terrestrial photogrammetry and visual observations for calving monitoring of Kronebreen, Svalbard. *Annals of Glaciology*, 51 (55): 34-40.

Copland, L., Sharp, M. J. & Nienow, P. W. (2003). Links between short-term velocity variations and the subglacial hydrology of a predominantly cold polythermal glacier. *Journal of Glaciology*, 49 (166): 337-348.

Corripio, J. G. (2006). *Geophotoref*. 1.0 ed. Georeferencing oblique terrestrial photogrammetryZrich: Institute of Enviromental Engineering, Swiss Federal Institute of Technology - ETH.

Dick, Ø. B. (2003). *Geomatikk - Kartfaglig bildebruk*. 1. ed., vol. 1. Oslo: GAN Forlag AS. 60 pp.

ESRI. (2008). *ArcMap*. 9.3.1 ed. ArcGISUSA.

Fountain, A. G. & Walder, J. S. (1998). Water flow through temperate glaciers. *Reviews of Geophysics*, 36 (3): 299-328.

Haslene, S. (2008). *Breboka*. 6. ed. Håndbok i brevandring, vol. 1. Oslo: DNT fjellsport. 240 pp.

Jacobsen, K. & Mostafa, M. M. R. (2001). Direct Georeferencing. *Photogrammetric Engineering & Remote sensing*, 67 (12).

Kimball, S. & Mattis, P. (2010). *GIMP*. 2.6.11. ed. GNU Image Manipulation Program. Photo retouching, image composition and image authoring. The GIMP Development Team.

Kääb, A. (2008). *Cias*. 1.0. ed. Image matching. Oslo: University of Oslo.

Lefauconnier, B., Hagen, J. O. & Rudant, J. P. (1994). Flow speed and calving rate of Kronebreen glacier, Svalbard, using SPOT images. *Polar research*, 13 (1): 59-65.

Melvold, K. (1992). *Studie av brebevegelse på Kongsvegen og Kronebreen, Svalbard*. Master thesis. Oslo: University of Oslo, Faculty of Mathematics and Natural Sciences. 60 pp.

Norwegian Meteorological Institute. (2010). *Weather- and climate data*. Ny-Ålesund: Norwegian Meteorological Institute,. Available at: sharki.oslo.dnmi.no/portal/page?_pageid=73,39035,73_39049&_dad=portal&_schema=PORTAL (accessed: 09.11.10).

Norwegian Polar Institute. (2010). *Svalbardkartet*. Digital, interactive and thematic map of Svalbard with detailed thopographic basis map, 1:100 000, 02.10.10. Ny-Ålesund: Norwegian Polar Institute.

Nuth, C. (unpublished). *Personal communication with Ph.D. student Christopher Nuth*. Oslo: Department of Geosciences, University of Oslo.

ReaSoft. (2010). *ReaJPEG*. 4.0 Pro ed. ReaSoft. Image converter. Seattle: ReaSoft Development.

Ritchie, J. B., Lingle, C. S., Motyka, R. J. & Truffer, M. (2008). Seasonal fluctuations in the advance of a tidewater glacier and potential causes: Hubbard Glacier, Alaska, USA. *Journal of Glaciology*, 54 (186): 401-411.

Rolstad, C. & Norland, R. (2009). Ground-based interferometric radar for velocity and calving-rate measurements of the tidewater glacier at Kronebreen, Svalbard. *Annals of Glaciology*, 50 (50): 47-54.

Schenk, T. (1999). *Digital Photogrammetry*. 1. ed. Image Matching Fundamentals & Advanced Image Matching methods, vol. 1. Ohio: TerraScience. 422 pp.

Spot Image. (2007). *SPIRIT Product*. Free DTMs / ortho-image over Polar Regions. Toulouse, France: Spot Image. Available at: www.spotimage.com/automne_modules_files/standard/public/p3163_f62084264e792ecb9756b2e5197a5fe9SPIRIT_tech_sheet-new.pdf (accessed: 27.10.10).

Spot Image. (2010). *FORMOSAT-2*. High resolution satellite images and daily revisit. Toulouse, France: Spot Image. Available at: www.spotimage.com/web/en/977--formosat-2-images.php (accessed: 10.11.10).

Stern, D. (2010). *IDL*. 7.1 ed. Interactive Data Language. Programming language in using Cias. Boulder, Colorado: David Stern & ITT Visual Information Solutions

Sund, M. (unpublished). *Personal communication with Ph.D. student Monica Sund*. Oslo: Department of Geosciences, University of Oslo (04.12.10).

The MathWorks. (2005). *MATLAB*. 7.1 ed. The Language Of Technical Computing. U.S. Patents.

Yushin, A. & Box, J. E. (2010). Glacier velocities from time-lapse photos: technique development and first results from the Extreme Ice Survey (EIS) in Greenland. *Journal of Glaciology*, 56 (198): 723-734.

Appendix

Appendix A: Poster presentation from IGS Nordic Branch meeting 2010

Appendix B: Offset between the images

Appendix C: MATLAB script for transformation of images into same reference frame

Appendix D: Example of result file from Cias

Appendix E: Example of result file from Geophotoref

Appendix F: Displacement showed in the reference image

Appendix G: MATLAB script for extracting the velocity from result files

Appendix H: Table of point coordinates, angle and distance from camera, ground pixel size and position accuracy.

Terrestrial photogrammetry for velocity measurement of Kronebreen calving front

Mari Svanem[1], Anne Chapuis[1], Monica Sund[2, 3] Cecilie Rolstad Denby[1], Andreas Kääb[2], Etienne Berthier[4]

1. Department of Mathematical Sciences and Technology, Norwegian University of Life Sciences, 1432 Ås, Norway. E-mail: mari.svanem@student.umb.no
2. Department of Geosciences, University of Oslo, P.O. Box 1047 Blindern, N-0316 Oslo, Norway 3. The University Centre in Svalbard, P.O. Box 156, N-9171 Longyearbyen 4. LEGOS, Toulouse, France

INTRODUCTION

Crevasse tracking in optical satellite images has successfully been used for mapping glacier velocities. Temporal resolution is restricted to the repeat orbit periods, and the spatial resolution according to recording geometry.

Terrestrial photogrammetry offers an advantage in both temporal and spatial resolution, but introduces other challenges. We have applied terrestrial photogrammetry close to the calving front of Kronebreen, in order to map velocities close to the terminus.

Kronebreen is a tidewater glacier that calves into Kongsfjorden, 14 km east of Ny-Ålesund.

METHOD

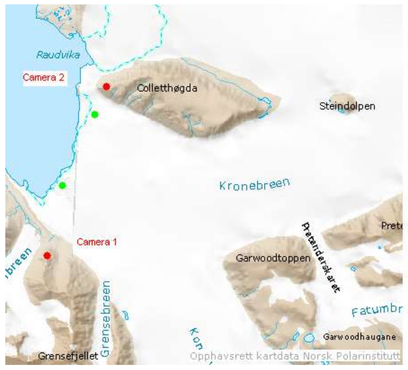

Camera 1, 2 km south

Camera 2, 1 km north

1. Two cameras are placed near the front: One is 2 km south west and one is 1 km north east of the glacier. Photographs are recorded every hour and every sixth hour.

2. Co-registration: We need to translate the images because of camera motion. If they are in exactly same reference frame, all the difference between them will be glacier displacement.

$$[x' \quad y'] = [x \quad y \quad 1] * \begin{bmatrix} 1 & 0 \\ 0 & 1 \\ t_x & t_y \end{bmatrix}$$

The target position probably changes because of unstable ground.

3. Matching: The software, Cias, use area based mathing to find displacement between two images from different times.

By repeating this for same image point in different images, you get the velocity through this terrain point in wanted period.

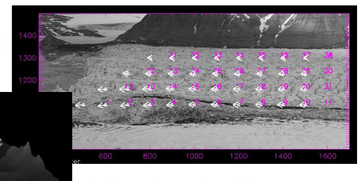

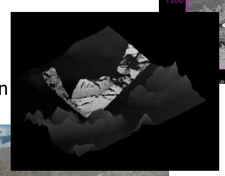

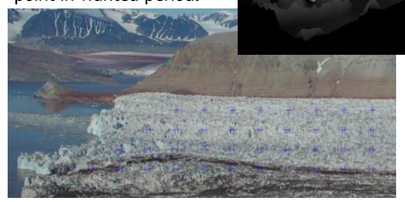

4. Georeferencing: The software, Geophotoref, use the result files from Cias.

It translates the displacement in pixels to displacement in terrain coordinates with help of a DEM, GCPs and camera parameters.

CHALLENGES

Uncertainties in measured velocities are from camera motion, weather conditions, incorrect matching, errors in terrain model, and spatial resolution in the images.

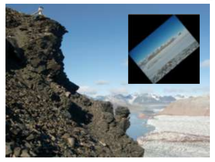

The camera is moving relative to the terrain, mainly with a displacement in y-direction in the image.

This results in changed reference systems, and difference between the images will not only stem from glacier motion.

A small rotation gives up to one pixel difference after translation.

Weather condition: Snow, fog, light, sun direction and shadow makes the images different and more difficult to find right match.

This is also a problem when finding the offset needed to translate the images in Matlab. There I need a homogenous area to decide the difference between the images.

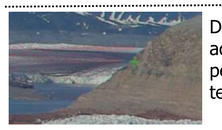

Difficult to adjust the image perfect to the terrain model.

I use the camera parameters and pick the matched target position from the elevation model in ArcGis. This is an inaccurate method and I need to proceed tentatively to get the best adjustment (Once for each reference system).

Incorrect adjustment gives wrong absolute position, not wrong velocity. – If we assume that the uncertainty is systematic for the two point positions, and the relative displacement of the points is accurately determined.

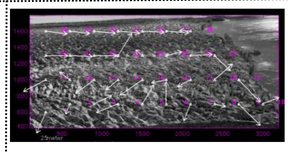

Incorrect match in Cias.

It is easier to match right point if the images look similar: Short time gives small displacement and similar weather conditions. However, it is more difficult to identify incorrect matching points with good temporal resolution.

Changing of block size and search area increase the chance of getting right match.

ACCURACY

Accuracy estimate will determine which temporal resolution that can be used. To determine how to improve the accuracy, we study the individual contributions to the total error:

1. Spatial resolution. The closest measured point has a ground pixel size of 23 cm.
2. Co-registration of images. By neglecting rotation difference up to one pixel can occur.
3. Matching technique. Block Size and search area size can show different displacement.
4. Glacier speed and temporal resolution decrease the percentage accuracy.
5. Image quality and weather conditions. Different shadows change the visibly point.
6. Georeferencing and accuracy of elevation model. 10 meters error in elevation gives 29 meters error in measured position.

VELOCITY

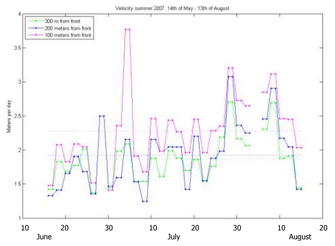

Velocity 2007:
The velocity accelerate towards the front.

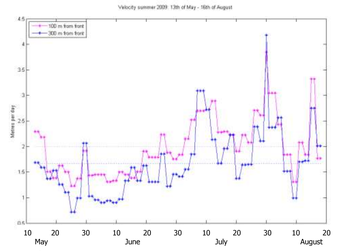

Velocity 2009:
The velocity accelerate towards the front.

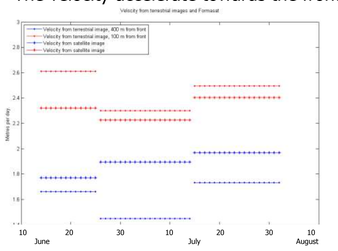

The difference in velocity between measurements in Formosat satellite images and terrestrial images.

Stdv. for period 1, 2 and 3 are 38, 96 and 88 cm.

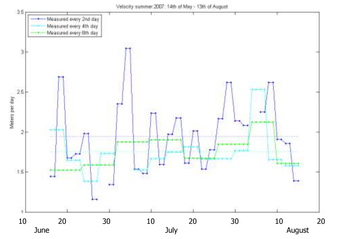

The velocity measured every 2nd, 4th and 8th day for the same period.

CONCLUSION

This method can give better temporal and spatial resolution than velocity measurement from satellite images.

Terrestrial images provides velocities for each day, but the pixel size, camera motion, weather conditions and matching technique reduce the accuracy of it. Several days between each match reduce the temporal resolution and improve the percentages accuracy. - However, it makes it more difficult to find correct matched points. The spatial resolution also depends of the distance between the camera and the matched points in the image. In this measurement do the ground pixel size varies between 23 and 100 cm.

All the applied photogramerical software are free and easy to use. Incorrect matching points and points without know terrain coordinates requires much editing. The method also requiers Matlab, GIMP, ArcGis and a terrain model.

REFERENCES

Chapuis, A., Rolstad, C. & Norland, R. (2010). Interpretation of amplitude data from a ground-based radar in combination with terrestrial photogrammetry and visual observations for calving monitoring of Kronebreen, Svalbard. *Annals of Glaciology, 51 (55).*

Norsk Polarinstitutt. (2010). *Svalbardkartet. Available at: http://eivind.npolar.no/Geocortex/Essentials/Web/viewer.aspx?Site=svbk_v01_no (accessed: 2nd of October).*

Appendix B: Offset (and rotation) between the images

Summer 2007		
Date	x	y
13.jun	-	-
14.jun	?	?
15.jun	?	?
16.jun	?	?
17.jun	?	?
18.jun	?	?
19.jun	-	-
20.jun	?	?
21.jun	?	?
22.jun	?	?
23.jun	?	?
24.jun	?	?
25.jun	?	?
26.jun	?	?
27.jun	?	?
28.jun	?	?
29.jun	?	?
30.jun	?	?
01.jul	?	?
02.jul	?	?
03.jul	?	?
04.jul	?	?
05.jul	?	?
06.jul	?	?
07.jul	?	?
08.jul	?	?
09.jul	?	?
10.jul	?	?
11.jul	?	?
12.jul	?	?
13.jul	?	?
14.jul	?	?
15.jul	?	?
16.jul	?	?
17.jul	?	?
18.jul	?	?
19.jul	?	?
20.jul	?	?
21.jul	?	?
22.jul	?	?
23.jul	?	?
24.jul	?	?
25.jul	?	?
26.jul	?	?
27.jul	?	?
28.jul	?	?
29.jul	?	?
30.jul	?	?
31.jul	?	?
01.aug	?	?
02.aug	?	?
03.aug	?	?
04.aug	?	?
05.aug	?	?
06.aug	?	?
07.aug	?	?
08.aug	?	?
09.aug	?	?
10.aug	-	-
11.aug	?	?
12.aug	?	?
13.aug	?	?

Summer 2009			
Date	x	y	rot deg
10.mai	-1	-50	0.23
11.mai	-2	-30	0.09
12.mai	-1	-30	0.09
13.mai	-2	-26	0.14
14.mai	-4	-16	0.12
15.mai	-2	-13	0.07
16.mai	-2	-13	0.05
17.mai	-1	-14	0.07
18.mai	-3	-12	0.07
19.mai	-4	-7	0.05
20.mai	-3	-6	0.05
21.mai	-3	-5	0.05
22.mai	-3	-5	0.02
23.mai	-3	-3	0.02
24.mai	-4	-4	0.02
25.mai	-3	-4	0.02
26.mai	-3	-4	0.02
27.mai	-	-	-
28.mai	-2	-6	0.05
29.mai	-3	-2	0.05
30.mai	-3	-2	0.03
31.mai	-2	-2	0.02
01.jun	-2	-2	0.02
02.jun	-2	-1	0
03.jun	-2	-1	0
04.jun	-2	-1	0
05.jun	-2	-2	0.02
06.jun	-2	-1	0.02
07.jun	-1	-2	0.02
08.jun	-1	-1	0
09.jun	-1	-2	0.02
10.jun	-1	-1	0.02
11.jun	-2	-1	0
12.jun	-1	0	0.02
13.jun	-2	1	0.02
14.jun	-	-	
15.jun	-1	0	0.02
16.jun	-2	1	0
17.jun	-2	1	0
18.jun	-1	0	0.02
19.jun	-1	-2	0
20.jun	-1	-1	0
21.jun	-	-	
22.jun	-	-	
23.jun	-1	0	0
24.jun	0	1	0.02
25.jun	0	-2	-0.02
26.jun	-1	1	-0.02
27.jun	-1	1	-0.02
28.jun	0	1	-0.02
29.jun	0	-1	0
30.jun	0	0	0
01.jul	0	0	0
02.jul	0	0	-0.02
03.jul	0	-2	0
04.jul	1	-3	-0.03
05.jul	1	-3	0
06.jul	1	-3	-0.02
07.jul	-	-	-
08.jul	1	-1	-0.05
09.jul	-	-	-
10.jul	1	0	-0.07
11.jul	0	-1	-0.07
12.jul	1	-1	-0.05
13.jul	1	-2	-0.05
14.jul	2	-2	-0.05
15.jul	1	-2	-0.05
16.jul	1	-1	-0.02
17.jul	-	-	
18.jul	2	-1	-0.05
19.jul	2	0	-0.05
20.jul	2	0	-0.05
21.jul	2	0	-0.07
22.jul	2	0	-0.07
23.jul	2	-1	-0.07
24.jul	3	-2	-0.07
25.jul	2	-2	-0.05
26.jul	1	-1	-0.05
27.jul	2	-1	-0.03
28.jul	1	-2	-0.05
29.jul	2	-1	-0.07
30.jul	-	-	
31.jul	-	-	
01.aug	2	-1	-0.07
02.aug	1	-1	-0.07
03.aug	1	-1	-0.09
04.aug	1	-1	-0.11
05.aug	-	-	
06.aug	1	-1	-0.10
07.aug	1	-1	-0.09
08.aug	2	-1	-0.11
09.aug	-	-	
10.aug	2	-1	-0.14
11.aug	2	-2	-0.14
12.aug	2	-2	-0.14
13.aug	2	-2	-0.14
14.aug	2	-3	-0.11
15.aug	-	-	-
16.aug	3	-2	-0.12

Autumn 2009		
Date	x	y
16.aug	0	-3
17.aug	0	-2
18.aug	0	-2
19.aug	0	-2
20.aug	0	-2
21.aug	0	-2
22.aug	0	0
23.aug	0	0
24.aug	-	-

25.aug	0	0	12.okt	0	20	12.mai	-2	-4	27.jun	-1	0
26.aug	0	0	13.okt	0	20	13.mai	-2	-2	28.jun	-1	0
27.aug	0	0	14.okt	-	-	14.mai	-2	-2	29.jun	-1	0
29.aug	0	0	15.okt	0	20	15.mai	-2	-2	30.jun	-1	0
30.aug	0	0	16.okt	-	-	16.mai	-2	-2	01.jul	-	-
31.aug	0	0	17.okt	0	20	17.mai	-2	-2	02.jul	-1	0
01.sep	0	0	18.okt	0	20	18.mai	-2	-2	03.jul	-1	0
02.sep	0	0	19.okt	0	20	19.mai	-2	-1	04.jul	-1	0
03.sep	0	0	20.okt	0	20	20.mai	-2	-1	05.jul	-1	0
04.sep	0	0	21.okt	0	20	21.mai	-2	-1	06.jul	-1	0
06.sep	0	0	22.okt	0	20	22.mai	-2	-1	07.jul	-1	0
07.sep	0	0	23.okt	0	20	23.mai	-2	-1	08.jul	-1	0
08.sep	0	0	24.okt	0	20	24.mai	-2	-1	09.jul	-1	0
09.sep	0	1	25.okt	-	-	25.mai	-2	-1	10.jul	-1	0
10.sep	-	-	26.okt	0	20	26.mai	-2	-1	11.jul	-1	0
11.sep	0	1	27.okt	-	-	27.mai	-2	-1	12.jul	-1	0
12.sep	0	1	28.okt	0	20	28.mai	-2	-1	13.jul	-1	0
13.sep	0	1	29.okt	0	20	29.mai	-2	-1	14.jul	-	-
14.sep	0	1	**Summer 2010**			30.mai	-2	-1	15.jul	-1	0
15.sep	0	1	**Date**	**x**	**y**	31.mai	-2	-1	16.jul	-1	0
16.sep	0	1	16.apr	-2	-5	01.jun	-2	-1	17.jul	-1	0
17.sep	0	1	17.apr	-2	-5	02.jun	-2	-1	18.jul	-1	0
18.sep	0	1	18.apr	-2	-5	03.jun	-2	-1	19.jul	-1	0
19.sep	0	1	19.apr	-2	-5	04.jun	-2	-1	20.jul	-1	0
20.sep	0	1	20.apr	-2	-5	05.jun	-2	-1	21.jul	-1	0
21.sep	0	1	21.apr	-2	-5	06.jun	-2	-1	22.jul	-1	0
22.sep	0	1	22.apr	-2	-5	07.jun	-2	-1	23.jul	-1	0
23.sep	0	5	23.apr	-2	-5	08.jun	-2	-1	24.jul	-1	0
24.sep	0	20	24.apr	-2	-5	09.jun	-2	-1	25.jul	-1	0
25.sep	0	20	25.apr	-2	-5	10.jun	-2	-1	26.jul	-1	0
26.sep	0	20	26.apr	-2	-5	11.jun	-2	-1	27.jul	0	0
27.sep	0	20	27.apr	-2	-5	12.jun	-2	-1	28.jul	0	0
28.sep	0	20	28.apr	-2	-5	13.jun	-	-	29.jul	0	0
29.sep	0	20	29.apr	-2	-5	14.jun	-2	-1	30.jul	0	0
30.sep	0	20	30.apr	-2	-5	15.jun	-2	0	31.jul	0	0
01.okt	0	20	01.mai	-2	-5	16.jun	-2	0	01.aug	0	0
02.okt	0	20	02.mai	-2	-5	17.jun	-2	0	02.aug	0	0
03.okt	0	20	03.mai	-2	-5	18.jun	-2	0	03.aug	0	0
04.okt	0	20	04.mai	-2	-5	19.jun	-1	0	04.aug	1	0
05.okt	0	20	05.mai	-2	-5	20.jun	-1	0	05.aug	1	0
06.okt	0	20	06.mai	-2	-5	21.jun	-1	0	06.aug	1	0
07.okt	0	20	07.mai	-2	-5	22.jun	-1	0	07.aug	1	0
08.okt	0	20	08.mai	-2	-4	23.jun	-1	0	08.aug	-	-
09.okt	0	20	09.mai	-2	-4	24.jun	-1	0	09.aug	1	0
10.okt	0	20	10.mai	-2	-4	25.jun	-1	0	10.aug	1	0
11.okt	0	20	11.mai	-2	-4	26.jun	-1	0			

Appendix C: MATLAB script for transformation of images into same reference frame

```
% PROCESS OBLIQUE IMAGERY
% Georeferencing images according to a master image to derive camera motion.
% - With  cross-correlation
% Make us of image processing toolbox
% Assumed inputs are .jpg
% image coordinates refered to as x,y ; map coordinates E,N or X for vector
% Basic code written by Martin Truffer, 2003
% Improvement made of Shad O'Neel, November 2008, to process glacier terminus
% Edited by Mari Svanem, 2010, to use the part of derive camera motion
%%%%%%%%%%%%%%%%%%%%%%%%%%%%%%%%%%%%%%%%%%%%%%%%%%%%%%%%%%%%%%%%%%%%%%%
% THIS SCRIPT USE ALL THE IMAGES FROM CAMERA 1, SUMMER 2009
clear all; close all; clc

mydir= 'C:/Documents and Settings/Mari Svanem/My Documents/Master';          % Folder with all the images
in_dir='/100929_2009a\Transformed_09a';                                       % Folder with the images from summer 2009
% GET FILENAMES
cd([mydir in_dir])                                                            % cd into input dir
list = dir('*.JPG');                                                          % creates structure
temp = struct2cell(list);                                                     % changes structure array into cell array
filename = char(temp(1,:));
MS = imread('master6_09.tif');                                                % reference image for image registration performed later
 camE=445884; camN=8754603; camz=340;                                         % CAMERA POSITON
 [nfiles junk]  = size(filename);
OFFSET = [];
for i = 1:nfiles                                                              % LOOP OF n FILES
   I = imread(filename(i,:));                                                 % eventually loop over files

   metadata = imfinfo(filename(i,:));                                         % grab some meta data
   % REGISTER IMAGE TO MASTER: Each processed image is compared to a master, to determine any camera motion.
   % The referencing is performed by cross correlating a pre-defined region between the two images.

   % CHOOSE REFERENCE AREA IN MASTER (COLLETTHØGDA)
   reg_region = [700 1000 2200 250];                                          % rectangle master: upper left corner, number pixels in x,y dirs
   MScrop = imcrop(MS,reg_region);                                            % figure(3);imshow(MScrop)

   % CHOOSE REFERENCE AREA IN THE OTHER IMAGE: SMALLER AREA INSIDE THE MASTER
   ith_region = [750 1050 2100 150];                                          % rectangle in other images
   icrop = imcrop(I,ith_region);                                              %  figure(4);imshow(icrop)

   cd('C:/Documents and Settings/Mari Svanem/My Documents/Master/Matlab_transformation');
   % CROSS CORRELATION. DECIDES THE OFFSET BETWEEN THE IMAGES
   offset = register_TLimages(icrop,MScrop, reg_region, ith_region);          % Own function, look at next page
   cd([mydir in_dir]);                                                        % Back to images
   OFFSET = [OFFSET offset];                                                  % Save all offsets together
   tx = offset(1);                                                            % Integer translation in x
   ty = offset(2);                                                            %  Integer translation in y
   matrix = [1 0 ; 0 1; tx ty];                                               % Trans formation matrix = translation matrix
   tform = maketform('affine',matrix);% Transformation
   I_trans = imtransform(I,tform,'XData',[1 metadata.Width],'YData',[1 metadata.Height]); % Transformed image
   % imshow(I), figure, imshow(I_trans);
   imwrite(I_trans, sprintf('%s.tif',metadata.Filename(1:8)))                 % Save transformed image in rgb
   I_g = rgb2gray(I_trans);                                                   % Make gray scale image
   imwrite(I_g, sprintf('%s%s.tif',metadata.Filename(1:8),'_g'))              % Save transformed image in gray scale
end
```

```
function offset = register_TLimages(icrop,MScrop, reg_region, ith_region)

%given subset of master image and ith image, perform spatial
%cross-correlation between the two regions to determine any camera
%translation during the sequence.

%input:
%MScrop = region that stays constant in master image, defined in main script
%icrop = smaller region in ith image to be cross-correlated

%output:
%offset = 2 field vector that contains x,y offset in pixels.

cmat = normxcorr2(icrop(:,:,1),MScrop(:,:,1)); % Crosscorrelation matrix
%figure(5); surf(cmat), shading flat

%find the offset
[max_c imax] = max(abs(cmat(:)));
[ypeak, xpeak] = ind2sub(size(cmat),imax(1));

corr_offset = [(xpeak - size(icrop,2))
        (ypeak - size(icrop,1))];

rect_offset = [(reg_region(1) - ith_region(1))
        (reg_region(2) - ith_region(2))];

offset = corr_offset + rect_offset;
```

Appendix D: Example of result file from Cias

This is an example of a result file from the image mathing software, Cias.
The inputs are images from 24th and 28th of June 2010. (IMGP6980 and IMGP7076),
Matched with a template of 70 pixels and a search window of 100 pixels.

X,Y,dx,dy,length,direction,corr_coeff

100.0000,	1150.0000,	-17.5000,	-1.5000,	17.5642,	265.1009,	0.5298
200.0000,	1150.0000,	-17.5000,	-1.5000,	17.5642,	265.1009,	0.5267
300.0000,	1150.0000,	-17.0000,	-1.2500,	17.0459,	265.7946,	0.4965
400.0000,	1150.0000,	-17.2500,	-0.2500,	17.2518,	269.1697,	0.5378
500.0000,	1150.0000,	-13.0000,	1.0000,	13.0384,	274.3987,	0.4911
600.0000,	1150.0000,	-12.5000,	2.0000,	12.6590,	279.0903,	0.6328
700.0000,	1150.0000,	-15.7500,	2.0000,	15.8765,	277.2369,	0.8332
800.0000,	1150.0000,	-15.2500,	1.7500,	15.3501,	276.5463,	0.8178
900.0000,	1150.0000,	-15.5000,	1.2500,	15.5503,	274.6107,	0.8439
1000.0000,	1150.0000,	-15.0000,	1.0000,	15.0333,	273.8141,	0.8751
1100.0000,	1150.0000,	-15.0000,	0.7500,	15.0187,	272.8624,	0.9130
200.0000,	1220.0000,	-17.5000,	-1.0000,	17.5285,	266.7295,	0.3286
300.0000,	1220.0000,	-11.5000,	1.2500,	11.5677,	276.2035,	0.4180
400.0000,	1220.0000,	-17.5000,	2.0000,	17.6139,	276.5198,	0.5801
500.0000,	1220.0000,	-17.5000,	2.0000,	17.6139,	276.5198,	0.8018
600.0000,	1220.0000,	-16.7500,	2.0000,	16.8690,	276.8091,	0.7260
700.0000,	1220.0000,	-16.5000,	1.5000,	16.5680,	275.1944,	0.6925
800.0000,	1220.0000,	-16.0000,	1.0000,	16.0312,	273.5763,	0.7458
900.0000,	1220.0000,	-15.5000,	1.0000,	15.5322,	273.6914,	0.8270
1000.0000,	1220.0000,	-15.2500,	1.0000,	15.2828,	273.7517,	0.8414
1100.0000,	1220.0000,	-14.7500,	1.0000,	14.7839,	273.8785,	0.8184
300.0000,	1290.0000,	-15.7500,	2.0000,	15.8765,	277.2369,	0.4469
400.0000,	1290.0000,	-14.7500,	2.0000,	14.8850,	277.7218,	0.5755
500.0000,	1290.0000,	-14.2500,	1.2500,	14.3047,	275.0131,	0.6472
600.0000,	1290.0000,	-14.0000,	1.0000,	14.0357,	274.0856,	0.7003
700.0000,	1290.0000,	-14.0000,	0.7500,	14.0201,	273.0665,	0.6488
800.0000,	1290.0000,	-14.0000,	0.7500,	14.0201,	273.0665,	0.6007
900.0000,	1290.0000,	-13.5000,	0.7500,	13.5208,	273.1798,	0.5606
1000.0000,	1290.0000,	-13.0000,	0.7500,	13.0216,	273.3019,	0.6572
1100.0000,	1290.0000,	-12.7500,	0.5000,	12.7598,	272.2457,	0.7195
400.0000,	1360.0000,	-10.0000,	1.5000,	10.1119,	278.5308,	0.6175
500.0000,	1360.0000,	-9.5000,	1.2500,	9.5819,	277.4959,	0.5489
600.0000,	1360.0000,	-10.0000,	1.2500,	10.0778,	277.1250,	0.4877
700.0000,	1360.0000,	-8.7500,	1.2500,	8.8388,	278.1301,	0.6725
800.0000,	1360.0000,	-8.7500,	1.5000,	8.8776,	279.7276,	0.7470
900.0000,	1360.0000,	-7.5000,	1.2500,	7.6035,	279.4623,	0.6575
1000.0000,	1360.0000,	-7.0000,	1.0000,	7.0711,	278.1301,	0.7155
1100.0000,	1360.0000,	-7.2500,	1.0000,	7.3186,	277.8533,	0.7055
1100.0000,	1360.0000,	-7.2500,	1.0000,	7.3186,	277.8533,	0.7055

This is an example of a result file from the Georeferencing software, Geophotoref.

The inputs are appendix D: Pixel displacement between images from 24th and 28th of June 2010.

X1,Y1,Z1,dx,dy,dz,direction,length,corr_coeff,pixels1,lines1

446335.906,	8756561.000,	32.239,	-6.500,	12.000,	-2.580,	331.557,	13.647,	0.530,	100.000,	1150.000
446372.344,	8756499.000,	40.232,	-8.531,	2.000,	-0.796,	283.194,	8.763,	0.527,	200.000,	1150.000
446414.000,	8756460.000,	44.642,	-6.594,	9.000,	-1.742,	323.772,	11.157,	0.496,	300.000,	1150.000
446447.781,	8756396.000,	53.089,	-5.969,	11.000,	-1.451,	331.515,	12.515,	0.538,	400.000,	1150.000
446488.000,	8756355.000,	57.906,	-5.000,	6.000,	-0.171,	320.194,	7.810,	0.491,	500.000,	1150.000
446539.219,	8756343.000,	57.982,	-4.250,	8.000,	0.119,	332.021,	9.059,	0.633,	600.000,	1150.000
446590.344,	8756327.000,	58.727,	-6.375,	7.000	0.391,	317.675,	9.468,	0.833,	700.000,	1150.000
446650.156,	8756326.000,	56.756,	-6.625,	6.000,	0.391,	312.166,	8.938,	0.818,	800.000,	1150.000
446718.594,	8756337.000,	52.804,	-8.719,	3.000,	0.706,	288.988,	9.220,	0.844,	900.000,	1150.000
446781.781,	8756330.000,	51.723,	- 6.938,	7.000,	-0.121,	315.257,	9.855,	0.875,	1000.000,	1150.000
446849.656,	8756327.000,	49.929,	-10.344,	0.000,	0.785,	270.000,	10.344,	0.913,	1100.000,	1150.000
446416.000,	8756673.000,	57.256,	-8.906,	4.000,	-0.989,	294.186,	9.763,	0.329,	200.000,	1220.000
446458.344,	8756621.000,	63.158,	-0.281,	23.000,	-1.936,	359.299,	23.002,	0.418,	300.000,	1220.000
446512.469,	8756607.000,	64.412,	-5.969,	14.000,	-0.359,	336.910,	15.219,	0.580,	400.000,	1220.000
446578.938,	8756624.000,	61.044,	-10.750,	0.000,	1.417,	270.000,	10.750,	0.802,	500.000,	1220.000
446651.281,	8756646.000,	56.858,	-6.063,	14.000,	-0.297,	336.586,	15.256,	0.726,	600.000,	1220.000
446731.000,	8756675.000,	51.654,	-12.406,	- 2.000,	1.575,	260.842,	12.566,	0.692,	700.000,	1220.000
446807.219,	8756685.000,	49.089,	-12.375,	-1.000,	1.149,	265.380,	12.415,	0.746,	800.000,	1220.000
446880.250,	8756679.000,	48.673,	-10.250,	4.000,	0.414,	291.318,	11.003,	0.827,	900.000,	1220.000
446950.813,	8756662.000,	49.758,	-7.500,	9.000,	-0.358,	320.194,	11.715,	0.841,	1000.000,	1220.000
447025.281,	8756646.000,	50.508,	-9.031,	6.000,	0.105,	303.598,	10.843,	0.818,	1100.000,	1220.000
446526.625,	8757078.000,	31.000,	0.000,	0.000,	0.000,	45.000,	0.000,	0.447,	300.000,	1290.000
**********,	**********,	**********,	**********,	**********,	**********,	87.086,	Inf,	0.576,	400.000,	1290.000
-NaN,	-NaN,	- NaN,	-NaN,	-NaN,	-NaN,	NaN,	-NaN,	0.647,	500.000,	1290.000
**********,	8757420.000,	**********,	**********,	264.000,	**********,	270.000,	Inf,	0.700,	600.000,	1290.000
446956.781,	8757235.000,	36.678,	-3.594,	22.000,	-1.956,	350.723,	22.292,	0.649,	700.000,	1290.000

447024.250,	8757181.000,	42.888,	-7.531,	12.000,	-0.629,	327.887,	14.168,	0.601,	800.000,	1290.000
447102.156,	8757148.000,	46.673,	-9.156,	8.000 ,	-0.191,	311.144,	12.159,	0.561,	900.000,	1290.000
447178.469,	8757108.000,	51.296,	-6.813,	12.000,	-0.655,	330.416,	13.799,	0.657,	1000.000,	1290.000
447256.094,	8757067.000,	56.037,	-6.750,	11.000,	-0.851,	328.465,	12.906,	0.720,	1100.000,	1290.000
446850.719,	8757701.000,	52.044,	0.750,	32.000,	-1.667,	1.343,	32.009,	0.618,	400.000,	1360.000
-NaN,	-NaN,	-NaN,	-NaN,	-NaN,	-NaN,	NaN,	-NaN,	0.549,	500.000,	1360.000
-NaN,	-NaN,	-NaN,	-NaN,	-NaN,	-NaN,	NaN,	-NaN,	0.488,	600.000,	1360.000
447232.250,	8757919.000,	36.832,	-5.906,	10.000,	0.434,	329.433,	11.614,	0.673,	700.000,	1360.000
447357.188,	8757943.000,	36.564,	-7.969,	6.000,	1.089,	306.978,	9.975,	0.747,	800.000,	1360.000
**********,	8768697.000,	**********,	**********,	-2306.000,	**********,	270.000,	Inf,	0.658,	900.000,	1360.000
**********,	8757771.000,	-6729193.500,	-19792624.000,	-26.000,	-494790.500,	270.000,	19792624.000,	0.715,	1000.000,	1360.000
-NaN,	8758954.000,	-NaN,	-NaN,	-75.000,	-NaN,	NaN,	-NaN,	0.706,	1100.000,	1360.000

The measurement are from 24th to 28th of June 2010, and the image are from 31st of July 2010.

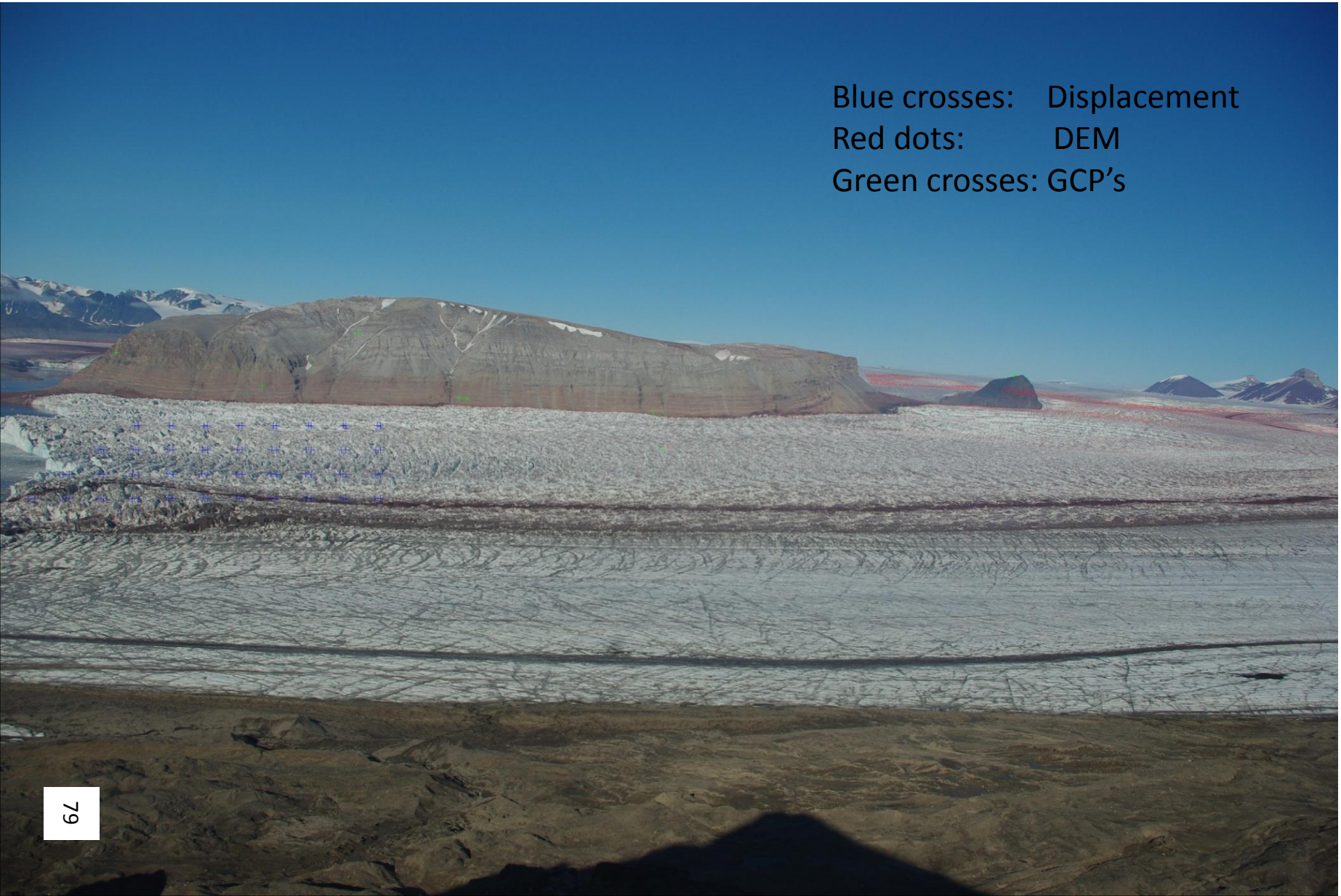

Appendix F: Displacement showed in the reference image.

Appendix F: MATLAB script for extracting the velocity from result files

```
% Velocity of Kronebreen, meter/day
% %%%%%%%%%%%%%%%%%%%%%%%%%%%%%%%%%%%%%%%%%%%%%%%%%%%%%%%%%%%%%%%%%%%%%%%%%%%%%%%%%%%%%
clc; clear all; format long g
% Use images from camera 1
% Matched every 4th day
% Summer 2009: 13th of May - 16th of August
may = [13:31];l_may=size(may,2);
june =[1:30];l_june=size(june,2);
july = [1:31];l_july=size(july,2);
august=[1:16];l_august=size(august,2);
days = l_may+l_june+l_july+l_august; %96

% Download all *.txt files (From Geophotoref) in the folder
%%%%%%%%%%%%%%%%%%%%%%%%%%%%%%%%%%%%%%%%%%%%%%%%%%%%%%%%%%%%%%%%%%%%%%%%%%%%%%%%%%%
cd('C:\Documents and Settings\Mari Svanem\My Documents\Master\100929_2009a\Resultat_2009a_4');

list = dir('*.txt');                      % creates structure of all txt.files
temp = struct2cell(list);                 % changes structure array into cell array
filename = char(temp(1,:));               % Vector av filnamn, char

[nfiles length_name] = size(filename);

for n = 1:nfiles
   number = num2str(1000 + n);
   file = strcat('res09_',number,'_4_ref.txt');
   stored = load(file);
   dX(:,n) = stored(:,4);                 % dX
   dY(:,n) = stored(:,5);                 % dY
   dZ(:,n) = stored(:,6);                 % dZ
   length(:,n) = stored(:,8);             % sqrt(dX^2+dY^2)
   res(:,:,n) = stored(:,:);              % All files togehter
   if( n == 1 )
      allLoaded = stored;
   else
      allLoaded = cat(2, allLoaded, stored );
   end

end

% SUMMERIZE, FIND AVERAGE VELOCITY FOR EACH POINT
%%%%%%%%%%%%%%%%%%%%%%%%%%%%%%%%%%%%%%%%%%%%%%%%%%%%%%%%%%%%%%%%%%%%%%%%%%%%%%%%%%%%%%%%%%
 [points nfiles] = size(length);
 SUM_dX = sum(dX');
 SUM_dY = sum(dY');
for p = 1:points
   SUM_velocity(p) = sqrt((SUM_dX(p))^2 + (SUM_dY(p))^2);
end
velocity_day = SUM_velocity./days;

% REMOVES WRONG MATCH
%%%%%%%%%%%%%%%%%%%%%%%%%%%%%%%%%%%%%%%%%%%%%%%%%%%%%%%%%%%%%%%%%%%%%%%%%%%%%%%%%%%%%%%%%%
res(34,:,1) = NaN; % point 34, 1st matching period
res(29,:,10) = NaN; res(13,:,19) = NaN; res(12,:,21) = NaN;res(13,:,21) = NaN;
```

```
% VELOCITY EACH DAY
%%%%%%%%%%%%%
for q = 1 :points
   pd(q,1)=res(q,8,1)/4;
   pd(q,2)=res(q,8,1)/4;
   pd(q,3)=res(q,8,1)/4;
   pd(q,4)=res(q,8,1)/4;
   pd(q,5)=res(q,8,2)/4;
   pd(q,6)=res(q,8,2)/4;
   pd(q,7)=res(q,8,2)/4;
   pd(q,8)=res(q,8,2)/4;
   pd(q,9)=res(q,8,3)/4;
   pd(q,10)=res(q,8,3)/4;
   pd(q,11)=res(q,8,3)/4;
   pd(q,12)=res(q,8,3)/4;
   pd(q,13)=res(q,8,4)/4;
   pd(q,14)=res(q,8,4)/4;
   pd(q,15)=res(q,8,4)/4;
   pd(q,16)=res(q,8,4)/4;
   pd(q,17)=res(q,8,5)/4;
   pd(q,18)=res(q,8,5)/4;
   pd(q,19)=res(q,8,5)/4;
   pd(q,20)=res(q,8,5)/4;
   pd(q,21)=res(q,8,6)/4;
   pd(q,22)=res(q,8,6)/4;
   pd(q,23)=res(q,8,6)/4;
   pd(q,24)=res(q,8,6)/4;
   pd(q,25)=res(q,8,7)/4;
   pd(q,26)=res(q,8,7)/4;
   pd(q,27)=res(q,8,7)/4;
   pd(q,28)=res(q,8,7)/4;
   pd(q,29)=res(q,8,8)/4;
   pd(q,30)=res(q,8,8)/4;
   pd(q,31)=res(q,8,8)/4;
   pd(q,32)=res(q,8,8)/4;
   pd(q,33)=res(q,8,9)/4;
   pd(q,34)=res(q,8,9)/4;
   pd(q,35)=res(q,8,9)/4;
   pd(q,36)=res(q,8,10)/4;
   pd(q,37)=res(q,8,10)/4;
   pd(q,38)=res(q,8,10)/3;
   pd(q,39)=res(q,8,10)/3;
   pd(q,40)=res(q,8,11)/3;
   pd(q,41)=res(q,8,11)/4;
   pd(q,42)=res(q,8,11)/4;
   pd(q,43)=res(q,8,11)/4;
   pd(q,44)=res(q,8,12)/4;
   pd(q,45)=res(q,8,12)/4;
   pd(q,46)=res(q,8,12)/4;
   pd(q,47)=res(q,8,12)/4;
   pd(q,48)=res(q,8,13)/4;
   pd(q,49)=res(q,8,13)/4;
   pd(q,50)=res(q,8,13)/4;
   pd(q,51)=res(q,8,13)/4;
   pd(q,52)=res(q,8,14)/4;
   pd(q,53)=res(q,8,14)/4;
   pd(q,54)=res(q,8,14)/4;
   pd(q,55)=res(q,8,14)/4;
   pd(q,56)=res(q,8,15)/4;
   pd(q,57)=res(q,8,15)/4;
   pd(q,58)=res(q,8,15)/4;
   pd(q,59)=res(q,8,15)/4;
   pd(q,60)=res(q,8,16)/4;
   pd(q,61)=res(q,8,16)/4;
   pd(q,62)=res(q,8,16)/4;
   pd(q,63)=res(q,8,16)/4;
   pd(q,64)=res(q,8,17)/4;
   pd(q,65)=res(q,8,17)/4;
   pd(q,66)=res(q,8,17)/4;
   pd(q,67)=res(q,8,17)/4;
   pd(q,68)=res(q,8,18)/4;
   pd(q,69)=res(q,8,18)/4;
   pd(q,70)=res(q,8,18)/4;
   pd(q,71)=res(q,8,18)/4;
   pd(q,72)=res(q,8,19)/4;
   pd(q,73)=res(q,8,19)/4;
   pd(q,74)=res(q,8,19)/4;
   pd(q,75)=res(q,8,19)/4;
   pd(q,76)=res(q,8,20)/3;
   pd(q,77)=res(q,8,20)/3;
   pd(q,78)=res(q,8,20)/3;
   pd(q,79)=res(q,8,21)/4;
   pd(q,80)=res(q,8,21)/4;
   pd(q,81)=res(q,8,21)/4;
   pd(q,82)=res(q,8,21)/4;
   pd(q,83)=res(q,8,22)/4;
   pd(q,84)=res(q,8,22)/4;
   pd(q,85)=res(q,8,22)/4;
   pd(q,86)=res(q,8,22)/4;
   pd(q,87)=res(q,8,23)/4;
   pd(q,88)=res(q,8,23)/4;
   pd(q,89)=res(q,8,23)/4;
   pd(q,90)=res(q,8,23)/4;
   pd(q,91)=res(q,8,24)/3;
   pd(q,92)=res(q,8,24)/3;
   pd(q,93)=res(q,8,24)/3;
   pd(q,94)=res(q,8,25)/3;
   pd(q,95)=res(q,8,25)/3;
   pd(q,96)=res(q,8,25)/3;
end
```

```
% STANDARD DERIVATION AND MEAN
%%%%%%%%%%%%%%%%%%%%%%%%%%%%%%%%%%%%%%%%%%%%%%%%%%%
for i = 1:points                   % For each point
   pd0 = pd(i,:);
   pd0 = pd0(~isnan(pd0));
   Mean_point(i,1) = mean(pd0);
   Std_point(i,1) = std(pd0);
   Min_point(i,1) = min(pd0);
   Max_point(i,1) = max(pd0);
end

pd2 = pd(~isnan(pd));         % For all points
Mean_all = mean(pd2);        % Average
Std_all = std(pd2);          % Standard derivation
Max_all = max(pd2);          % Maximum value
Min_all = min(pd2);          % Minimum value

% GRAPHS
%%%%%%%%%%%%%%%%%%%%%%%%%%%%%%%%%%%%%%%%%%%%%%%%%%%%%%%%%%%%%%%%%
x = [may,june+31,july+31+30,august+31+30+31];

figure (1);
plot(x,pd(13,:),'- . ','LineWidth',2,'Color',[0,0,1]); hold on;
plot(x,Mean_point(13)*ones(days,1),': b'); hold on;
plot(x,pd(14,:),'- . ','LineWidth',2,'Color',[0,0,0]); hold on;
plot(x,Mean_point(14)*ones(days,1),': k'); hold on;
plot(x,pd(15,:),'- . ','LineWidth',2,'Color',[0,1,0]); hold on;
plot(x,Mean_point(15)*ones(days,1),': g'); hold on;
title({'Velocity summer 2009';'Acceleration towards the front'});
xlabel('Days');
ylabel('Meters per day');
legend('Point 200 m from the front','Mean','Point 300 m from the front',...
   'Mean','Point 400 m from the front','Mean','Location','NorthWest');

disp('Min, Max, Mean, Std: ');
out = [Min_point(13),Max_point(13),Mean_point(13),Std_point(13);...
   Min_point(14),Max_point(14),Mean_point(14),Std_point(14);...
   Min_point(15),Max_point(15),Mean_point(15),Std_point(15)]
```

Appendix H: Table of point coordinates, angle and distance from camera, ground pixel size and position accuracy.

Point (x, y)	Distance, m	Vertical angle, degrees	Horizontal angle, degrees	Ground pixel size, m	dH = 14 m, m	dH = 8 m, m	dH = 20 cm, m
Camera 2							
447375,8758600	1085	-17.97	256.87	0.24026	43.17	24.67	0.62
447311,8758631	1073	-18.41	253	0.23773	42.06	24.03	0.60
447251,8758669	1059	-18.78	249.06	0.23442	41.18	23.53	0.59
447196,8758716	1037	-19.07	245.07	0.22971	40.50	23.14	0.58
447137,8758749	1036	-19.26	241.11	0.22936	40.06	22.89	0.57
447084,8758791	1027	-19.37	237.17	0.22739	39.82	22,75	0.57
446974,8758753	1127	-19.40	233.3	0.2495	39.76	22.72	0.57
447387,8758325	1338	-13.83	260.17	0.29628	56.88	32.50	0.81
447302,8758331	1352	-14.28	256.45	0.29947	55.00	31.43	0.79
447221,8758366	1342	-14.68	252.63	0.29721	53.43	30.53	0.76
447148,8758421	1315	-15.02	248.74	0.29131	52.16	29.80	0.75
447078,8758474	1296	-15.30	244.83	0.28691	51.18	29.25	0.73
447013,8758535	1271	-15.52	240.89	0.28148	50.43	28,82	0.72
447275,8757760	1905	-10.17	259.73	0.42186	78.07	44.61	1.12
447173,8757847	1843	-10.56	256.06	0.40805	75.18	42.92	1.07
447080,8757949	1771	-10.92	252.28	0.39211	72.55	41.45	1.04
446986,8758028	1729	-11.23	248.45	0.38283	70.49	40.28	1.01
447235,8756628	3018	-6.14	262.83	0.66831	130.06	74.32	1.86
447073,8756765	2909	-6.50	259.31	0.6442	122.88	70.22	1.76
446784,8757077	2680	-7.16	251.93	0.59352	111.43	63.68	1.59
446647,8757206	2607	-7.45	248.15	0.57729	107.02	61.16	1.53
Minimum value	1027	-19.40	233.30	0.2274	39.76	22.72	0.57
Mean value	1610	-13.86	250.38	0.3566	65.39	37.37	0.93
Maximum value	3018	-6.14	262.83	0.6683	130.06	74.32	1.86

Point (x, y)	Distance, m	Vertical angle, degrees	Horizontal angle, degrees	Ground pixel size, m	dH = 14 m, m	dH = 8 m, m	dH = 20 cm, m
Camera 1							
446319,8756650	2115	-8.35	77.995	0.71305	95.41	54.52	1.36
446367,8756596	2073	-8.35	76.391	0.69868	95.34	54.48	1.36
446410,8756533	2022	-8.35	74.745	0.68162	95.34	54.48	1.36
446454,8756475	1978	-8.35	73.06	0.66676	95.41	54.52	1.36
446493,8756407	1924	-8.33	71.337	0.64874	95.60	54.63	1.37
446551,8756394	1931	-8.31	69.583	0.65106	95.87	54.79	1.37
446618,8756400	1961	-8.28	67.794	0.6612	96.25	55.00	1.37
446689,8756408	1997	-8.24	65.966	0.67319	96.70	55.26	1.38
446759,8756406	2025	-8.19	64.121	0.68251	97.32	55.61	1.39
446827,8756394	2045	-8.13	62.235	0.68925	97.99	55.99	1.40
446893,8756375	2059	-8.06	60.351	0.69421	98.86	56.49	1.41
446479,8756791	2285	-7.11	74.785	0.7703	112.31	64.18	1.60
446537,8756753	2264	-7.09	73.097	0.76334	112.60	64.34	1.61
446616,8756774	2308	-7.06	71.378	0.77819	113.08	64.62	1.62
446690,8756775	2334	-7.02	69.63	0.78694	113.68	64.96	1.62
446774,8756787	2376	-6.98	67.836	0.80092	114.35	65.34	1.63
446866,8756810	2433	-6.93	66.022	0.82026	115.20	65.83	1.65
447040,8756806	2506	-6.80	62.303	0.8447	117.34	67.05	1.67
447114,8756768	2507	-6.73	60.402	0.84519	118.64	67.79	1.69
446678,8757530	3049	-5.86	74.815	1.0278	136.44	77.97	1.95
446763,8757501	3044	-5.82	73.136	1.0261	137.27	78.44	1.96
446847,8757469	3039	-5.78	71.423	1.0245	138.29	79.02	1.98
446931,8757428	3028	-5.73	69.672	1.0207	139.46	79.69	1.99
447011,8757378	3010	-5.68	67.888	1.0147	140.80	80.46	2.01
447088,8757316	2983	-5.62	66.068	1.0054	142.31	81.32	2.03
447167,8757261	2966	-5.55	64.227	0.9997	144.08	82.33	2.06
447241,8757195	2939	-5.48	62.363	0.99084	146.07	83.47	2.09
447322,8757141	2930	-5.39	60.468	0.98771	148.25	84.71	2.12
446974,8758207	3777	-4.56	73.176	1.2733	175.59	100.34	2.51
447102,8758235	3843	-4.50	71.462	1.2954	177.72	101.56	2.54
447432,8758101	3836	-4.30	66.125	1.2932	185.99	106.28	2.66
447573,8758109	3902	-4.23	64.281	1.3154	189.36	108.20	2.71
447713,8758104	3960	-4.15	62.42	1.335	193.17	110.38	2.76
447846,8758076	3999	-4.06	60.532	1.3481	197.34	112.77	2.82
Minimum value	1924	-8.35	60.35	0.64874	95.34	54.48	1.36
Mean value	2690	-6.57	68.15	0.90671	128.51	73.44	1.84
Maximum value	3999	-4.06	78.00	1.3481	197.34	112.77	2.82